

# The Feni River Closure Dam Reviewed

Report of the final thesis

August 1993

F.M. Stroeve

---





**FINAL REPORT OF THE THESIS**

**THE FENI RIVER CLOSURE DAM  
REVIEWED**

**AN UPDATE AND ANALYSIS OF THE DESIGN OF THE  
GEOMETRIC DAM PROFILE AND SEA SIDE SLOPE PROTECTION**

**BY F.M. STROEVE  
nr: 813071**



## PREFACE

In May 1992 the consultant Haskoning presented a study proposal to the Faculty of Civil Engineering of the University of Technology in Delft. This proposal comprised a study to re-examine the cross section of the Feni River Closure Dam in Bangladesh that had already been designed by this consultant in 1983 and subsequently built in 1985. The proposed study was thought to be the basis for a paper for the PIANC congress in 1994. Subject 4 of this congress reads among others: "It will be of particular interest to be informed about the comparison between the current situation concerning morphology and defence works with earlier predictions."

The student F.M. Stroeve was willing to perform this study as a part of his final thesis with the intention to obtain his Masters degree. The work was carried out in Bangladesh for one month and at the office of Haskoning in Nijmegen in the Netherlands during the remainder of the study. The author wants to thank Haskoning for providing the guidance and the accommodation in Bangladesh and in the Netherlands.

Furthermore the author owes gratitude to the Lamminga Fund, which paid for the flight to Bangladesh.

For the collection of information in both the Netherlands and Bangladesh, a lot of people have been approached. The author wants to thank all these people, without whom this study had not been possible at all. Since it is impossible to mention all the people who contributed to the success of this study, only a few of them are mentioned below:

Mr. F.G. Koch	Land Reclamation Project
Mr. A.J.M. Shamsuddin	Systems Rehabilitation Project
Mr. J. Houterman	Systems Rehabilitation Project
Mr. F. Cooper	Systems Rehabilitation Project (EEC)
Mr. H. Dahl	Cyclone Protection Project II (FAP 7)
Mr. A. Macdonald	Surface Water Simulation Modelling Programme, phase II
Mr. D.S. Shamsul Abedin	South East Region Water Resources Development Program

Furthermore, gratitude is indebted to the Bangladesh Water Development Board, the Bangladesh Inland Water Transport Authority and the Bangladesh Meteorological Department for supplying the necessary information.

Last but not least, the author wants to thank the people who provided study guidance and advice. These are among others: Ir. B. the Slaa and ir. R. Noppeney of Haskoning and the Commission of Graduation:

Prof. ir. K. d'Angremond,  
Ir. J. van Duivendijk,  
Ing. K. Bezuijen and  
Ir. N. Booij.

## ABBREVIATIONS

BIWTA	= Bangladesh Inland Water Transport Authority
BWDB	= Bangladesh Water Development Board
CD	= Chart Datum
CO <sub>2</sub>	= Carbon Dioxide
CPP	= Cyclone Protection Project
FAP	= Flood Action Plan
HYV	= High Yield Variety (rice variety)
LAT	= Lowest Astronomical Tide
MIP	= Muhuri Irrigation Project
MSF	= Fortnightly constituent of the tide
MSL	= Mean Sea Level
NPV	= Net Present Value
NTD	= Neap Tide Dam
PV	= Present Value
PWD	= Public Works Datum
SOB	= Survey Of Bangladesh
SWL	= Still Water Level
TDS	= Total Dissolved Solids
WSTD	= Winter Spring Tide Dam

## TABLE OF CONTENTS

1	<u>ABSTRACT</u> .....	9
2	<u>INTRODUCTION</u> .....	13
2.1	GENERAL DESCRIPTION AND EVALUATION OF ORIGINAL DESIGN .....	13
2.1.1	Historical background .....	13
2.1.2	General description of original design .....	13
2.1.3	General evaluation of original design .....	16
2.2	STUDY OBJECTIVES .....	17
2.3	STUDY ASSUMPTIONS .....	19
3	<u>NATURAL CONDITIONS</u> .....	21
3.1	INTRODUCTION .....	21
3.2	TIDE .....	21
3.3	SEASONAL CHANGE OF MEAN SEA LEVEL .....	21
3.4	MORPHOLOGICAL CHANGES .....	22
3.5	CYCLONE PHENOMENON .....	22
3.6	CO <sub>2</sub> WARMING .....	24
4	<u>DATUM ANALYSIS</u> .....	25
4.1	INTRODUCTION .....	25
4.2	DESCRIPTION OF USED DATUMS .....	25
4.3	RELATION BETWEEN CD AND MSL .....	25
4.4	RELATION BETWEEN PWD AND MSL .....	27
5	<u>OBJECTIVES OF THE FENI RIVER CLOSURE DAM</u> .....	29
6	<u>ORIGINAL DESIGN METHOD</u> .....	31
6.1	INTRODUCTION .....	31
6.2	ORIGINAL DESIGN CRITERIA .....	31
6.3	WATER LEVEL PROBABILITY DISTRIBUTION USED FOR THE ORIGINAL DESIGN .....	31
6.4	WAVE CHARACTERISTICS USED IN THE ORIGINAL DESIGN .....	32
6.5	ORIGINAL DESIGN OF THE GEOMETRIC DAM PROFILE .....	32
6.5.1	<u>Macro slope stability analysis</u> .....	32
6.5.2	<u>Sea side slope angles of original dam profile</u> .....	33
6.5.3	<u>Crest levels of the original dam design</u> .....	33
6.5.3.1	Wave run-up for the main dam .....	33
6.5.3.2	Geotechnical settlement and long term sea level rise .....	34
6.5.3.3	Applied crest levels .....	34

6.6	ORIGINAL DESIGN OF THE SEA SIDE SLOPE PROTECTION	35
6.6.1	<u>Slope protection principle</u>	35
6.6.2	<u>Calculation of the block sizes</u>	35
7	<u>REDESIGN OF FENI RIVER CLOSURE DAM</u>	37
7.1	DESIGN CRITERIA	37
7.1.1	<u>Introduction</u>	37
7.1.2	<u>Distinction between monsoon and cyclone conditions</u>	37
7.1.3	<u>Design criteria for overtopping</u>	37
7.1.3.1	Polder system	38
7.1.3.2	Monsoon criterion for overtopping of the Feni dam	39
7.1.3.3	Cyclone criterion for overtopping of the Feni dam	39
7.1.4	<u>Design criterion for the slope protection</u>	40
7.2	ACCRETION PROCESS IN FRONT OF THE DAM	41
7.3	WATER LEVELS	43
7.3.1	<u>Introduction</u>	43
7.3.2	<u>Probability distribution for monsoon conditions</u>	43
7.3.2.1	General probability distribution for Sonapur station	44
7.3.2.2	Probability distribution for Azimpur station during monsoon conditions	44
7.3.3	<u>Probability distribution for cyclone conditions</u>	45
7.3.3.1	Methodology	45
7.3.3.2	Results of the calibration of the model complex	46
7.3.3.3	Derivation of probability distribution for Chittagong	46
7.3.3.4	Derivation of probability distribution for the Feni Dam	47
7.4	WAVE CLIMATE	49
7.4.1	<u>Methodology</u>	49
7.4.2	<u>Limitations of Hiswa</u>	49
7.4.3	<u>General distinction between wave sources</u>	50
7.4.4	<u>Assessment of wave conditions caused by swell</u>	50
7.4.5	<u>Assessment of wave conditions during monsoon winds</u>	51
7.4.5.1	Determination of design wind velocity	51
7.4.5.2	Determination of the governing wind direction	52
7.4.5.3	Determination of wave parameters during monsoon conditions	52



7.4.6	<u>Assessment of wave conditions during cyclones</u> . . . . .	53
7.4.6.1	Schematization of cyclones as a stationary and uniform situation . . . . .	53
7.4.6.2	Determination of governing points of landfall . . . . .	54
7.4.6.3	Wind velocity probability distribution during cyclonic conditions . . . . .	54
7.4.6.4	Determination of the wave climates for cyclonic conditions . . . . .	56
7.5	REDESIGN OF GEOMETRIC DAM PROFILE . . . . .	57
7.5.1	<u>Introduction</u> . . . . .	57
7.5.2	<u>Slope stability analysis</u> . . . . .	57
7.5.2.1	Required safety factors and design conditions . . . . .	57
7.5.2.2	Geotechnical parameters of subsoil and dam body . . . . .	58
7.5.2.3	Results of biseis calculations . . . . .	59
7.5.3	<u>Optimization procedure of geometric dam profile</u> . . . . .	59
7.5.3.1	Variables for optimization . . . . .	59
7.5.3.2	Costs . . . . .	60
7.5.3.3	Benefits . . . . .	61
7.5.3.4	Calculation of Net Present Value . . . . .	61
7.5.4	<u>Geometric dam profile without sedimentation influence</u> . . . . .	62
7.5.4.1	Results of the optimization procedure . . . . .	62
7.5.4.2	Sensitivity analysis for expected annual damage . . . . .	62
7.5.4.3	Verification of monsoon criterion . . . . .	63
7.5.4.4	Geotechnical settlement . . . . .	63
7.5.4.5	Dam profile when the CPP II criteria would be applied . . . . .	63
7.5.5	<u>Geometric dam profile including sedimentation influence</u> . . . . .	64
7.6	DETAILED DESIGN OF THE SLOPE PROTECTION . . . . .	65
7.6.1	<u>Introduction</u> . . . . .	65
7.6.2	<u>Choice of the sub layers of the slope protection</u> . . . . .	65
7.6.3	<u>General description of the analytical method for the design of the slope revetment</u> . . . . .	65
7.6.4	<u>Design loading conditions for the slope protection without accretion influence</u> . . . . .	67
7.6.4.1	Design conditions for the main dam . . . . .	67
7.6.4.2	Design loading conditions for the left flank embankment . . . . .	67
7.6.4.3	Design loading conditions for the right flank embankment . . . . .	68

7.6.5	<u>Generation of alternatives for the filter and cover layers</u>	69
7.6.5.1	Cover layer options	69
7.6.5.2	Filter layer options	70
7.6.5.3	Choice of the filter fabric	71
7.6.5.4	Resulting alternatives	72
7.6.6	<u>Calculation of the cover layer thickness for the alternatives</u>	72
7.6.7	<u>Design of slope protection without sedimentation influence</u>	73
7.6.7.1	Design of slope protection for the main dam	73
7.6.7.2	Design of slope protection for the left flank embankment	75
7.6.7.3	Design of slope protection for the Right flank embankment	76
7.6.8	<u>Design of slope protection including sedimentation influence</u>	76
8	<u>INFLUENCE OF IMPROVED DESIGN METHODS AND MORPHOLOGICAL CHANGES</u>	77
8.1	INTRODUCTION	77
8.2	INFLUENCE OF THE APPLICATION OF NUMERICAL MODELS	77
8.3	INFLUENCE OF ADVANCED WAVE RUN-UP FORMULAS	78
8.4	INFLUENCE OF OPTIMIZATION METHOD FOR THE GEOMETRIC DESIGN	79
8.5	INFLUENCE OF ADVANCED DESIGN METHOD FOR PLACED BLOCK REVETMENTS	79
8.6	INFLUENCE OF A HYPOTHETICAL METHOD TO PREDICT THE SEDIMENTATION PROCESS	81
9	<u>FINAL CONCLUSIONS</u>	83
10	<u>REFERENCES</u>	85

## ANNEXES

ANNEX A	Distribution analysis for water levels during monsoon conditions
ANNEX B	The set-up of a numerical storm surge model
ANNEX C	Model calibration
ANNEX D	Derivation of water level distribution for cyclone conditions
ANNEX E	The set-up of a numerical wave hindcast model
ANNEX F	Design procedure for the geometric dam profile
ANNEX G	Calculations using the analytical method for the design of placed block revetments
ANNEX H	Cost calculation of the original and redesign

## 1 ABSTRACT

The subject of this study is the Feni River Closure Dam in Bangladesh, which was designed in 1983 and subsequently built in 1985. In this final report the influence is analyzed of advanced design methods, which have become available since 1983, on the geometric dam profile and sea side slope protection. For this purpose the Feni dam was redesigned using these advanced design techniques.

First the methods used for the original design were analyzed, with regard to the geometric profile and sea side slope protection.

Subsequently the Feni dam was redesigned, using advanced design methods and considering the afore mentioned items. Contrary to the original design, the distinction between monsoon and cyclone conditions was made, because of the different character of both hydraulic situations. As a result of the closure of the Feni river by means of the Feni dam, a huge area downstream of the dam has accreted. The geometric redesign and structural redesign of the slope protection was carried out twice: With and without accretion influence. In this way, the influence of a hypothetical method to predict the morphological process, which was not available at the time the original design was originally made, is demonstrated.

In order to derive the hydraulic loading conditions first the water levels were analyzed. The influence of the accretion process on the water levels near the dam was assumed to be zero. By analyzing gauge readings near the dam site, a probability distribution for water levels during monsoon conditions was derived. The probability distribution of water levels for cyclone conditions was obtained by means of a numerical storm surge model. After calibrating this model, 40 synthetic situations were derived, of which the probability of occurrence could be derived from the meteorological cyclone record since 1900. By computing the maximum water levels for these 40 situations and by means of relations between gauge stations the probability distribution for cyclone conditions near the Feni dam could be obtained.

For the wave climate the influence of the accretion process is not negligible. As no wave observations have been carried out in the neighbourhood of the Feni dam, again a numerical model was used. By means of a wave hindcast model, the wave climate could be estimated during cyclones and monsoon winds and for the two cases: with or without accretion influence.

It was found out that the wave height 3 years after closure was about 10 to 20% lower than at the time of closure for the same probability of exceedance. This effect is caused by the accretion of the fore shore.

When the hydraulic boundary conditions were derived, the geometric dam profile was designed including and excluding the accretion influence. In contrast with monsoon conditions, sea water is permitted to overtop the structure during cyclone conditions. By estimating the annual benefits and costs of the Feni River Closure Dam, an economic optimization procedure could be carried out. The dam profile was determined to be the most economic profile during cyclone conditions. The geotechnical macro stability was checked and it was concluded, that this profile fulfils the monsoon design criterion imposed to the dam.

Using the analytical method to design a slope protection consisting of placed block revetments, the sea side slope protection was redesigned. Again, this was done with and without accretion influence, using the same materials as applied for the original design.

Finally, the influence of the advanced design methods was analyzed. By means of numerical computer models, an economic optimization procedure, new wave run-up formulas and an advanced method to design the slope protection, a dam design without accretion influence was obtained, which is only about 4% cheaper than the original design. A further cost reduction of only 1% can be reached when the accretion process in front of the Feni dam could be anticipated accurately. This small influence is mainly caused by the fact that the positive effect of the wave height reduction is more or less equal to the negative effect of the reduction of the wave steepness.

When the original design of the slope protection was analyzed using the newly available analytical method, the applied slope protection turned out to be far from stable for the concerned return period!



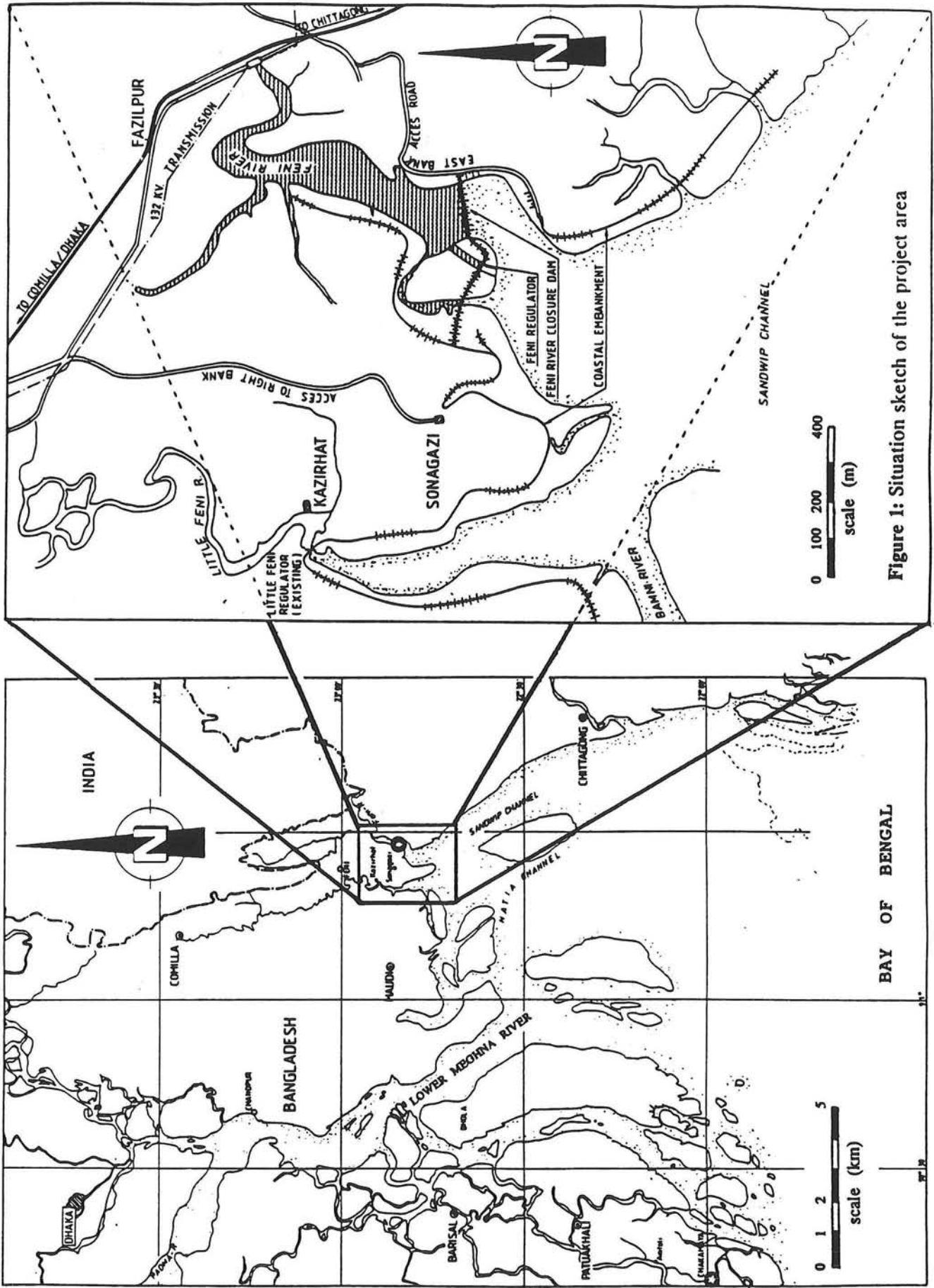


Figure 1: Situation sketch of the project area

## **2 INTRODUCTION**

In this chapter, the study objectives and study assumptions are described in Section 2.2 and 2.3. First a general description of the original design is given in Section 2.1.

### **2.1 GENERAL DESCRIPTION AND EVALUATION OF ORIGINAL DESIGN**

In order to understand the descriptions mentioned in the study objectives and assumptions, the Feni dam is briefly described in this section first. In Section 2.1.1 a historical background is given. Subsequently in Section 2.1.2 a general description of the Feni dam is given as it was designed in 1983. Finally the general evaluation of this design is described in Section 2.1.3.

#### **2.1.1 Historical background**

In the south eastern part of Bangladesh three rivers; the Feni River, the Muhuri River and the Kalidash Paharia Khal River, discharge into the Bay of Bengal. In this area the Muhuri Irrigation Project was started in the early eighties. This project comprised an agricultural development consisting of about 27,000 ha. of arable land, located in the tidal zone of the Noakhali and Chittagong District. This project area was affected by saline intrusion from the tidal basin, was distressed by flooding in the wet season and was subject to loss of fresh water in the dry season. The most important facility to overcome these burdens, was the construction of the Feni River Closure Dam to permit storage of fresh water and to prevent floodings and saline intrusion. The closure of the Feni river estuary formed the last and most important part of the Muhuri Irrigation Project. Haskoning, Royal Dutch Consulting Engineers, which was asked to design and to supervise the construction of the Feni River Closure Dam, started its work on January 14th 1983. The construction of the dam was completed two and a half years later in August 1985.

#### **2.1.2 General description of original design**

At the previously determined location of the closure dam, the river mouth was approximately 1160 meters wide, while there were two gullies and a shoal in between. Before starting the closure operation, the construction of the Feni regulator was completed. The function of this regulator is to control the reservoir water level by sluicing fresh river water into the sea. The general situation of the project area is shown in Figure 1. Two flank embankments had to be constructed. The position of the right and left flank embankment is given in Figure 2.

The right flank embankment connects the main dam to the Feni Regulator at the western side and the left flank embankment connects the main dam to the existing coastal embankments at the eastern side. The design of the cross-section of the main dam consists of several parts, depending on the different phases of construction. These parts are described below, for which Figure 3 is referred to.

#### **Bed protection**

In order to stabilize the river bed, a mattress was placed both in the gullies and on the shoals. This mattress consisted of a composite fabric (woven and non-woven), connected to bamboo and reed rolls. For ballasting the bed protection river boulders were used.

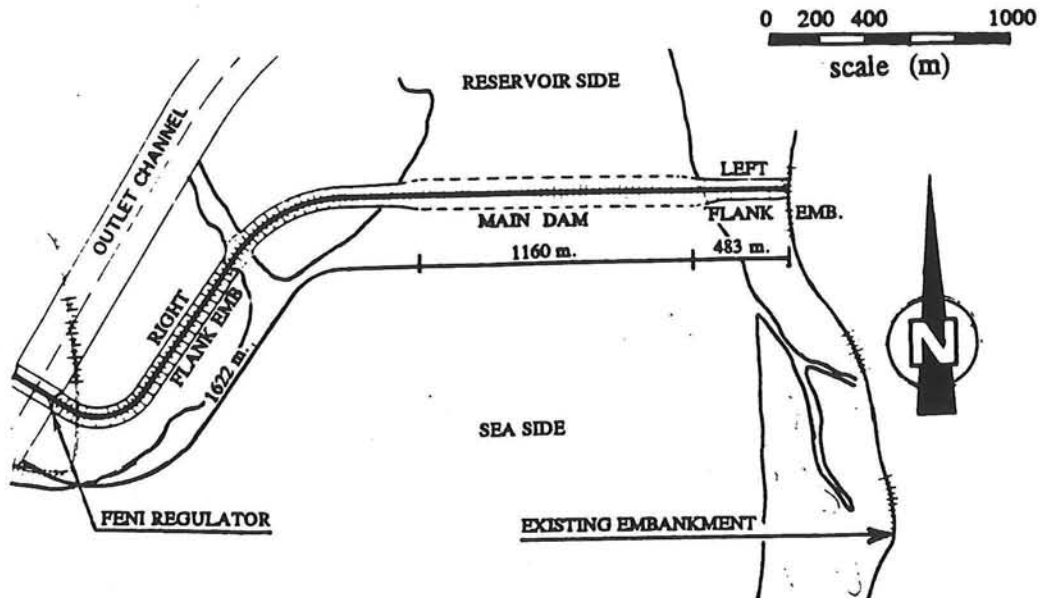


**Figure 2:** Project site and dam sections.

### Sill

A sill had to be constructed to create a uniform depth and flow condition over the whole river mouth as a starting point for the closure operation. This would fill out the gullies. The original design consisted of a sill, made out of dumped boulders over a width of 70 meters, that would have to be grouted under the Neap Tide Dam to prevent leakage after construction. The sill slopes were covered with bed protection mattresses.

### Neap Tide Dam (NTD)

After construction of the sill, the actual closure operation could start. The winter season was chosen for this operation, because of the minimal mean sea level and the large availability of labour in that period. Furthermore the closure operation took place during neap tide, because of the small tidal range. The job would be executed by approximately 12,000 labourers, who had to close the Feni estuary, by moving 1,200,000 clay bags from 12 stock piles to the closure gap by hand. This operation lasted for only about 6 hours, during low water. In this way a barrier against high water during neap tide was obtained, which was called the Neap Tide Dam (NTD).

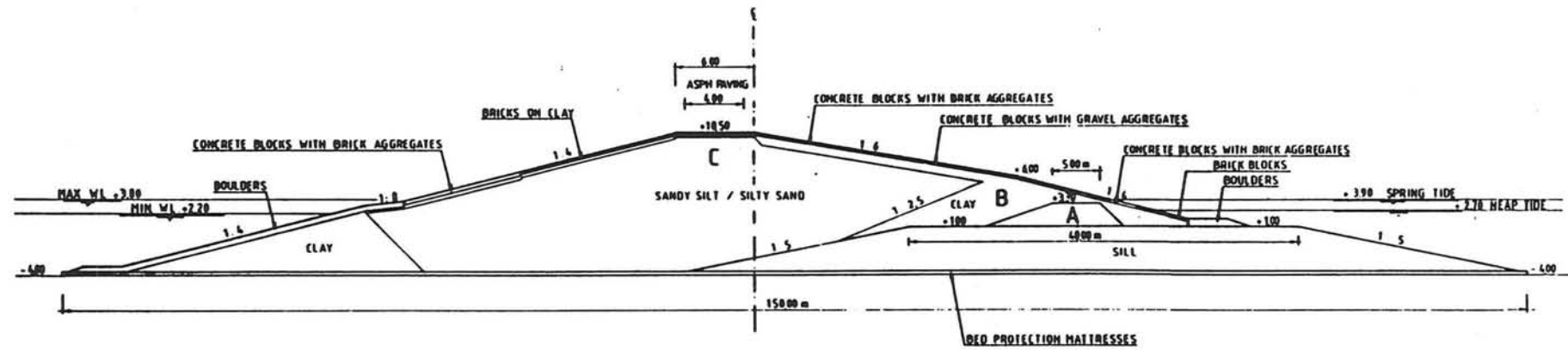
### Winter Spring Tide Dam (WSTD)

After the closure, the Neap Tide Dam had to be elevated to a level that would be sufficient to block the high water levels during spring tide, which would occur 8 days later. This dam totally consisted of clay and was called the Winter Spring Tide Dam (WSTD).

### Main dam body

After the construction of the WSTD the final dam profile had to be realised by moving earth on top and at the reservoir side of the WSTD. This earth was obtained from dredging operations in the neighbourhood. This operation had to be finished before the start of the monsoon season, during which the working conditions would be very bad.





Cross section Fenl River Closure Dam

- A : Neap Tide Dam (NTD)
- B : Winter Spring Tide Dam
- C : Final Profile

Figure 3: Cross section of the main dam, levels above SOB = 0.46 m. + PWD.

### **Slope protection**

As a base for the slope protection at the sea side of the dam a clay layer was applied on top of the final dam profile. This clay was covered by a filter fabric. On top of this the block revetments were placed on a layer of chipped bricks. Depending on the position on the slope the cover layer comprised concrete blocks made with either gravel or brick aggregates or so-called brick blocks (blocks consisting of bricks and mortar in between).

### **Toe structure**

At the sea side of the dam, a toe structure was constructed, to ensure stability of the block revetments and to establish a flexible transmission to the bed protection. This toe comprised a concrete horizontal slab beneath the block revetments with vertical joints. In front of this beam boulders were placed. The construction of the toe was hampered due to the accretion process in front of the dam at the sea side, that started immediately after the day of closure.

### **2.1.3 General evaluation of original design**

In 1983 no means were available to estimate the water levels during cyclone conditions. Furthermore, no wave observations have been carried out in the area of the lower Meghna estuary. Furthermore, during and after construction of the Feni River Closure Dam, a huge accretion took place at the sea side of the dam. As a reliable theory to predict the speed of this sedimentation process accurately was not available, the consultant decided not to take any foreshore accretion into account.

For the design of the cross section and the revetments, methods were applied, which were commonly used in 1983, but which are out of date nowadays.

Due to all these items the design of the Feni River Closure Dam can be considered to be a rather conservative one, mainly with respect to the crest level, the slope angles and the revetments.

## 2.2 STUDY OBJECTIVES

In general the objective of this study is to examine the influence of various improved design methods and morphological changes since the year 1983 on the design of the Feni River Closure dam.

The objective can be divided into several parts:

- 1 To describe the original design method with regard to the geometric dam profile and its sea side slope protection.
- 2 To design the dam profile and sea side slope protection by means of the following improved design methods and tools to anticipate morphological developments:
  - Better computational tools such as computer hardware and software which enable a more accurate estimation of extreme water levels and wave climates for various conditions.
  - Wave run-up formulas which became available recently.
  - Economic optimization procedure to be used for the design of the geometric dam profile.
  - Analytical method to design a placed block revetment. This method was developed through extensive research in the field of the behaviour of placed block revetments under various hydraulic loads.
  - Hypothetical method to anticipate the morphological changes caused by the construction of a dam structure accurately. Until now such a method is not available. For the redesign the observed accretion figures downstream of the dam will be taken into account.
- 3 To analyze the influence of the improved design methods and morphological changes on the geometric design of the Feni dam profile and the structural design of the sea side slope protection.  
This will be carried out by comparing the construction costs of the original design to the costs of the redesign.



### 2.3 STUDY ASSUMPTIONS

Due to the limited time available for this study, it is not possible to examine all design aspects of the Feni River Closure Dam. For this reason, only a few items will be studied in detail and assumptions have to be made for the remaining parts of the design. In this way the study is clearly defined. The following assumptions have been made: (for a description of the used parameters reference is made to Section 2.1.2.)

- 1) For this study the location of the Feni regulator and the design of the regulator itself will not be re-examined.
- 2) No attention shall be paid to the closure method and the execution of this closure operation.  
This automatically implies that the following items will not be reconsidered:
  - The dam location in the Feni river estuary.
  - The river bed protection.
  - The sill.
  - The Neap Tide Dam.
- 3) The Winter Spring Tide Dam will not be redesigned.
- 4) The slope angle and the slope protection at the reservoir side shall not be reconsidered.
- 5) The protection at the crest of the dam will not be re-examined.
- 6) The possibility of applying a berm at the sea side will not be analyzed.
- 7) No redesign of the various toe protection works will be carried out.
- 8) The geotechnical settlement and liquefaction phenomenon will not be reconsidered. Since 1983, no appreciable improved methods to calculate these items have been developed and no additional geotechnical data of the Feni dam site have become available. So there is no reason to re-examine these items.
- 9) The type of the sea side slope protection will not be changed.  
In order to enable a sound comparison between the original design and the redesign, a cover layer consisting of placed blocks was assumed. The sub layer was determined to consist of clay covered with a filter fabric, like the original design.

As far as these items are considered, the study results and properties of the original design will be taken as a starting point for this study.

Consequently, only the geometric design of the crest level and the sea side slope angles and the structural design of the sea side slope protection will be updated and subsequently the influence of advanced design methods and morphological changes since 1983 on these items will be analyzed.

For the redesign, the same unit prices as in the year 1985 will be taken into account, in order to compare the redesign with the original design in an accurate manner.



### **3      NATURAL CONDITIONS**

#### **3.1      INTRODUCTION**

The Feni dam is subject to many different natural conditions, which should be taken into account for the redesign. The hydraulic conditions concerning the tide and the seasonal change of MSL are briefly described in Sections 3.2 and 3.3. In Section 3.4 the morphological processes which affect the Feni dam are explained. At last the meteorological situations with regard to cyclones and CO<sub>2</sub> warming are illustrated in Sections 3.5 and 3.6.

#### **3.2      TIDE IN THE FENI ESTUARY**

The Feni estuary is connected to the Bay of Bengal by means of the Hatia and Sandwip channels. See for this Figure 1 of section 2.1. Here the tide is predominantly semi diurnal with daily inequities. The tidal amplitude may reach a value of 4 meters near the dam site. The consultant Haskoning noticed an uneven distribution between flood and ebb. On an average the flood lasts less than three hours and the ebb lasts approximately 9 hrs. 30 min. The current reversal at the end of the ebb tide is almost instantaneous and was often accompanied by a tidal bore, which is a propagating hydraulic jump.

Investigations have shown that, besides the diurnal and semi-diurnal constituents, the tidal constituent having a period of one fortnight is significant in the area. Before a tidal wave reaches the coast near the Feni River Closure Dam, it propagates over an extensive area of shallow water, through the Sandwip and Hatia channels. Due to damping of the tidal wave by friction, kinetic energy is transformed among others into potential energy. This results in a variation of the mean water level, with a cycle of 2 weeks.

#### **3.3      SEASONAL CHANGE OF MEAN SEA LEVEL**

There is a rise of MSL in the wet season, which may reach to about 1 meter relative to the MSL in the dry season. This seasonal change of MSL can be ascribed to the following causes:

- An increase of the hydraulic gradient of the lower Meghna river due to an increase of the discharge in the wet season. This subsequently causes an elevation of MSL in the lower Meghna estuary.
- A change of the magnitude and strength of predominant winds from the dry to the monsoon season.
- A general change in atmospheric pressure.
- Changes in salinity differences between the coast and the deep sea.

When the magnitude of the MSL change is considered, the first three reasons can contribute only to some degree. A MSL change of about 1 meter, can only be explained by a change of the salinity gradient. This is caused by the seasonal variations of the fresh water discharge of the main rivers in the area, the Meghna, the Ganges and the Jamuna. The main mechanism behind this water level difference is that the density is larger for saline sea water than for fresh water. It requires a higher column of fresh water to balance out the gravity of a corresponding column of sea water.

### 3.4 MORPHOLOGICAL CHANGES

The lower Meghna river supplies a huge volume of sediment to the lower Meghna estuary. See Figure 1 of chapter 2. A part of this load settles in the low lying lands in the Meghna delta. This is the main cause of the rapid changes of the coastlines and bathymetry in the area. As a result, the hydraulic situation is also influenced by this phenomenon. Directly in front of the dam, huge areas have accreted, which resulted in an elevation of the foreshore downstream of the Feni dam after closure. In chapter 7.2 this process is described more in detail. The influence of this sedimentation process on the dam design was analyzed in this study.

### 3.5 CYCLONE PHENOMENON

In history, the Bangladeshi coast was often struck by cyclones. Cyclones, which are very low depressions, are classified according to their maximum attained wind speed. Nowadays the following nomenclature is used:

Classification	Interval of maximum wind speed
Depression	up to 62 km per hour
Cyclonic storm	63 - 87 km per hour
Severe cyclonic storm	88 - 118 km per hour
Severe cycl. storm with hurricane intensity	above 118 km per hour

**Table 1:** Classification of cyclones.

A cyclones life can be divided into several stages.

In the formative stage the origin of a cyclone can be traced back to an area of low pressure on the ocean. The clouds begin to organise themselves into a coherent system.

When the sea surface temperature is 27° or more in areas of low pressure, a warm air advection from the ocean surface to the mid-troposphere can develop and the cyclone is likely to intensify. This is the growth stage of the cyclone. In the centre of the cyclone, air pressures start falling over a small and circular area. This centre is generally called 'the eye' of the cyclone. This is accompanied by an organization of clouds into a more or less circular pattern.

During the mature stage the central pressure does not decrease any more and maximum wind speeds do no longer increase. The storm only expands horizontally a little while it is heading for the coast line.

When the storm reaches land or a colder sea region it will decay very quickly during the last stage of the cyclone's life.

A cyclone can be characterized by its maximum pressure drop:  $\Delta p$ , its radius to maximum wind speed:  $R_{max}$  and the maximum wind speed  $V_{max}$ . In Figure 4 the air pressure and the wind velocities over a cross-section of a cyclone are given.



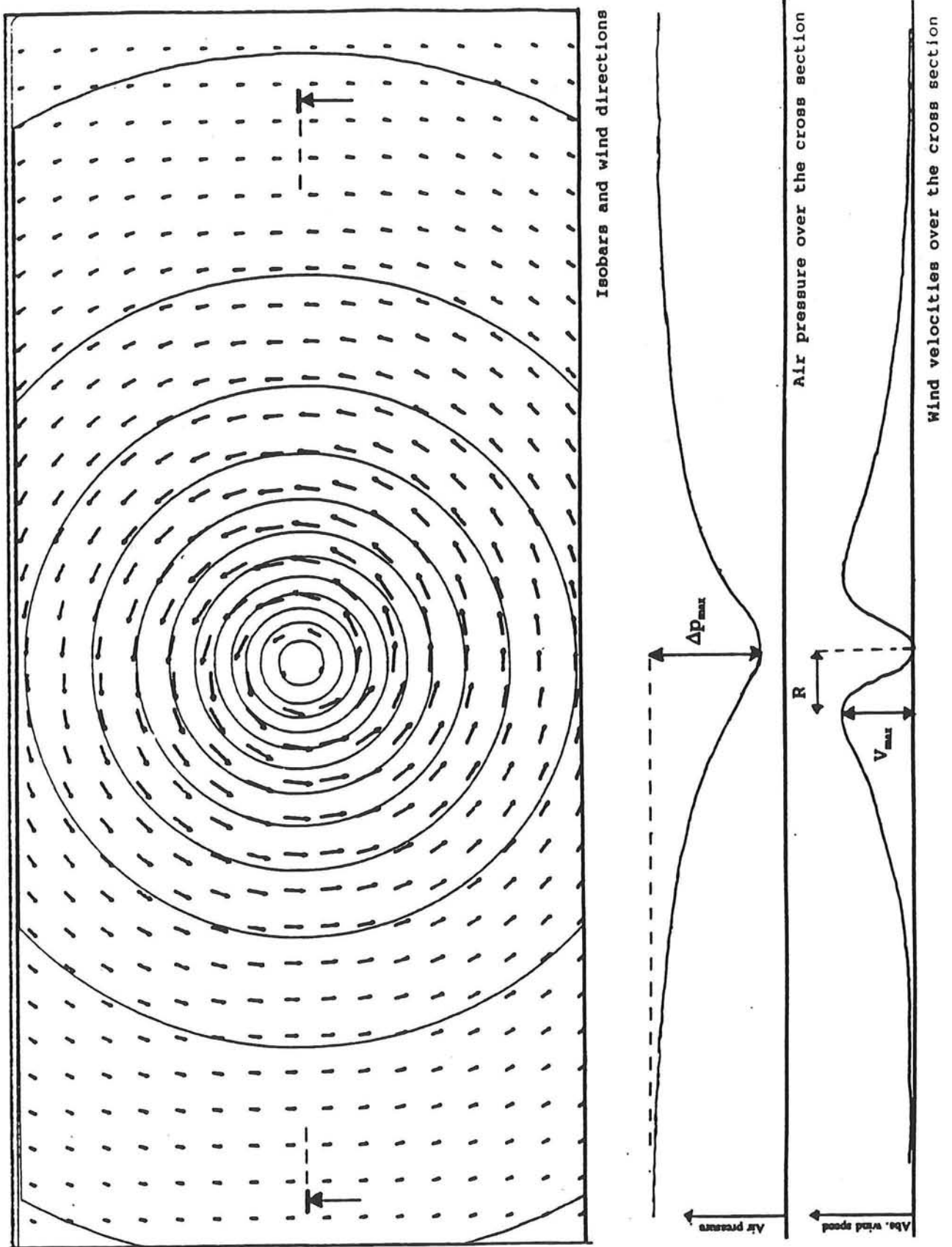


Figure 4: Wind velocities and air pressures in a cyclone

### 3.6 CO<sub>2</sub> WARMING

It is generally believed that the carbon dioxide (CO<sub>2</sub>) concentration in the air has increased dramatically over the last decennia, due to human impact on the global environment. This will probably lead to an increase of global temperatures, which is called the 'greenhouse effect'. If these expectations become reality, this may affect Bangladesh in several ways.

First of all studies indicate that the mean sea level will rise due to the rise of temperature. If this is going to happen, this effect will cause an increase of the inundation probability in the future. A lot of research has been performed to estimate the long term sea level rise. The results of these studies vary between 31 and 350 cm. by the year 2100. Because of these large differences, the estimations of this long term effect can be considered to be rather unreliable. For the original design this effect was not considered. In order to enable a good comparison with the original design, the long term sea level rise will neither be taken into account for the redesign.

Secondly, the greenhouse effect may possibly cause an increase of the intensity of tropical cyclones in the Bay of Bengal. Because of the increase of sea surface temperatures, considerably more water vapour is available for conversion to kinetic energy. The minimum attainable central pressure in a cyclonic storm will decrease and the maximum wind speed will increase as a result. Since accurate estimations are not available, this effect will neither be taken into account.

## **4      DATUM ANALYSIS**

### **4.1    INTRODUCTION**

Many different reference levels are encountered when the hydraulic situation in the northern part of the Bay of Bengal is studied. For clearness of this report all these reference datums should be transformed to one datum. The relations between the datums are given in this chapter. First the used datums are described in Section 4.2. Subsequently in Section 4.3 and 4.4, the relations between these datums are derived.

### **4.2    DESCRIPTION OF USED DATUMS**

The most important levels used in the concerned region are:

- PWD** This stays for "Public Works Datum" and is installed by the Bangladeshi government at 0.46 meter below MSL of the ocean. Nowadays this reference level is mainly used by the Bangladesh Water Development Board (BWDB). This datum is not subject to seasonal changes.
- SOB** This level, meaning "Survey Of Bangladesh" was used for the original Feni Dam design, but not for recent projects any more. This reference level is equal to the mean sea level of the ocean and therefore SOB is constant in time and in place like PWD.
- MSL** This stays for the Mean Sea Level. The annual mean sea level varies in place. Mainly due to salinity differences, the water density in the lower Meghna estuary is lower than in the ocean. This yields a higher MSL in the lower Meghna estuary. In this study the annual MSL will be used as a reference datum for calculations using numerical models.
- CD** This abbreviation stays for Chart Datum, which is used both by the Bangladesh Inland Water Transport Authority (BIWTA) and by the British Admiralty. This datum is the level below which the tide seldom comes and is approximately the Lowest Astronomical Tide (LAT). As the tidal range is not constant, the Chart Datum will vary considerably over the eastern Meghna estuary.

For the clearness of this report, all data and computational results are transformed to one reference level: PWD.

### **4.3    RELATION BETWEEN CD AND MSL**

The relation between CD and MSL is mainly depending on the tidal range and is thus depending on the location along the coast. In order to obtain this relation, the Bangladesh and British Admiralty tide tables (ref. [1] and [2]) were used. From these tables, the relation was obtained for several tidal gauge stations used by the Bangladesh Inland Water Transport Authority (BIWTA). The locations of these stations are given in Figure 5. In Table 2 these relations are given. From these figures it is clear that the tidal range increases from Hiron Point in the west to Sandwip near the Feni River Closure Dam, where it reaches its maximum. From there the tidal range decreases to Shahpuri Island in the south east.

Gauge Station	level of MSL above CD (m)
Hiron Point	1.700
Char Changa	2.037
Sandwip	3.243
Khal no. 10	2.664
Sadarghat	2.481
Cox's Bazar	1.995
Shahpuri Island	1.874

Table 2: Relation between CD and MSL.

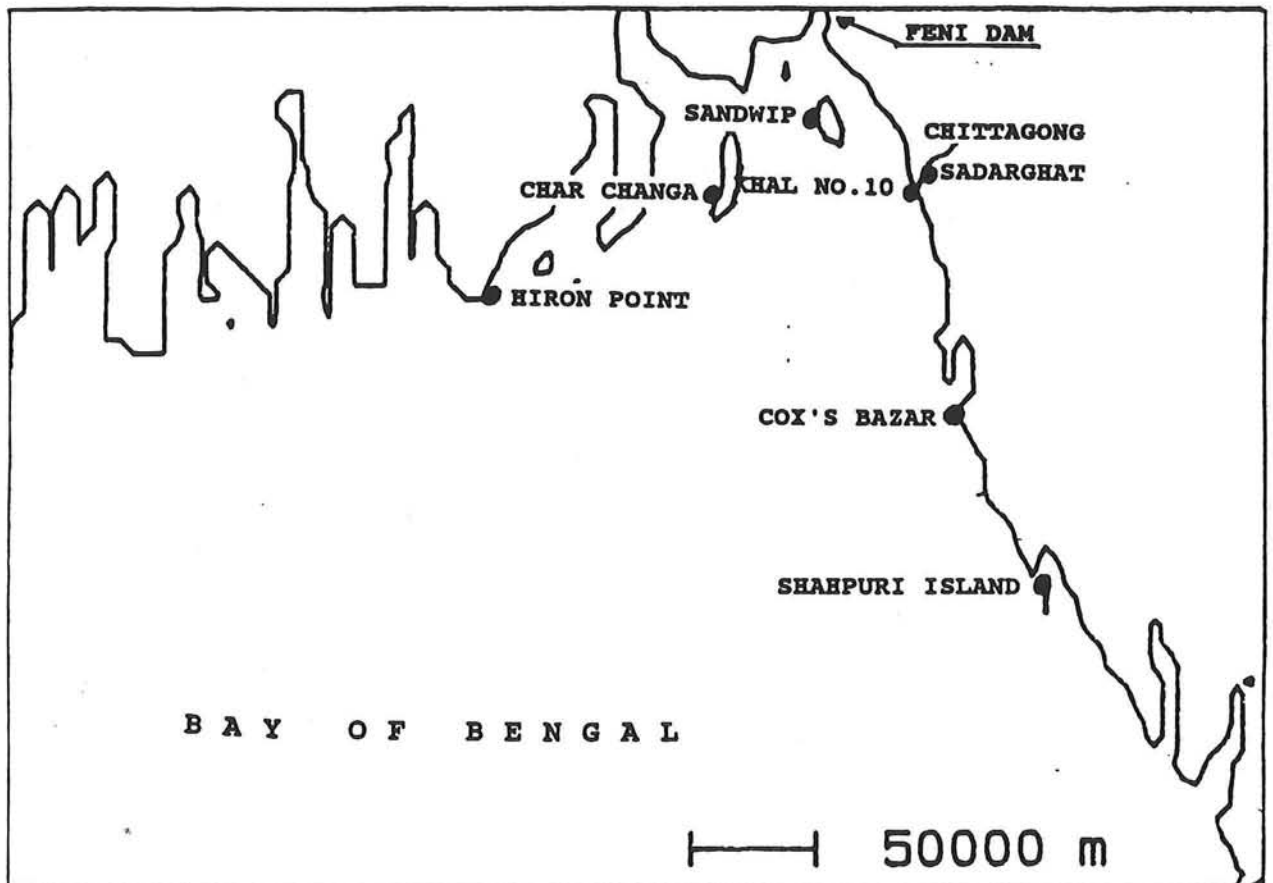


Figure 5: Location of tidal (BIWTA) gauge stations

#### 4.4 RELATION BETWEEN PWD AND MSL

It appeared to be very difficult to determine this relation, because an accurate geographic information system is not available. From the Bangladesh Tide Tables (ref. [2]) the bench mark heights in some stations are known relative to both CD and PWD. This can be used to determine the relation between these two reference levels. Table 3 shows how these relations were derived.

gauge station	Bench mark above CD	Bench mark above PWD	PWD minus CD	MSL minus CD	MSL minus PWD
Sandwip	6.907 m.	4.687 m.	2.220 m.	3.243 m.	1.023 m.
Char Changa	4.996 m.	(3.826 m.)	1.170 m.	2.037 m.	0.867 m.
Cox's Bazar	4.836 m.	3.931 m	0.905 m.	1.995 m.	1.050 m.

Table 3: Calculation of relation between PWD and CD.

In this table, the accuracy of the value between brackets is doubted, for the corresponding figure in the tide tables is hand written. This is why the relation in Char Changa has been neglected. For the lower Meghna estuary the relation between the two datums is schematized to be constant over the area. For the design calculations the average relation between CD and PWD near Sandwip and Cox's Bazar was taken into account. Thus the PWD level in the concerned region was determined to be  $(1.023 + 1.050) * 0.5 = 1.037 \approx 1.0$  meter below the mean sea level in the concerned region. For clearness sake a definition sketch of the various datums is given in Figure 6.

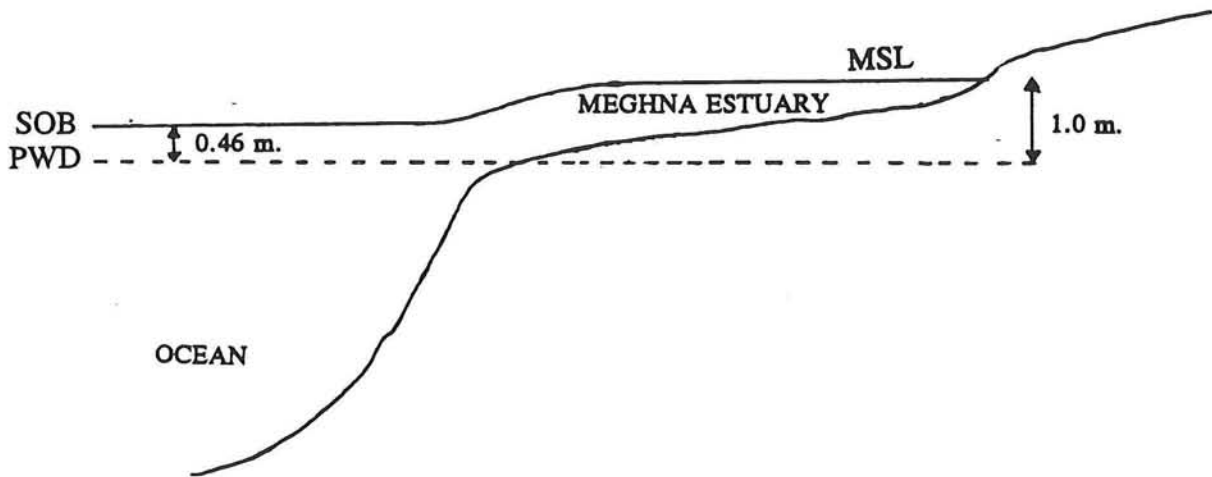


Figure 6: Definition sketch of several reference levels



## **5      OBJECTIVES OF THE FENI RIVER CLOSURE DAM**

For the redesign of the Feni River Closure Dam, it is important to know what are the objectives of the hydraulic structure.

**Main objective of the Feni dam is:**

To enable irrigation for at least two crops per year for the Muhuri Irrigation Project.

This objective can be divided into three parts:

- To create a fresh water storage capacity to enable cultivation of two crops per year. These crops are HYV (= High Yield Variety) Aus, which is planted in March / April and harvested in June / July and HYV Aman, which is planted from July till September during the monsoon and harvested from November till January.
- To prevent intrusion of sea water into the reservoir and thus to protect the reservoir water against getting saline.
- To decrease the head difference between the reservoir and the irrigation channels. As the irrigation channels have a higher piezometric head than the reservoir, fresh reservoir water has to be pumped to the irrigation channels by means of low-lift pumps. In order to enable the cultivation of rice, this head difference should be relatively small.

**Sub objective of the Feni dam is:**

To reduce the risk of inundation of the upland by shortening of the coastline and to protect the hinterland, during the passage of a cyclone.

This sub-objective can also be divided into several parts:

- protection of human lifes,
- protection of livestock and
- protection of infrastructure, buildings, roads, communication lines, etc, in the hinterland.





## 6 ORIGINAL DESIGN METHOD

### 6.1 INTRODUCTION

In order to be able to compare the design methods used in the original and redesign, first the procedure used in the original design had to be analyzed. For this mainly the Final Design Report of 1983 (ref. [3]) and the Design report of 1981 (ref. [4]) were used. In Section 6.2 the original design criteria are given. Subsequently, it is described in Sections 6.3 and 6.4 how the design water levels and wave conditions were derived in the original design. The original geometric design of the dam profile and the structural design of the sea side slope protection are explained in Sections 6.5 and 6.6.

### 6.2 ORIGINAL DESIGN CRITERIA

After studying the original design method, the design criteria could be derived. For this study the criteria could be divided into overtopping and slope protection criteria. In these criteria, no division was made between the two possible weather conditions, monsoon storms and cyclones, probably because the tools to derive hydraulic boundary conditions during cyclones were not available.

The overtopping criterion was defined for a situation with a return period of 50 years, during which only 2% of the waves were permitted to overtop the structure.

The criterion concerning the slope protection was defined for a situation with the same return period of 50 years, during which nearly no damage to the slope protection was tolerated.

### 6.3 WATER LEVEL PROBABILITY DISTRIBUTION USED FOR THE ORIGINAL DESIGN

The water level probability distribution used for the original design was based on water level data obtained from the Design report of 1981 (ref. [4]). These data comprised monthly mean and extreme water levels, during the years 1957 - 1977 derived from observations in the gauge station Azimpur, which is located in the Feni estuary. See Figure 10 of section 7.3.2. From these figures the annual mean and extreme values were derived. In Annex A these data are given. After considering these figures, the consultant Haskoning concluded, that the gauge readings are unreliable from the year 1967 onwards. Therefore, the statistics for the original design were only based on data of the period 1957 - 1967. Assuming that the annual extreme water levels are Gumbel distributed, Table 4 could be derived:

Return period in years	1	10	20	50
Water level in m. + PWD	6.44	7.51	7.95	8.52

Table 4: Water levels for various return periods near the Feni dam.

The accompanying distribution reads:

$$p \{ \text{water level} \geq x \} = e^{-e^{-1.635 \cdot x - 10.03}}$$

Contrary to the method followed for the redesign study, the division between monsoon and cyclone conditions was not made for the original design. Later in this report it will be analyzed, whether cyclonic surges do occur in the used annual extremes.

#### 6.4 WAVE CHARACTERISTICS USED IN THE ORIGINAL DESIGN

The wave characteristics used as a basis for the original design were obtained from ref. [4]. In this report two situations were calculated.

First, the wave climate caused by incoming waves from the ocean was estimated. This was done by transforming the wave parameters at the ocean to the shore, including breaking and shoaling in the Hatia Channel. In this way, a significant wave height  $H_{sig} = 1.70$  m. and a significant period  $T_{sig}$  of 7.0 seconds was found. Furthermore, the governing wave propagating direction was thought to be south-west and thus, the angle between the wave fronts and the dam axis,  $\beta$ , was determined to be  $30^\circ$ .

Secondly, the waves generated by local winds were estimated to have a  $H_{sig}$  of about 1.4 meter and a  $T_{sig}$  of about 4.8 seconds.

For the design the first situation was taken into account.

As far as the impact of water depths on wave heights is concerned, in the year 1983 no reliable method and insufficient data were available to predict the sedimentation speed in front of the Feni dam accurately. This is why this process was not taken into account. The bathymetry seaward of the dam was assumed not to change in the course of the time.

#### 6.5 ORIGINAL DESIGN OF THE GEOMETRIC DAM PROFILE

In this section the method used for the original geometric design of the dam profile is given. First the minimum possible sea side slope angle was derived by means of a geotechnical macro slope stability analysis. How this was done is described in Section 6.5.1. In Section 6.5.2 and 6.5.3 the original determination of the sea side slope angles and crest levels are given for all considered dam sections.

##### 6.5.1 Macro slope stability analysis

First the maximum possible slope angle was derived for the main dam. This was done by schematizing the whole dam body as one uniform material. For this material a relatively low friction angle ( $\phi = 20^\circ$ ) and cohesion ( $c = 5$  KN/m<sup>2</sup>) was taken into account. Then the worst loading condition was considered with a filled reservoir and low tide in conjunction with a horizontal acceleration due to earth-quakes of 0.1 times the acceleration of gravity. The subsoil is then likely to be subject to liquefaction. The maximum slope angle was determined by considering straight failure planes and by analyzing previous studies for comparable situations. According to the consultant, no analysis of the macro slope stability for circular failure planes was carried out. In this way, the tangent of the maximum slope angle was estimated to be 1:3.5 .

### **6.5.2 Sea side slope angles of original dam profile**

In this study, the total Feni dam is divided into three sections:

- The main dam,
- the right flank embankment, connecting the main dam to the regulator at the west side and
- the left flank embankment, connecting the main dam to the existing coastal embankments at the east side. For an illustration of this, reference is made to Figure 2 of section 2.1.

#### **Main dam**

First the slope was divided into two parts; above and below the crest level of the Winter Spring Tide Dam at 6.46 m. + PWD. For construction and maintenance purposes, the lower slope angle was chosen to be 1:4. The upper slope angle was reduced to 1:6 in order to decrease the wave run-up.

#### **Right flank embankment**

For the mayor part of the right flank embankment, parallel to the outlet channel (see Figure 2, section 2.1), the wave impact was assumed to be reduced, as its dam axis is almost perpendicular to the governing wave fronts. This is why steeper slopes were applied than for the main dam. The tangent of the chosen slope angle for the right flank embankment is 1:4, which is less than the maximum slope angle, which was thought to be geotechnically permissible. The part of this embankment, adjacent to the regulator is severely attacked by waves. The slope protection of this part was determined to be equal to the main dam.

#### **Left flank embankment**

The slope angle of the left flank embankment was determined to be equal to the slope angle of the main dam, because this part of the dam is lying in one line with the main dam axis.

### **6.5.3 Crest levels of the original dam design**

In this section it is described what was the original method used to derive the crest levels. With regard to the original design criterion, the wave run-up was calculated. This procedure is explained in Section 6.5.3.1. After estimating the geotechnical settlement in Section 6.5.3.2 the original determination of the crest levels is given in Section 6.5.3.3.

#### **6.5.3.1 Wave run-up for the main dam**

The crest level of the main dam was determined following the overtopping criterion. For the chosen upper slope angle at the sea side and for a situation with a return period of 50 years the run-up, which would be exceeded by 2% of the waves, was calculated. For this calculation a formula was applied, which was generally used in 1983.

This formula reads:

$$z_{2\%} = 8 * f * H_{sig} * \tan \alpha * \cos \beta$$

in which:

$z_{2\%}$	= wave run-up exceeded by 2% of the waves	[ m ]
$f$	= friction coefficient, which was determined to be 0.95 for concrete blocks.	[ - ]
$H_{sig}$	= significant wave height at the foot of the dam slope	[ m ]
$\alpha$	= upper slope angle	[ ° ]
$\beta$	= angle between the wave fronts and the dam axis.	[ ° ]

When the necessary parameters are introduced in the formula, the run-up can be determined.

$$z_{2\%} = 8 * 0.95 * 1.7 * \frac{1}{6} * \cos 30^\circ = 1.86 \text{ m.}$$

In ref. [3] it is pointed out that the run-up may turn out to be higher in reality. Nevertheless, a higher percentage of overtopping waves can be accepted, because of the facts that the dam crest is paved, the major part of the slopes is covered by revetments, the application of gentle slopes and the fact that the damage to the hinterland (i.e. reservoir) due to wave overtopping is relatively small.

#### 6.5.3.2 Geotechnical settlement and long term sea level rise

For the main dam and the flank embankments, settlements in the sub soil and dam body of 0.3 to 0.5 meters were calculated. Due to a relatively short consolidation period, the major part of this settlement would develop during the construction stage. As mentioned in Section 3.5, the mean sea level will probably rise in the following decennia, caused by CO<sub>2</sub> warming. In the original design however, this effect was not taken into account.

#### 6.5.3.3 Applied crest levels

##### Main dam

The crest level of the main dam was derived by adding the wave run-up and the geotechnical settlement to the design still water level. For the considered return period of 50 years, the SWL was 8.06 m. + SOB = 8.52 m. + PWD, which can be seen from Table 4 of Section 6.3. The crest level was thus determined to be 8.06 m. + SOB + 1.86 m. + 0.5 m. = 10.42 m. + SOB ≈ 10.5 m. + SOB = 10.96 m. + PWD.

##### Flank embankments

For the main part of the right flank embankment the wave run-up was assumed to be reduced dramatically, because its dam axis is almost perpendicular to the governing wave fronts ( $\beta \approx 80^\circ$  à  $90^\circ$ ). Consequently the crest level was chosen lower than the main dam. As the left flank embankment is connected to the embankment of the neighbouring polder, the crest level of this embankment had to be regarded.

Both crest levels were chosen equal to the regulator crest. In this way the crest levels of both flank embankments were determined to be at 9.46 m. + PWD including geotechnical settlement. Compared to the main dam crest level this meant a difference of 1.5 meters.

## **6.6 ORIGINAL DESIGN OF THE SEA SIDE SLOPE PROTECTION**

In this section it is described how the slope protection was originally designed. In Section 6.6.1 the slope protection principle is described for the main dam and both flank embankments. Subsequently in Section 6.6.2 the method used to calculate the required block sizes is given.

### **6.6.1 Slope protection principle**

#### **Main dam**

Except for the winter spring tide dam, a clay layer having a thickness of 0.6 meter was put on the core of silty sand. Then the whole slope was covered with a filter fabric on top of which a filter layer was placed having a thickness of 0.10 meter and consisting of chipped bricks. The cover layer of the sea side slope protection was determined to consist of placed blocks. Between the levels 5.46 m. and 9.46 m.

+ PWD concrete blocks with aggregates made from crushed boulders were applied, having a specific density of 2250 kg/m<sup>3</sup>. Here the wave attack was assumed to be relatively high. For the slope above 9.46 m. + PWD and beneath 5.46 m. + PWD to a level of 2.46 m. + PWD concrete blocks with chipped bricks as an aggregate were applied, having a specific density of 1850 kg/m<sup>3</sup>.

#### **Left flank embankment**

Like the main dam, the slope protection of the left flank embankment consists of placed blocks on chipped bricks on filter fabric on clay. Although the text of ref.[3] and its drawings contradict each other about the applied cover layer and the consultant could not recall the reason for it, the revetment is assumed to consist of concrete blocks with brick aggregates.

#### **Right flank embankment**

For the cover layer of the right flank embankment, brick blocks were applied, which are blocks consisting of bricks and mortar in between, having a specific density of 1600 kg/m<sup>3</sup>. This relatively cheap option was preferred here, because the wave attack is relatively moderate. Furthermore, the clay layer and filter fabric were omitted. A fine granular filter was placed instead, underneath the layer of chipped bricks.

### **6.6.2 Calculation of the block sizes**

#### **Main dam**

As there was no accurate theory to estimate block sizes for placed block revetments, the well known Hudson formula was used. Originally, this formula was meant to calculate the necessary block weight for a cover layer, consisting of dumped stones, such as rip-rap.

However, this formula could be adapted to placed block revetments by means of changing the  $K_d$  factor. See following formula. Through model research, a  $K_d$  factor of 8.0 was advised in order to use the Hudson Formula to calculate the necessary block weight for placed block revetments. The Hudson formula reads:

$$G = \frac{\rho_{\text{block}} * g}{\Delta^3 * K_d} * H_{\text{sig}}^3 * \tan\alpha, \quad \Delta = \frac{\rho_{\text{block}} - \rho_{\text{seawater}}}{\rho_{\text{seawater}}}$$

in which:

$G$	= weight of the blocks	[ N ]
$g$	= acceleration of gravity,	[ m/s <sup>2</sup> ]
$\rho_{\text{block}}$	= specific density of the blocks	[ kg/m <sup>3</sup> ]
$\rho_{\text{sea water}}$	= specific density of water	[ kg/m <sup>3</sup> ]
$K_d$	= coefficient depending on the material used	[ - ]
$H_{\text{sig}}$	= significant wave height	[ m ]
$\alpha$	= slope angle for the upper slope	[ ° ]

The following values were introduced:

$g$	= 9.81 m/s <sup>2</sup> ,
$\rho_b$	= 2250 kg/m <sup>3</sup> for concrete with gravel aggregates
$\rho_w$	= 1016 kg/m <sup>3</sup>
$K_d$	= 8 for placed blocks
$H_{\text{sig}}$	= 1.7 m.
$\tan \alpha$	= 1/6

$G$  turned out to be 1260 N. The used relationship between the block thickness and the rib size was thought to be  $\frac{1}{2} - \frac{1}{3}$  for practical purposes. You may call this sound engineering judgement. For the chosen thickness of 0.25 meter square blocks having a rib size of 0.50 meter fulfilled the requirement ( $G = 1380$  N).

#### Right flank embankment

For this dam section the same block sizes as for the main dam were applied. Brick blocks were used for the part parallel to the outlet channel and concrete with gravel aggregates for the part adjacent to the regulator. The latter part of the right flank embankment was determined to have the same slope protection as the main dam.

#### Left flank embankment

The applied block size for this dam section was determined to be the same as for the main dam (0.50 m \* 0.50 m \* 0.25 m). The block material was assumed to be concrete made with brick aggregates.

## **7 REDESIGN OF FENI RIVER CLOSURE DAM**

### **7.1 DESIGN CRITERIA**

#### **7.1.1 Introduction**

In this section the design criteria used for the redesign are drawn up. For the present study the distinction between monsoon and cyclone conditions was made. These conditions are clearly defined in Section 7.1.2. Two types of design criteria were considered; criteria for overtopping and criteria for the slope protection. In section 7.1.3 the design criteria for overtopping and in 7.1.4 the design criteria to be imposed to the slope protection are given.

#### **7.1.2 Distinction between monsoon and cyclone conditions**

For the present study the distinction was made between monsoon and cyclone conditions, because these conditions have a different character. The annual extremes during monsoon conditions are caused by long term wind set-up. The monsoon winds in a monsoon storm are mainly directed north and they will generally prevail for several days. This will cause extreme storm surges near the Feni dam during several successive tides. During cyclone conditions however, the extreme water levels are caused by an air pressure drop and high wind velocities which are present for only several hours. A cyclonic storm surge will generally cause extreme high water levels during only one period of high tide.

These differences merit the use of different design criteria. In this study the definitions used for monsoon and cyclonic conditions are given below.

##### **Cyclonic conditions**

These conditions were defined to occur, when a cyclone is crossing the Bangladeshi coast. These extreme hydraulic situations near the Feni dam are supposed to correspond to a different probability distribution than situations caused by other weather conditions.

##### **Monsoon conditions**

These conditions were defined as weather conditions, during periods when no cyclones are crossing the Bangladeshi coast. The maximum water levels during these conditions are mainly caused by monsoon weather systems having a lower intensity than cyclonic storms.

#### **7.1.3 Design criteria for overtopping**

The design criteria for overtopping determine the geometric dam profile, which includes the crest levels and the slope angles. In order to draw up the criteria for overtopping, the locations of the various embankments in the area near the Feni dam were analyzed first. This is done in Section 7.1.3.1. The overtopping criteria were divided into two different criteria, concerning monsoon and cyclone conditions. In Section 7.1.3.2 the monsoon criteria for overtopping are defined and in Section 7.1.3.3 the overtopping criteria for cyclone conditions are treated.

### 7.1.3.1 Polder system

For the definitions of the overtopping criteria the volume of sea water, which flows into the Feni reservoir during a storm surge had to be considered. It should be analyzed, whether a part of this sea water had initially overtopped the coastal embankments adjacent to the Feni dam. If this is not the case, the design of the Feni dam could be made independent of the crest levels of the adjacent coastal embankments. For this analysis the polder system near the Feni dam should be studied. The polder system is the location of the various coastal and polder embankments in the area. In the south-eastern part of Bangladesh, land used for irrigation purposes is divided into separate polders. For a situation sketch Figure 7 is referred to.

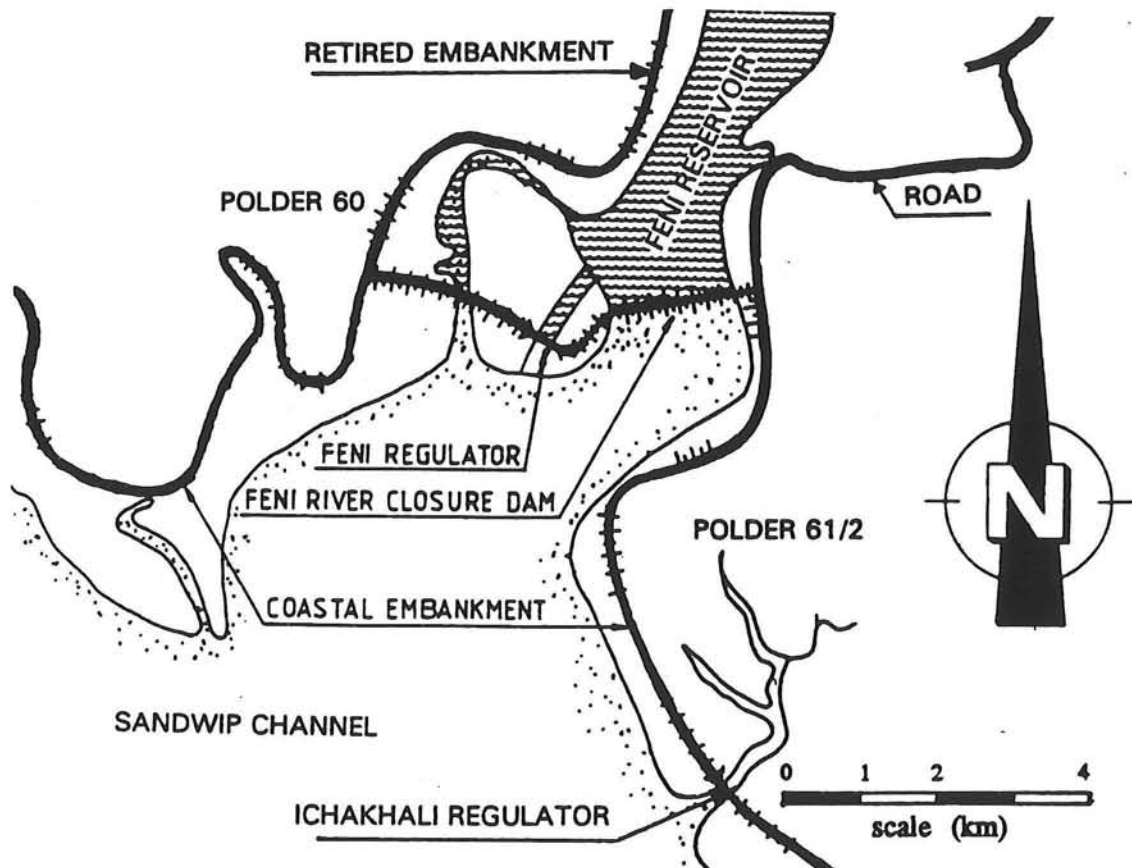


Figure 7: Polder system

The Feni reservoir borders on polder 60 at the western side. When a huge amount of water overtops the coastal embankment of this polder, the retired embankment between this polder and the reservoir is assumed to prevent this overtopped sea water from flowing into the reservoir. At the eastern side, the reservoir borders on polder 61/2, separated by a road. Local inspection resulted in the opinion, that the road leading to the Feni dam serves as an embankment. During an extreme high water period, this road is thought to avoid that sea water, that overtopped the coastal embankment of polder 61/2, will flow into the Feni reservoir. After the high water period, this polder is assumed to be drained by means of the Ichakhali regulator.

Accordingly, it was assumed, that the Feni reservoir will not be affected by water that overtopped the neighbouring coastal embankments. The Feni reservoir can be considered as a separate polder. For this reason the design of the Feni dam could be made independent of the crest levels of the adjacent coastal embankments.



### **7.1.3.2 Monsoon criterion for overtopping of the Feni dam**

In Bangladesh no design criteria for hydraulic structures are imposed by the government. The design criterion for monsoon conditions was decided to be chosen more or less arbitrarily. The design criterion used as a basis for the original design was adapted for monsoon conditions. The monsoon design criterion for overtopping has thus been defined as follows:

For a monsoon situation having a return period of 50 years only 2% of the waves may overtop the Feni River Closure Dam.

The mentioned 50 years return period was taken into account to enable a decent comparison with the original design.

For comparison only, the cyclone criteria imposed to the coastal embankments, which are subject to the Cyclone Protection Project II, are given below. See ref. [5]. This project aims to design coastal embankments for the parts of the Bangladeshi coast which were severely damaged during the killer cyclone of 1991. The used monsoon criterion for overtopping was that less than 13% of the waves may overtop the structure for a situation having a return period of 5 years. This criterion was considered to be very gentle and was chosen arbitrarily. There are no indications that these criteria were imposed by the Bangladeshi government. Because of these considerations and because of the assumption that the Feni dam could be designed independent of the profiles of the adjacent coastal embankments, this overtopping criterion is neglected.

The afore mentioned monsoon criterion to be imposed to the Feni dam was thought to be more reasonable.

### **7.1.3.3 Cyclone criterion for overtopping of the Feni dam**

In Bangladesh the design philosophy with respect to wave overtopping during cyclonic storms is generally based on the thought that a reasonable amount of water may overtop a coastal embankment. One possibility to define the cyclone criteria is to choose the return periods for certain overtopping situations arbitrarily, like the monsoon overtopping criterion. The other possibility, which was applied here, is to derive the dam crest levels and slope angles, that yield the most economic dam profile during cyclone conditions. For this procedure the Bangladeshi guidelines (ref. [15]) were followed to a certain extent. These guidelines should be applied to all projects carried out in the scope of the Flood Action Plan, set up by the Bangladeshi government following the disastrous floods of 1987 and 1988. In accordance with these guidelines, the economic feasibility of the FAP projects should be demonstrated. One manner to do so is to calculate the Net Present Value, which indicates the economic feasibility. The higher the NPV, the higher the economic feasibility. The definition of the NPV is described in Section 7.5.3. In this study this NPV is optimized by varying the slope angles and crest levels of the dam. The profile that yields the highest NPV was thought to be the most economic profile during cyclone conditions. If this geometric profile would meet the monsoon criterion as well, this profile would be chosen for the redesign.

Again the cyclone criteria imposed to the coastal embankments, which are subject to the Cyclone Protection Project II, are given below for comparison only, . See ref. [5]. The return periods of cyclonic storm design conditions in this study have been set to:

- (a) 20 years, where flooding due to wave overtopping of the sea facing embankment should not result in an average water depth in the polder exceeding 1.0 m.
- (b) 40 years, where the crest level should not be lower than the still water level.

It is emphasized that these criteria were chosen arbitrarily and that there are no indications that these criteria were imposed by the Bangladeshi government.

#### **7.1.4 Design criterion for the slope protection**

In order to define the design criterion for the slope protection, first the repair philosophy will be analyzed. The following considerations were made:

- When the slope protection is damaged due to a cyclonic storm, this damage is assumed to be repaired directly after the passage of the cyclone. This is very important, when the cyclone damage occurs in the pre-monsoon. Subsequent monsoon storms could possibly extend the damage, which will ultimately lead to failure of the dam; a dam breach. Due to the relatively smooth weather conditions after a cyclone, repair of damage is thought to be easier than during monsoon weather conditions.
- The duration of a cyclonic weather situation will generally be smaller than the duration of a monsoon storm. For cyclonic storms, the duration of the maximum wind speed and thus the extreme wave climate is relatively short. Accordingly, initial damage of the slope protection will ultimately affect a larger part of the slope revetment during monsoon storms than during cyclonic storms.

For the design criterion for the slope protection, the governing situation was thought to be the monsoon situation. During this weather condition, the slope protection was designed to be stable for a situation having a return period of 50 years. This is the same return period as used for the original design, to enable a decent comparison with the original design.

## 7.2 ACCRETION PROCESS IN FRONT OF THE DAM

In the course of the years an extensive landmass has accreted downstream of the Feni River Closure Dam. In a study by D.M. Barua (ref. [6]) the accretion was concluded to develop exponentially in time, according to the following formula:

$$h_t = h_0 * e^{-q * (t - t_0)}$$

in which:

$t - t_0$	= time after closure	[ years ]
$h_0$	= initial water depth before closure for high water spring (HWS)	[ m ]
$h_t$	= water depth after a period t for HWS	[ m ]
q	= a coefficient	[ - ]

This relation could more or less be demonstrated by the surveys, carried out downstream of the Feni dam. The bathymetry downstream of the Feni dam was surveyed in the following months:

- March 1982. This was considered to be the bathymetry before the time of the closure.
- March 1986, 1987 and 1988. This is respectively approximately one, two and three years after closure.

As an illustration the observed elevation of the fore shore as a function of time is given in the following Figure 8 for a point in a gully and a point on a tidal flat, according to ref. [6]. For the location of the points and the present accretion, reference is made to Figure 9.

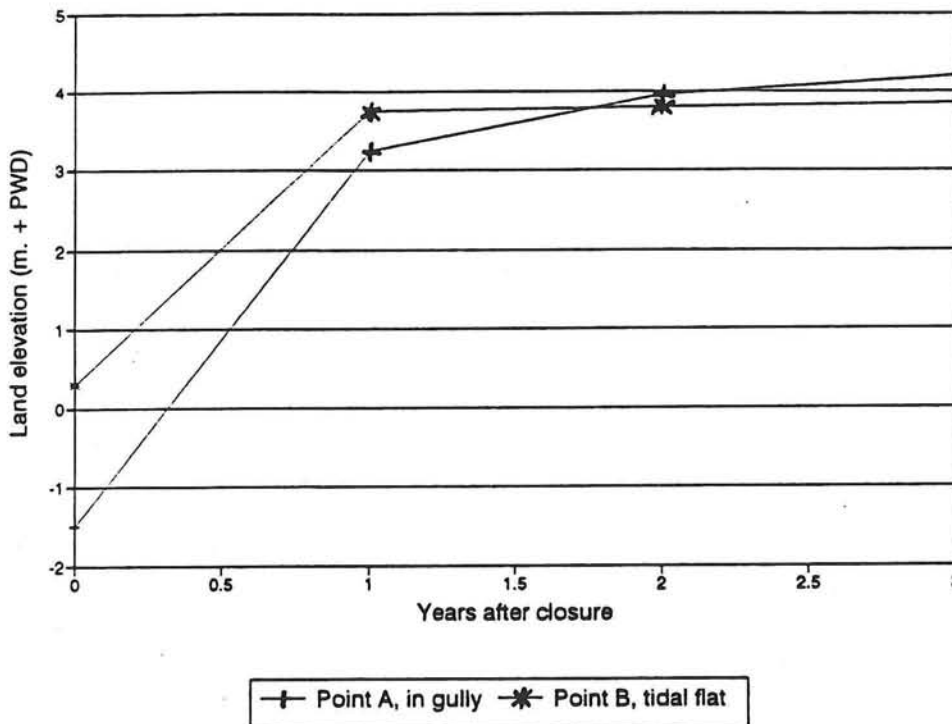
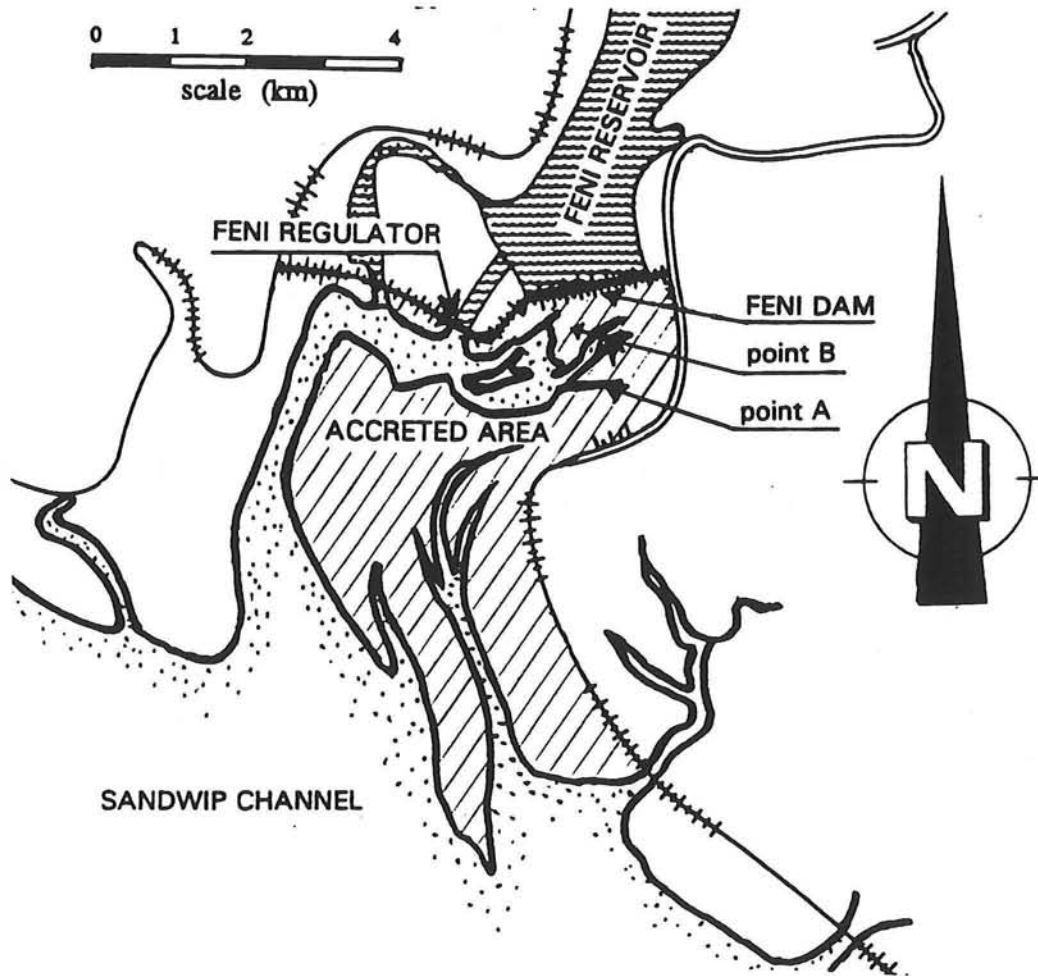


Figure 8: Observed land elevation in front of the Feni dam related to the time after closure.



**Figure 9:** Present accretion downstream of Feni dam

It was assumed, that the elevation of the fore shore downstream of the Feni dam will affect the wave climate. By the reduction of the water depths more waves are likely to break. This will result in a lower significant wave height which subsequently was thought to result in a more economical design.

Since 1983 a lot of research has been carried out with the objective to describe morphological processes. Until now, it is not possible to anticipate the accretion speed in front of a hydraulic structure accurately. Only rough estimations can be made by analyzing similar situations in the same region. Numerical models to describe morphological processes are in the developing stage at this moment. The result of models are only indicative.

For the design of the cross-section of the Feni dam, two cases were considered. First of course, the original situation, for which no accretion influence was taken into account. Secondly, the case, when the accretion speed could have been anticipated accurately, using a hypothetical method, which was not available at the actual time the design was originally made. For the second case, accretion figures after the closure were used, which were obtained from ref. [7].

## 7.3 WATER LEVELS

### 7.3.1 Introduction

As a hydraulic boundary condition for the redesign, the probability distributions should be derived for the water levels near the Feni River Closure Dam. In contrast with the original design, the distinction between monsoon and cyclone conditions was made for this.

First the water level distribution for monsoon conditions was derived in Section 7.3.2.

Subsequently, the probability distribution for cyclone conditions was estimated. As the available gauge readings comprise a period which is too short, this was done by means of a numerical storm surge model. This method is described in Section 7.3.3.

The extent of the accretion area near the dam is small in relation to the tidal wave length.

Accordingly, changes of the bathymetry in the course of the years were assumed not to influence the water level distributions.

### 7.3.2 Probability distribution for monsoon conditions

Because the distinction between cyclonic and monsoon conditions was made, the probability distribution for the water level had to be calculated for both circumstances. This is done in this section for monsoon conditions. In order to analyze, whether the distribution used for the original design is reliable, the probability distribution was derived for water levels at Sonapur station in Section 7.3.2.1. This is a gauge station nearby the gauge station Azimpur, which was used for the original design. For the locations of these gauge stations, reference is made to Figure 10. Finally, the monsoon probability distribution was derived in Section 7.3.2.2 by omitting the cyclonic surges, occurring in the annual extremes.

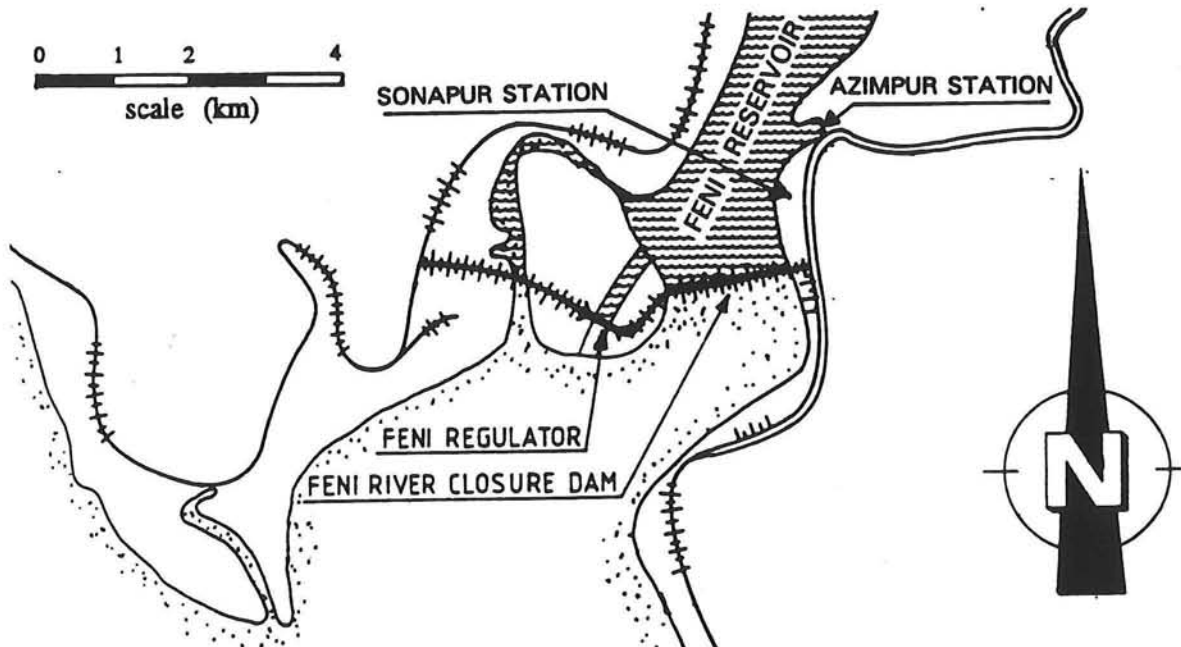


Figure 10: Locations of gauge stations near the Feni dam.

### 7.3.2.1 General probability distribution for Sonapur station

The gauge station Sonapur is located at the reservoir side of the Feni dam, close to Azimpur station, whose observations were used as a basis for the original design. In order to analyze, whether the water level readings of Azimpur station are reliable, the probability distribution at Sonapur station was derived. The water level readings at Azimpur station were thought to be reliable when its probability distribution would more or less correspond to the distribution of Sonapur station, because of the small distance between the two stations.

Records of Sonapur station were obtained from the BWDB in Dhaka. After the closure of the Feni estuarium, water levels near this station have not been influenced by the tide any more and this is why the water levels after the closure date have not been used.

After analyzing the data, 11 years of record were used for the distribution analysis. The description of the derivation of the probability distribution for Sonapur station is given in Chapter 1 of Annex A. Finally the water levels for the different return periods could be calculated. It is emphasized that in this stage no attention was paid to the question whether cyclonic surges are present in the used annual extreme water levels. In this way it is possible to compare the probability distribution for Sonapur station with the one used for the original design. For this, see Table 5.

Return periods (years)	2.33	5	10	20	25	50	100
Water level at Sonapur (m. + PWD)	6.28	6.92	7.43	7.92	8.08	8.56	9.04
Water level of orig. design at Azimpur (m. + PWD)	6.48	7.05	7.51	7.95	8.08	8.52	8.94

**Table 5:** Water levels for return periods using the theoretical distribution for Sonapur compared with the ones used on the original design. In meters above PWD.

When the results are considered, the correspondence of the two distributions is clear. However, the accuracy of the used theoretical distributions was considered to be rather small. Nevertheless, it could be concluded, that the readings of Azimpur station are rather reliable, because the originally used distribution corresponds well to the probability distribution derived for Sonapur station. As a result, the water level readings of Azimpur station will be used for the redesign. Based on these data, a probability distribution for monsoon conditions will be derived in the next section.

### 7.3.2.2 Probability distribution for Azimpur station during monsoon conditions

For the determination of the probability distribution during monsoon conditions, the cyclonic surges had to be filtered out of the used records. In order to do so, first the cyclones occurring during the period of observation were analyzed. This was done using the cyclone records obtained from the Bangladesh Meteorological Department. During each month in which a cyclone hits the coast of Bangladesh, it has been analyzed, whether the concerned monthly extreme is equal to the annual extreme as well.

After studying the cyclones, two cyclonic surges appeared in the annual extremes: the cyclone of May 1961 and the cyclone of October 1966. For the concerned two years the annual extremes were determined once again without taking the months into account, that contain the cyclonic surges.

From these newly obtained annual extremes a probability distribution for monsoon conditions was derived. See chapter 2 of Annex A for more computational details. Finally the water levels for various return periods are given in Table 6.

Return periods (years)	2.33	5	10	20	25	50	100
Water level (m. + PWD)	6.21	6.62	6.95	7.27	7.37	7.69	8.00

**Table 6:** Water levels for return periods during monsoon conditions for Azimpur station.

As explained in Annex A, the observed extreme water levels do not exactly correspond to the theoretical Gumbel distribution. The inaccuracy turned out to be considerable. This is due to the fact that the number of years of observation is very small.

### 7.3.3 Probability distribution for cyclone conditions

#### 7.3.3.1 Methodology

In this section the methodology is described how the probability distribution for cyclone conditions was derived. Because of the following reasons it turned out to be rather unreliable to derive this distribution just by analyzing the gauge readings in the area.

First the available water level readings near the Feni dam comprise only 10 years, in which only 2 cyclonic surges appear. See section 7.3.2.2. This period is too short to achieve a probability distribution which is sufficiently reliable.

Secondly, it is doubtful whether the gauge was read accurately by the time the cyclone passed the gauge station. Furthermore, the measuring device could have been damaged or destroyed by the cyclonic winds.

Contrary to the gauge readings, meteorological information on historic cyclones that crossed the Bangladeshi coast is sufficiently available. Information on cyclone properties have been collected from the 19th century onwards by the Bangladesh Meteorological Department. Especially in the last decennia the accuracy of this information is considerable, because of the introduction of data collection from satellite pictures.

It was thus decided to use a numerical storm surge model, by means of which the hydraulic situation could be simulated during cyclones using the meteorological information. For this purpose the program Duchess was used.

Duchess is a numerical computer program intended to perform two-dimensional tidal and storm surge computations. This program is based on a finite difference approximation of the two-dimensional shallow water equations. For a grid comprising the model area, among others the bottom depths, wind velocities and bottom friction values have to be introduced. The model is capable to calculate the hydraulic situation in each grid point at certain time intervals. For an explanation of this program, provided by the Faculty of Civil Engineering of Delft University of Technology, reference is made to Duchess user manual (ref. [8]).

First the model was set-up as described in Annex B. In order to achieve reliable results, which represents reality well, the model should be calibrated. This procedure is explained in Annex C. In Section 7.3.3.2 the results of the calibration are given. Here it is described that the model could only be calibrated for Chittagong, a city located south of the Feni dam. See Figure 5 of Chapter 4.

In the following Section 7.3.3.3 the derivation of the probability distribution for Chittagong using the numerical model is given. Finally, in Section 7.3.3.4 it is briefly described how the probability distribution for the Feni dam could be derived.

### 7.3.3.2 Results of the calibration of the model complex

In Annex C the calibration results of the model complex are given. Here it was determined, that the calibrated model is only valid for cyclones crossing the coast of the lower Meghna estuary. This was done, because the model appeared not to be able to generate water levels in the northern part of the lower Meghna estuary, which correspond to reality, when cyclones are crossing the Bangladeshi coast relatively far away from the dam.

Furthermore, it turned out to be impossible to simulate reality well in the area near the Feni dam, where the hydraulic situation is very complex. It was concluded that the model could not be calibrated for the area close to the Feni dam. This is probably caused by the fact that the present model has a mesh size which is too large for a good simulation in this region. Here a mesh refinement is needed, which could be introduced in the model by means of a so-called nest. Such a nest would comprise a smaller model area with a smaller mesh size, that uses the results of the general model as a boundary condition. Due to the limited time available for this study, it is impossible to construct this nested model for this study.

After calibration, the ultimate model is assumed to be able to represent the water level near Chittagong well, this is to say, only for cyclones that cross the lower Meghna estuary. For the location of Chittagong, reference is made to Figure 5 Section 4.3. Reference is made to Annex C for a more detailed explanation of the calibration procedure.

### 7.3.3.3 Derivation of probability distribution for Chittagong

As mentioned in the former section, the model is able to reproduce reliable extreme water levels near Chittagong. In this section it is briefly explained how a probability distribution was derived for cyclonic water levels near Chittagong. The idea was to construct several synthetic boundary conditions for the model using the meteorological cyclone record from the year 1900 onwards. By running the model for these boundary conditions, the maximum water levels near Chittagong could be computed. As the probability of occurrence could be estimated for every synthetic situation from history, the probabilities of exceedance of the computed maximum water levels near Chittagong could be derived as well. First the various synthetic situations had to be generated. In Annex D it is described how the various boundary conditions were derived. After running the Duchess model for these situations, the extreme water levels could be derived. Finally, the probability distribution for the water level near Chittagong could be obtained from these results as explained in Annex D. The resulting water levels for the various return periods are given by Table 7.

Return period (years)	5	10	20	25	50	100	200
Water level (m)	3.55	4.82	6.04	6.42	7.61	8.79	9.97

**Table 7:** Water levels for various return periods for Chittagong during cyclone conditions.



### 7.3.3.4 Derivation of probability distribution for the Feni Dam

From the probability distributions during monsoon conditions near Chittagong and the Feni dam, a relation could be derived between the water levels at the two locations. The resulting water levels near the Feni dam using this relation are given in Table 8 for various return periods, as explained in Annex D.

Return period (years)	5	10	20	25	50	100
Water level (m. + PWD) Cyclone conditions Feni dam, derived from monsoon relation	6.25	7.56	8.81	9.20	10.44	11.65

**Table 8:** Water levels for various return periods for the Feni dam during cyclone conditions, derived from the monsoon relation between Chittagong and the Feni dam.

The monsoon relation can be queried however. When the water level rises higher than the crest level of the coastal embankments, land will be flooded. Caused by the topography, which is more mountainous near Chittagong than near the Feni dam, relatively more land will be flooded near the Feni dam. Probably, this will result in a lower water level near the Feni dam than calculated from the monsoon relation between the two locations.

For an estimation of the water level reduction because of the inundation of the hinterland, the Duchess model cannot be used, because this numerical model could not be calibrated in the concerned area. Furthermore, it is doubted whether the hydraulic situation near the embankments can be simulated accurately in Duchess. For these embankments behave like free fall weirs during the overtopping period.

In order to estimate the water level reduction, the hydraulic situation near the Feni dam was schematized very roughly. The water level reduction was calculated by means of estimating the loss of water, caused by overtopping of the coastal embankments near the Feni dam. In Annex D this calculation is given. The resulting water level reductions due to inundation of dry land are a very rough estimation.

In Annex D it is demonstrated that the water level reduction will be smaller in reality than calculated by these schematizations. The water levels which were derived from the monsoon relation can be considered as an upper limit and the reduced water level which were derived by means of the overtopping schematization, can be considered as a lower limit. In reality the extreme water level will be somewhere in between the two values.

For further design purposes the extreme water levels during cyclone conditions near the Feni dam are estimated to be the average of the upper and lower limit. For various return periods, the water level values are given in Table 9.

Return period (years)	10	20	25	40	50	100
<b>A:</b> Water level (m + PWD) cyclone conditions Feni dam derived from monsoon relation.	7.56	8.81	9.20	10.02	10.44	11.65
<b>B:</b> Water level (m + PWD) cyclone conditions Feni dam after overestimated reduction due to inundation.	7.56	8.55	8.71	8.96	9.06	9.33
<b>(A+B)/2:</b> Water level (m + PWD) cyclone conditions Feni dam used for further design.	7.56	8.68	8.96	9.50	9.75	10.49

**Table 9:** Derivation of the water levels for cyclone conditions, used as a basis for the redesign, for various return periods.

## 7.4 WAVE CLIMATE

### 7.4.1 Methodology

Here, the distinction between monsoon and cyclonic conditions had to be made again for the short waves. As wave observations near the Feni River Closure Dam have never been carried out, other means to determine the wave climate at this location had to be found. The faculty of Civil Engineering of Delft University of Technology, provided a computer program which enables to set-up a stationary two dimensional numerical model to estimate the wave climate in shallow water. For this numerical wave hindcast model the bathymetry has to be introduced for a defined grid, comprising the model area. At each grid point the wave parameters can be derived. By refining the grid, the computations can be made more accurate. This program, called HISWA, was used to determine the wave climate near the Feni Dam. For an explanation of Hiswa, reference is made to the Hiswa user manual (ref. [9]). The model set-up is described in Annex E.

In Section 7.4.2 the limitations of Hiswa are drawn up. The main restriction of the model was the fact that the model could not be calibrated, because wave observations have never been carried out near the Feni dam. Due to these limitations, the reality could not be simulated accurately. In order to cope with this problem the design wave characteristics were obtained by overestimating the input parameters a little bit.

First a distinction between the wave sources was made in Section 7.4.3. In Section 7.4.4 the wave conditions caused by swell at the ocean is assessed by means of Hiswa model runs. Waves near the Feni dam caused by the second wave source, local winds, is described in the subsequent sections. The assessment of wave conditions is given in Section 7.4.5 for monsoon winds and in Section 7.4.6 for cyclonic winds.

### 7.4.2 Limitations of Hiswa

A few limitations are encountered when Hiswa is used. These limitations cause schematizations of reality and thus these will result in an error. The most important limitations are drawn up below:

- Hiswa is a stationary model. The model assumes a water level and boundary conditions, which are constant in time. For the reproduction of waves caused by cyclonic winds, this implies a considerable error.
- Hiswa assumes a fetch limited growth, which means that a wind field is prevailing for a relatively long time, which implies that the wave growth will only be limited by the fetch length. The minimum duration of a certain wind field which is necessary to establish a fetch limited growth has to be estimated.
- Hiswa is not capable to represent a wave situation well, whose energy distribution is comprising two peaks. Knowing this, the situations which result in the two different peaks, have to be analyzed separately.
- Moreover the model cannot be calibrated, because wave observations are not available in the lower Meghna estuary. As a result, the default values of the Hiswa program had to be used.

Accordingly, the results are thought to be rather inaccurate and can only serve as a first estimation of the wave conditions in the area. Yet, as no other means are available to derive the wave conditions, this model was used for design purposes. By introducing parameters, that are a little bit overestimated, the design wave conditions could be derived.

### 7.4.3 General distinction between wave sources

In general, short waves near the dam can be divided into two sources.

- Waves generated by oceanic depressions at the Indian Ocean in deep water. This is also called swell. These waves have a particular wave period of about 12 seconds and travel through the Bay of Bengal and arrive via the Hatia and Sandwip Channel at the dam site. (see Figure 1 of Chapter 2)
- Waves generated by local wind fields in the model area, either during monsoon or cyclone conditions. Generally these waves have smaller wave periods that can be estimated to be about 6 seconds.

Because of these two aspects, the energy distribution of the wave climate near the Feni River Closure Dam is thought to incorporate two peaks at different frequencies.

As Hiswa is not capable to represent a wave climate well, whose energy distribution has two peaks, the computation of the wave climate near the Feni dam had to be carried out separately for both situations.

### 7.4.4 Assessment of wave conditions caused by swell

For this situation only waves at the southern model boundary of the model had to be introduced. The wave climate at the southern model boundary is assumed not to be influenced by the bottom. Consequently, the wave climate at this location can be estimated to be more or less the same as the wave climate in the deeper Bay of Bengal, where wave observations are available.

In total 18,294 wave observations were carried out by ships in the Bay of Bengal. Out of these values, the probability distributions for the significant wave heights and wave periods were derived for the Cyclone Protection Project II, as explained in ref. [10]. Only the waves coming from south-eastern to south-western direction were taken into account for this distribution analysis. This is thought to be the governing situation. The used wave observations were based on 12 hours duration. Because of the improbability that waves are observed by ships during cyclones, these wave observations were assumed to represent monsoon conditions. The off-shore wave climate for various return periods is given in Table 10.

Furthermore, a joint probability was assumed for waves coming from the ocean and water levels during monsoon conditions. This was assumed, because of the fact that an extreme water level and an extreme wave height is thought to be caused by the same monsoon weather system with mainly southern winds. The water levels during monsoon conditions were derived for various return periods previously in this study. In the Table 10 these values are given.

Return period (years)	5	10	20	50	100
Offshore significant wave height (m)	7.6	8.2	8.8	9.6	10.2
Offshore significant wave period (sec)	11.7	12.2	12.5	13.1	13.6
Water level near the Feni dam for monsoon conditions (m. + PWD)	6.62	6.95	7.27	7.69	8.00

**Table 10:** Boundary conditions for generation of wave conditions caused by swell, for various return periods.

For each return period which is mentioned in the table the wave characteristics and water level were introduced in Hiswa. After carrying out the computer runs, the results could be drawn up in Table 11.

Return period (years)	5	10	20	50	100
Significant wave height near the dam (m)	0.060	0.064	0.068	0.075	0.079
Significant wave period near the dam (s)	11.7	12.2	12.5	13.1	13.6

**Table 11:** Resulting wave characteristics near the Feni dam, caused by intrusion of swell generated at the ocean.

Although the wave periods almost stay the same, the resulting significant wave heights turned out to have been reduced dramatically when they arrive at the Feni River Closure Dam. This can be explained as follows: The energy of the waves generated at the ocean is reduced through dissipation by friction, breaking etc, when the waves are travelling over an extensive area of relatively shallow water. For the concerned wave frequency, no energy is added by local winds. In the study, the waves generated at the ocean were neglected, because of the small influence.

#### 7.4.5 Assessment of wave conditions during monsoon winds

In this section the wave conditions during monsoon winds are derived. As mentioned before, the input parameters are a little bit overestimated. The two main input parameters, the design wind velocity and the design wind direction are determined in Section 7.4.5.1 and 7.4.5.2. After introducing these input parameters in the Hiswa model and running it, the design wave parameters could be obtained for various return periods in Section 7.4.5.3.

##### 7.4.5.1 Determination of design wind velocity

In order to analyze the wave conditions caused by local monsoon winds, the probability distribution of the wind velocity for various wind directional intervals was required. These wind records were obtained from ref. [11]. However, only 5 years of wind observations are available. The available wind velocity record is given in Table 12.

Average wind speed (m/s)	5	7.5	10	12.5	15	17.5	20	25
Duration (hours per year)	19	120	100	36	10	4	1	0

**Table 12:** Duration and average wind speed as recorded for the years 1981 - 1985 and obtained from ref. [11].

Using these data it was impossible to derive an accurate probability distribution during monsoon conditions for relatively large return periods. So, during monsoon winds a design value had to be introduced in the Hiswa model for the generation of the wave climate. During the considered 5 years, no wind speed of 25 m/s was observed and according to the BMD this value has never been exceeded during observations in monsoon conditions. Thus it was decided to take this wind velocity into account for the redesign, during monsoon conditions.

### 7.4.5.2 Determination of the governing wind direction

In order to derive the design values for the wind generated wave characteristics, the governing wind direction had to be determined. For an arbitrarily chosen wind speed of 20 m/s and a water level of 8.0 meters + PWD the wind direction was varied. The wind direction that yielded the highest wave height was considered to be the governing direction. Table 13 could be derived:

Wind direction (°), south=0°, west=90°	-30	0	15	30	45	60	0
H <sub>sig</sub> (m)	0.84	0.93	0.92	1.07	0.92	0.91	0.52

**Table 13:** Resulting wave heights for various wind directions for a wind velocity of 20 m/s and a water level of 8.0 m. + PWD.

From this it could be concluded that the governing wind direction is 30°, which is more or less south west. From theory this result can be confirmed. When Figure 1 is considered, the fetch length is maximal in this direction. This will generally yield the highest waves, generated by winds, because the wave growth is assumed to be fetch limited.

### 7.4.5.3 Determination of wave parameters during monsoon conditions

Then the wave climate during monsoon conditions could be determined for several return periods at the foot of the main dam. This was done by introducing the water level corresponding to the concerned return period and by keeping the wind velocity and direction equal to the design value. The wave conditions were thought to be sensitive for the accretion process downstream of the Feni dam. In order to analyze the influence of this sedimentation process, four bathymetries were introduced, for the year of closure and 3 years afterwards.

In this way an estimation of the wave characteristics during monsoon conditions could be achieved. The results are given in the Table 14.

Return period (years)	Water level (m+PWD)	years after closure							
		0		1		2		3	
		H <sub>sig</sub>	T <sub>z</sub>	H <sub>sig</sub>	T <sub>z</sub>	H <sub>sig</sub>	T <sub>z</sub>	H <sub>sig</sub>	T <sub>z</sub>
5	6.62	1.18	4.3	0.92	4.4	0.89	4.3	0.86	4.3
10	6.95	1.35	4.6	1.03	4.6	0.99	4.5	0.94	4.6
20	7.27	1.40	4.6	1.12	4.7	1.07	4.6	1.04	4.7
25	7.37	1.40	4.6	1.14	4.7	1.09	4.7	1.07	4.7
50	7.69	1.41	4.6	1.21	4.7	1.16	4.7	1.14	4.7
100	8.00	1.48	4.7	1.28	4.7	1.23	4.7	1.21	4.7

**Table 14:** Results of the derivation of the wave conditions during a monsoon wind of 25 m/s for various return periods and years after closure at the foot of the main dam.

As was to be expected, the significant wave height decreases during the first years after the closure. The situation of 3 years after closure is thought to stay constant hereafter. Moreover it can be seen that the wave period almost stays the same. This parameter is not influenced by the accretion.

#### 7.4.6 Assessment of wave conditions during cyclones

In this section the wave conditions during cyclones are estimated. As Hiswa is a stationary model, the cyclonic wind field should be schematized as a stationary situation as well. Furthermore, the cyclonic situation was schematized as a uniform wind field in order to simplify the computational calculations. These schematizations are dealt with in Section 7.4.6.1. In Section 7.4.6.2 the governing points of landfall of cyclones are determined, which had to be taken into account. In contrast with the derivation of wave conditions during monsoon winds, where one constant wind velocity was introduced for various return periods, the wind velocity during cyclone conditions was estimated for each return period separately. For this purpose the wind velocity probability distribution had to be derived from the historic cyclone record as explained in Section 7.4.6.3. Finally the wave conditions during cyclones resulting from the model runs are given in Section 7.4.6.4.

##### 7.4.6.1 Schematization of cyclones as a stationary and uniform situation

Hiswa is a stationary model which assumes stationary wind fields. This is in contrast to cyclones. These are dynamic weather systems that will result in a variation of the water level, the wind velocity and the wind direction in time. In this section it is described how a cyclone can be schematized as a stationary and uniform wind field.

For the development of the waves, Hiswa assumes a fetch limited growth. This means that the model assumes an unlimited storm duration. In this way the wave growth caused by wind influence is only limited by the fetch length. This is the distance over which energy is added to the waves by means of wind. The minimum duration of a certain wind field to establish a fetch limited growth could be derived from Figure 11, in accordance with ref. [12].

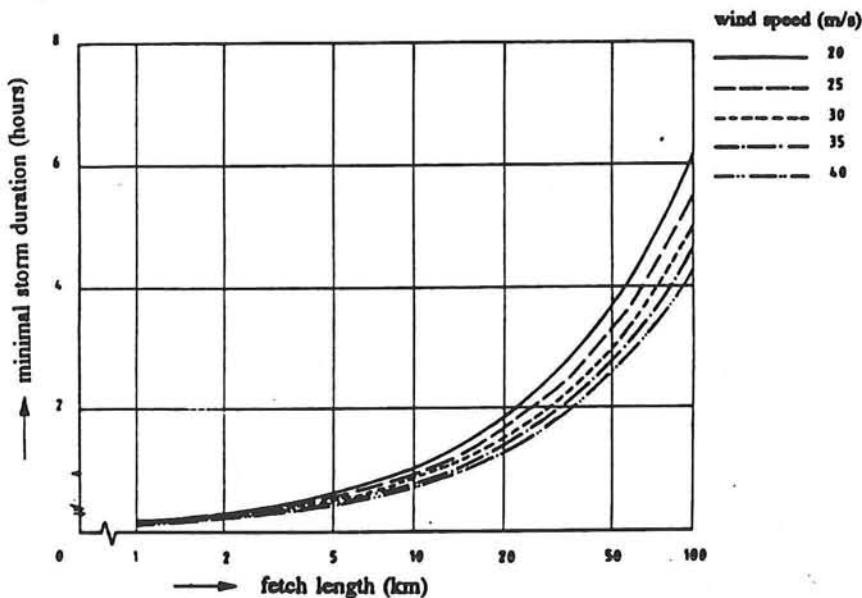


Figure 11: Minimum storm duration to establish a fetch limited growth, according to ref. [12].

For the governing wind direction, which is south west, the fetch length is approximately 20 km. When an average cyclone having a maximum wind velocity of about 40 m/s was considered, the minimum duration for a fetch limited growth was estimated to be about one hour.

The propagation speeds of the 1991 and 1985 cyclones were estimated to be about 25 and 40 km per hour respectively when they reached the coast.

During the minimum time, necessary for a fetch limited growth, the cyclone can thus move over a distance of about 40 km. This movement of the cyclone is relatively small compared to the size of the cyclone, represented by the average radius to maximum wind speed which was estimated to be 65 km. Accordingly, it seems reasonable that the water level, wind speed and wind direction was assumed to be constant during this time like a stationary situation.

Furthermore the cyclone wind field was schematized to be uniform as follows. The wave characteristics near the Feni dam are only influenced by winds over an area whose length is equal to the fetch length. The governing fetch length for the Feni Dam was determined to be about 20 km. This is relatively small compared to the radius to maximum wind speed of an average cyclone, which is about 65 km. This fact makes the assumption reasonable that the real wind field can be schematized as a uniform wind field near the dam and that the water surface can be schematized as a horizontal plane.

#### 7.4.6.2 Determination of governing points of landfall

In reality the cyclone wind field is not uniform. A cyclone is a very deep depression turning in counterclockwise direction at the northern hemisphere, when it is heading for the coast. At a location near the point of landfall, the wind direction will vary during the time that the cyclone is crossing the coast. When a cyclone's point of landfall is located east of the Feni dam, the wind direction will change from east via north to west during this cyclone passage. For a point of landfall west of the Feni dam, the wind direction will change from east via south to west. Thus, when the cyclone is crossing the coast west of the Feni Dam, the wind direction will attain the governing direction, which is south west, for a while. This situation governs the dam design. As a result, only cyclones with a point of landfall located west of the Feni Dam was considered. See Figure 12 for the cyclonic situation which yields the governing wind direction and velocity.

#### 7.4.6.3 Wind velocity probability distribution during cyclonic conditions

As mentioned before, the wind velocity and the water level were assumed to be statistically dependent. For the same return period the water level and the wind velocity during cyclone conditions had to be introduced in the Hiswa model. The probability distribution of the wind velocity during cyclone conditions near the Feni Dam had to be determined for this.

In contrast with monsoon conditions, a probability distribution for the wind velocity during cyclonic conditions can be derived from the historic meteorological records.

As explained in Annex D, the probability of exceedance of the maximum wind speed occurring in a cyclone ( $V_{max}$ ), when this cyclone is crossing the Bangladeshi coast, is determined to be:

$$p \{ V_{max} \geq x \mid \text{cyclone hits Bangladesh} \} = 1 - e^{-e^{-0.027 * x + 2.72}}$$

From the historic record the probability of occurrence of a cyclone hitting the coast of the lower Meghna estuary can be estimated to be about 0.2. As mentioned in section 7.4.6.2, the wind direction will only be south east for some time, when the cyclone is crossing the coast west of the Feni Dam.



The probability of occurrence of a cyclone that crosses the coast in the lower Meghna estuary west of the Feni Dam was estimated to be about 0.5 times the probability of a cyclone crossing the coast of the complete lower Meghna estuary.

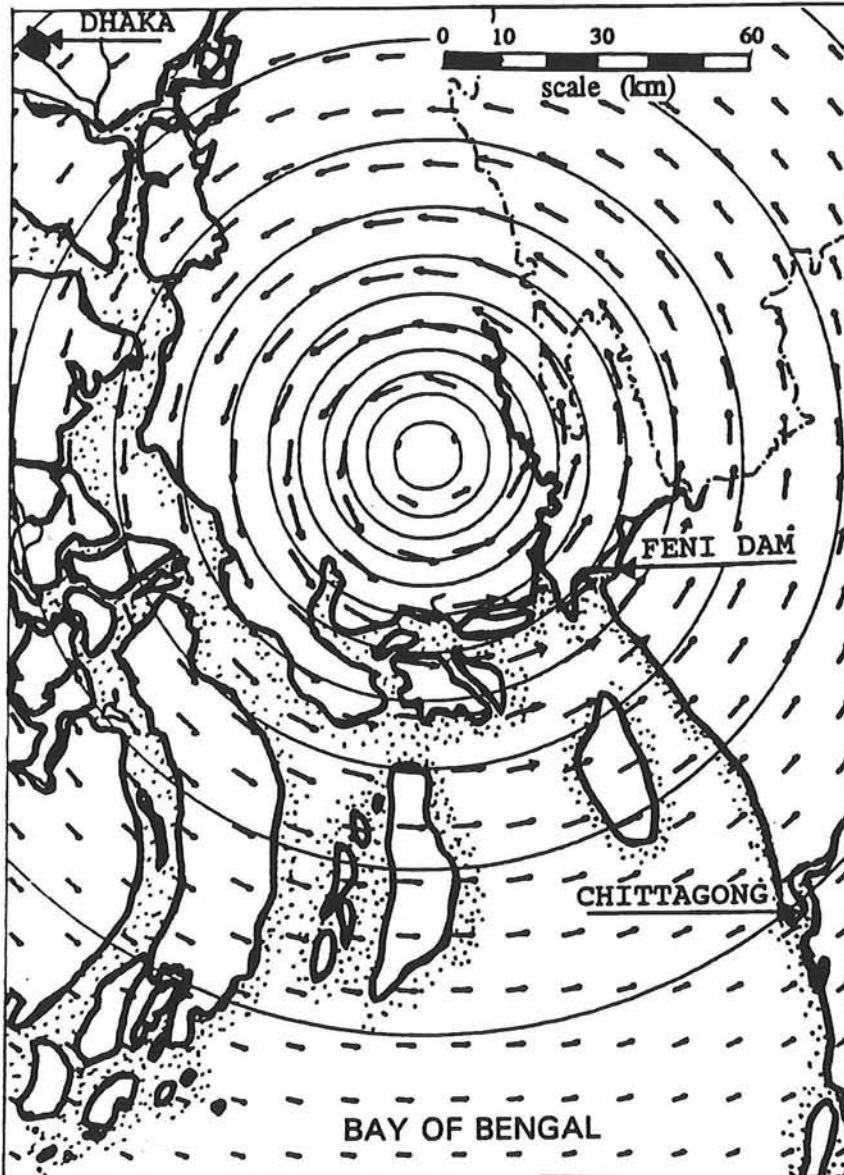


Figure 12: Cyclone situation (isobars and wind velocity vectors), which yields the governing wind direction and wind velocity.

The annual probability of occurrence of a cyclone, occurring in the concerned region and having a maximum wind speed larger than  $x$ , could be described by the following equation:

$$p \{ \text{point of landfall west of dam and } V_{\max} \geq x \} = 0.1 * (1 - e^{-0.027 * x + 2.72})$$

From this equation, the wind velocity for various return periods could be derived. See Table 15.

Return period (years)	20	25	40	50	100
Wind velocity (km/h)	115	126	147	156	184

**Table 15:** Wind velocities near the Feni dam for various return periods, cyclone conditions.

#### 7.4.6.4 Determination of the wave climates for cyclonic conditions

In order to determine the design wave climates near the Feni Dam, some design assumptions were made:

- During the coastal passage of the cyclone the governing wind direction which is south-west prevails for at least one hour in order to establish a fetch limited growth.
- During this complete period, the wind velocity near the Feni dam is equal to the maximum wind speed in the cyclone.

The probability distribution for wind speeds near the Feni dam was thus assumed to be equal to the afore mentioned equation. By means of these assumptions, the resulting wave characteristics were thought to be a little bit overestimated, which will probably result in a relatively save design. For various return periods computer runs were executed using four different bathymetries, corresponding to the various years after the closure. The results are used as a basis for the redesign and are listed in the Table 16.

Return period (years)	Water level (+ pwd)	Years after clo- sure							
		0		1		2		3	
		H <sub>sig</sub>	T <sub>z</sub>	H <sub>sig</sub>	T <sub>z</sub>	H <sub>sig</sub>	T <sub>z</sub>	H <sub>sig</sub>	T <sub>z</sub>
20	8.68	1.84	5.1	1.56	5.1	1.51	5.1	1.49	5.1
25	8.96	1.98	5.4	1.68	5.3	1.63	5.3	1.60	5.3
40	9.50	2.19	6.4	1.93	6.4	1.88	6.4	1.85	6.4
50	9.75	2.26	6.6	2.02	6.6	1.97	6.6	1.94	6.6
100	10.49	2.41	7.9	2.29	7.7	2.25	7.8	2.24	7.8

**Table 16:** Resulting wave characteristics near the Feni dam during cyclone conditions for various return periods and years after closure.

## **7.5 REDESIGN OF GEOMETRIC DAM PROFILE**

### **7.5.1 Introduction**

In this chapter the geometric dam profile is determined. As a starting point, the minimum slope angle is derived for which the dam is thought to be sufficiently stable. When the slope angle would be chosen too large, the slope may become unstable. In Section 7.5.2 the geotechnical macro slope stability is analyzed using the Bishop Simplified Method. Subsequently, the geometric profile is chosen for cyclone conditions using an economic optimization procedure, which is described in Section 7.5.3. In Section 7.5.4 the most economic profile is determined, when no influence of the elevation of the fore shore in front of the dam would be taken into account. In Section 7.5.5 the results of the optimization procedure including the accretion influence are given. In both Section 7.5.4 and 7.5.5 it is checked, whether the chosen dam profile fulfils the monsoon criterion as well.

### **7.5.2 Slope stability analysis**

For the original design, the maximum slope angle was determined without analyzing the macro slope stability for circular failure planes. Since 1983, computer programs to analyze the slope stability have become available.

In order to analyze the slope stability of the sea facing side, a computer program Biseis was used, which is based on the Bishop Simplified Method and which was provided by the consultant Haskoning. By means of this program, the most critical circular failure plane and the accompanying safety factor could be derived for various slope angles. For more information on this method, see ref. [13]. In Section 7.5.2.1 the required safety factors and design conditions are given which are in accordance with the international guidelines. Subsequently the geotechnical parameters which are necessary to perform the Biseis calculations are described in Section 7.5.2.2. Finally, the results of the Biseis computations are given in section 7.5.2.3.

#### **7.5.2.1 Required safety factors and design conditions**

According to international design codes, and to other recent studies in Bangladesh, two situations having different required minimum safety factors were used.

##### **Required safety factor for static loading**

For the static situation, the same loading condition as for the original design was taken into account. This loading condition comprised a filled reservoir ( 5.45 m. + PWD) in conjunction with low tide at the sea side. For this static situation a minimum safety factor of 1.5 is applied, in accordance with the international design codes as mentioned in ref. [16].

##### **Required safety factor for static and dynamic loading**

For this loading condition, a horizontal acceleration, which is caused by earth-quakes, was added to the static situation. This load was introduced in the calculations by means of a seismic coefficient, representing the horizontal acceleration as a part of the acceleration of gravity. In the original design a seismic coefficient of 0.1 was applied.

According to ref. [14], seismic zones were determined in Bangladesh. The area of the Feni dam is located in zone II, for which a seismic coefficient of 0.05 is advised. As the sub layers of the Feni dam are very sensitive for liquefaction, the slope stability was checked, using a seismic coefficient of both 0.05 and 0.1 . The minimum safety factor for these situations was determined to be 1.1, according to the guidelines as mentioned in ref. [16].

### 7.5.2.2 Geotechnical parameters of subsoil and dam body

No detailed information on the geotechnical parameters of the dam body is available. For all these parameters conservative values were introduced in the program Biseis. The geotechnical parameters are given in the Table 17. For the definition of the layers, see Figure 13.

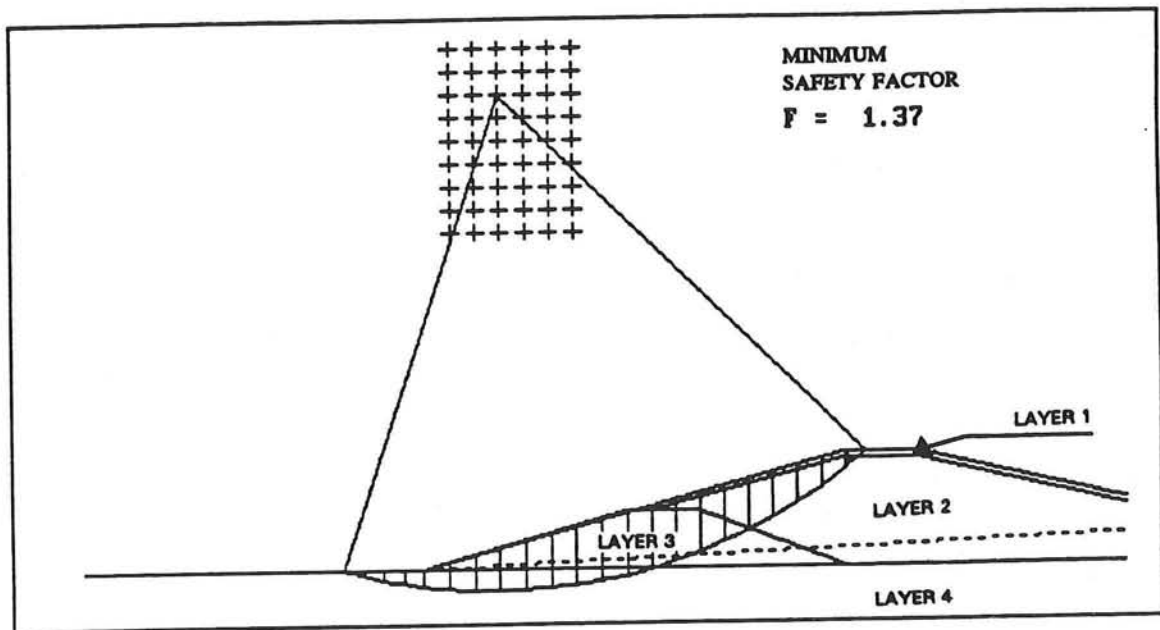


Figure 13: Critical circular failure plane for earth quakes and description of the used layers.

	Layer 1	Layer 2	Layer 3	Layer 4
$\gamma_{dry}$ (KN/m <sup>3</sup> )	16	19	16	19
c (KN/m <sup>2</sup> )	5	0	5	0
$\phi'$ (°)	20	25	20	25

Table 17: The used geotechnical parameters, of the different layers, in which:

$\gamma_{dry}$  = relative weight when the material is dry [ KN/m<sup>3</sup> ]  
 c = cohesion [ KN/m<sup>2</sup> ]  
 $\phi'$  = angle of internal friction [ ° ]

### 7.5.2.3 Results of biseis calculations

The results of the calculation using the Biseis program for a crest level of 10.50 m. + PWD are given in Table 18:

Tangent of slope angle	1 : 4.0		1 : 3.5		1 : 3.0	
Seismic coefficient	0.05	0.10	0.05	0.10	0.05	0.10
Safety factor incl. earthquakes	1.48	1.24	1.37	1.16	1.24	1.08
Safety factor excl. earthquakes	1.82		1.64		1.45	

**Table 18:** Safety factors resulting from Biseis computations.

From these results it could be concluded that for both seismic coefficients a slope having a tangent of 1 : 3.5 is sufficiently stable. A tangent of 1:3 results in safety factors, which do not meet the requirements. A slope angle having a tangent of 1:3.5 is thought to be the maximum possible slope angle at the sea side. This was also concluded in the original design study, where only straight failure planes were considered.

It can thus be concluded that the required slope angles resulting from both methods are equal. It is emphasized that the geotechnical stability analysis in this study was just carried out to check the values obtained in the original design.

### 7.5.3 Optimization procedure of geometric dam profile

In this section the optimization procedure is described, which was applied to derive the most economic dam profile for cyclone conditions. In accordance with the Bangladeshi guidelines for Flood Action Plan projects (ref. [15]), one of the main indicators of the economic feasibility is the Net Present Value, as mentioned before in Section 7.1.3.3. The geometric dam profile which yields the highest NPV is thought to be the most economic profile. The NPV was defined as the sum of the discounted differences of the annual costs and benefits over the economic life time of the structure.

First variables, which govern the dam profile, were defined in Section 7.5.3.1. By systematically varying these variables several dam profiles were obtained, for which the NPV could be calculated. In order to calculate the NPV as explained in Section 7.5.3.4, the method used to derive the annual costs is given in Section 7.5.3.2. and the procedure to derive the annual benefits is described in Section 7.5.3.3.

#### 7.5.3.1 Variables for optimization

Like the original design, the sea side slope was divided into two parts; below and above the crest of the Winter Spring Tide Dam at 6.46 m + PWD. Below this level, the same slope angle was chosen as for the original design, namely 1:4 . This is approximately equal to the maximum slope angle, required for the macro slope stability. The upper slope angle could be varied, but not steeper than the maximum slope angle required for the geotechnical macro stability.

Both this upper slope angle and the crest level of the main dam, excluding geotechnical settlement, were used as variables for the optimization procedure. In order to find the most economic dam profile, a number of profiles had to be generated, by means of varying these parameters.

The slope angles and crest levels of the flank embankments were assumed to be depending on the parameters for the main dam.

As the left flank embankment is lying in the same line as the main dam, the sea side slope angle was chosen to be equal to the main dam. The slope angle for the right embankment was determined to be 1:4.

As far as the crest levels are concerned, the following considerations were made:

The wave attack at the left embankment is reduced compared to the main dam, because this embankment is located on a relatively high fore shore. As the fore shore of this embankment is much higher compared to the main dam, the wave height is thought to decrease.

Wave heights at the right embankment are lower compared to the main dam, because of the direction of the dam axis, which is more or less parallel to the propagating direction of the waves.

Accordingly, the wave run-up will be lower for both flank embankments.

For economic reasons, it is desirable that the volume of overtopping sea water per linear meter of the dam is more or less equal for all dam sections. In order to establish this situation, the crest levels of both flank embankments can be chosen lower than the main dam. For the original design, the crest levels of the flank embankments were chosen 1.5 meters lower than the crest level of the main dam. As the exact reduction of the wave run-up could not be estimated well, the crest levels of the right and left embankments are determined to be 1.5 meters lower than the main dam as well.

#### 7.5.3.2 Costs

For each year of the structures life time, the costs had to be determined. For these costs various definitions are commonly used, which are explained in the Annex F. For the procedure of cost calculation the Bangladeshi guidelines for project assessment (ref. [15]) were used. In general, two types of costs can be considered; investment costs and operation, maintenance and replacement costs.

##### Investment costs

For each combination of the crest levels and upper slope angles, the total basic construction costs could be calculated out of the unit rates. The used unit rates for the various materials were estimated using the unit rates as mentioned in ref. [3] and ref. [24]. These are given in Annex F. The earthfill costs result directly from the two variables. The costs for the slope protection were derived, by means of estimating the necessary cover layer thickness. This was done using the global method, which is described in Annex F. As the design of the slope protection depends on the slope angle only, the cover layer thickness and accordingly the costs were estimated for each slope angle.

In order to derive the total construction costs, physical contingencies had to be introduced to cover unforeseen works. These contingencies are defined as a percentage of the total base costs.

Furthermore, engineering costs had to be taken into account. These costs comprise costs for survey, investigation, design, preparation of tender documents and supervision of construction.

The total investment costs are defined as the sum of the total construction costs and the engineering costs. These costs have to be made in the year of construction.

### **Operation, maintenance and replacement costs**

These costs include among others costs for technical staff, operation and maintenance of structures and costs for annual repair. These costs were taken into account for every year of the economic life time of the Feni dam.

#### **7.5.3.3 Benefits**

As the main objective of the Feni River Closure Dam is to provide irrigation possibilities, the benefits are assumed to be dealing with agricultural aspects only. In general, more benefits can be considered. For example benefits for fisheries in the Feni reservoir, social benefits with respect to the protection of human lives and infrastructure, etc. For this study, the benefits of the construction of the Feni dam were defined as the agricultural yield when the dam would be built (the [W] case) minus the yield without construction of the Feni dam (the [WO] case).

It is not exactly known what was the agricultural yield of the area before the Feni dam was built, thus in the [WO] case. As the yield was relatively small, the annual yield is assumed to be zero for the [WO] case. Accordingly, the annual benefit is assumed to be equal to the expected annual yield in the [W] case.

The annual benefit can then be defined to be the potential yield minus the average annual damage due to overtopping waves. For the determination of the benefits, first the potential yield had to be determined. See Annex F. This is the agricultural yield for the hypothetical situation of zero damage.

Then the average annual damage was estimated for each different dam profile. The crop damage can be caused by several effects. The main cause is the poor water quality in the reservoir, through which no irrigation is possible any more. This poor water quality is mainly caused by sea water overtopping the dam, which makes the reservoir saline. For the optimization procedure, only the damage to the crop due to overtopping waves was considered. The so-called damage-frequency curve had to be estimated, for which Annex F is referred to. The surface area under this curve, below the probability of exceedance of the design condition (0.02) has to be determined. The resulting value is equal to the annual expected damage.

Subsequently, the annual benefit could be estimated. Furthermore, this annual benefit is thought to increase each year, due to an economic growth. In accordance with the Bangladeshi guidelines (ref. [15]), an annual growth of 3% per year was taken into account.

#### **7.5.3.4 Calculation of Net Present Value**

The Net Present Value is a generally used parameter to estimate the economic feasibility of the project. The discounting period has to be determined for this.

The discounting period is assumed to be the economic life time of the structure. According to the Bangladeshi guidelines, 30 years is advised for the discounting period. As there is no reason to deviate from this, a period of 30 years will be considered for this study as well.

For each year of the discounting period, the discounted difference of the benefits and the costs had to be calculated. According to the guidelines, a discount rate of 12 % was applied. This discount rate is also called the opportunity cost of capital. The sum of these discounted differences over the discounting period is defined to be the Net Present Value.

#### **7.5.4 Geometric dam profile without sedimentation influence**

In this section the derivation of the geometric dam profile is given, for the situation when the elevation of the fore shore is neglected. In the original design, this effect was neglected as well. Through breaking of the waves on the elevated fore shore, the wave heights will be reduced. Thus, neglecting this effect will probably result in a relatively save design. In Section 7.5.4.1 the results of the optimization procedure are given. As the method used to derive the annual damage values is rather inaccurate, a sensitivity analysis is carried out in Section 7.5.4.2.

In Section 7.5.4.3 it is checked, whether the dam profile resulting from this optimization procedure during cyclone conditions fulfils the monsoon criterion as well. The overheight of the crest level due to geotechnical settlement is determined in Section 7.5.4.4. For an illustration only, the dam profile was derived in Section 7.5.4.5, when the design criteria used for the Cyclone Protection Project II would be imposed to the dam.

##### **7.5.4.1 Results of the optimization procedure**

The NPV could be calculated for each combination of the two variables; the crest level and the upper slope angle of the main dam. By systematically varying these parameters, the highest NPV could be derived. The geometric dam profile which yields the highest NPV is assumed to be the most economic profile. The resulting profile was chosen for the new dam design. For the optimization procedure, reference is made to Figure 3 of Annex F. The calculation of the NPV for the chosen profile is given in this annex too. The results are given in Table 19.

Slope angle	1:4	1:4.5	1:5	1:5.5	1:6
Optimum crest level (m. + PWD)	10.4	10.3	10.1	10.1	10.1
NPV (million Taka's)	4985.0	4994.9	4996.3	4990.8	4986.3

**Table 19:** Results of the optimization procedure

The dam profile, which yields the highest NPV comprised a crest level of 10.1 m + PWD and a slope angle of 1:5.

##### **7.5.4.2 Sensitivity analysis for expected annual damage**

The annual damage, and therefore the annual benefit is thought to be rather inaccurate. This is caused by the fact that the estimations of the damage costs in historic damage cases is not available. In order to solve this problem, several assumptions and schematizations had to be made. See Annex F.

In order to find out what is the influence of varying the annual damage on the most economic dam profile, a sensitivity analysis was carried out. The annual damage was increased with 20 %, which can be considered to be a considerable increase. Successively, the optimization procedure was carried out again. The results using this annual damage, are given in Table 20.



Slope angle	1:4	1:4.5	1:5	1:5.5	1:6
Optimum crest level (m. + PWD)	10.7	10.6	10.4	10.4	10.4
NPV (million Taka's)	4969.0	4980.6	4983.2	4977.2	4972.4

**Table 20:** Results of optimization procedure for an expected annual damage which is increased with 20% .

Again, a slope angle of 1:5 appeared to yield the highest NPV's. The slope angle turned out not to be very sensitive to the damage increase. The crest level, however, is 0.30 meter higher than the value calculated earlier. For a rather large increase of the expected annual damage, the increase of the crest level is thought to be relatively small. Accordingly, the described method is assumed to be a suitable method to estimate the most economic geometric dam profile.

#### 7.5.4.3 Verification of monsoon criterion

It had to be checked whether the most economic dam profile for cyclone conditions fulfils the monsoon criterion. For this, the run-up for a slope angle of 1:5 had to be added to the still water level for a situation having a return period of 50 years. This is described in Annex F. For a slope angle of 1:5 the run-up appeared to be 2.31 meter. For a SWL of 7.69, the required crest level for monsoon conditions is  $7.69 + 2.31 = 10.0$  meters. This is less than the crest level obtained by means of the optimization method. Finally the crest level was determined to be 10.1 m. + PWD and the slope angle was determined to be 1:5.

#### 7.5.4.4 Geotechnical settlement

For the geotechnical settlement the same values as used in the original design will be applied. The estimated geotechnical settlement of the sub soil and dam body is 0.5 meter for the main dam. This value had to be added to the achieved crest levels. The resulting crest level is  $10.1 + 0.5 = 10.6$  m. + PWD.

#### 7.5.4.5 Dam profile when the CPP II criteria would be applied

Just for comparison, the geometric dam profile was derived, which results from the design criteria applied by the CPP II project. In Annex F a detailed calculation and explanation is given. The monsoon criterion reads: Less than 13% of the waves should overtop the structure for a situation with a return period of 5 years. For a slope angle having a tangent of 1:5 the required crest level is calculated in Section F.5 of Annex F to be about only 8.07 m. + PWD for this criterion. The first cyclone design criterion reads: For a return period of 20 years the water level elevation of the polder (here: reservoir) should be less than 1.0 meter. The required crest level for a slope angle having a tangent of 1:5 turned out to be about 8.0 m. + PWD. The second cyclone criterion reads: For a return period of 40 years, the water level should be lower than the crest level. For this situation, the water level should be at least 9.50 meter + PWD.

The governing crest level using these CPP II criteria appears to be 9.50 meter + PWD. This is only 0.60 meter lower than the crest level chosen for the redesign of the Feni dam. It is reasonable to apply higher crest levels for the Feni dam than for the coastal embankments, because of the additional objectives of the Feni dam.

#### 7.5.5 Geometric dam profile including sedimentation influence

Now the case is considered, when the sedimentation speed could have been anticipated sufficiently accurate at the time when the design was originally made. For this, the same optimization procedure was carried out, but now introducing reduced significant wave heights for each year after the closure of the Feni river, due to the accretion process. In Table 21 the results are given.

Tangent of the slope angle	1:4	1:4.5	1:5	1:5.5	1:6
Optimum crest level (m + PWD)	10.3	10.1	9.9	9.9	9.9
NPV (million Taka's)	5003.9	5011.9	5011.4	5006.1	5001.9

**Table 21:** Results of optimization procedure when sedimentation could be predicted.

The dam profile, which yields the highest NPV, comprised a crest level of 10.1 m. + PWD and a slope angle of 1:4.5 .

Although a slope angle of 1:4.5 yields a higher NPV, a slope angle of 1:5 was chosen for a comparison with the redesign, when the sedimentation speed would be neglected. Then the crest level resulting from the optimization procedure is 9.90 meters + PWD.

When the situation three years after closure is considered, the monsoon criterion yields a wave run-up of 2.15 m. and a SWL of 7.69 m. + PWD, which results in a minimum necessary crest level of 9.84 meters + PWD for a sea side slope angle of 1:5 . This is less than the crest level resulting from the optimization for cyclone conditions. Accordingly, the cyclone condition is governing the redesign here as well. When the accretion process could have been anticipated accurately, the resulting geometric profile would comprise a crest level of 9.90 m. + PWD and a slope angle of 1:5 .

This crest level is 0.20 meter lower for the same slope angle than the resulting dam profile when no sedimentation influence was taken into account. This will thus yield a more economical solution. The calculation of the cost difference is given in chapter 8.

## 7.6 DETAILED DESIGN OF THE SLOPE PROTECTION

### 7.6.1 Introduction

In this chapter the detailed redesign of the sea side slope protection of the Feni dam is described. In general, a slope protection consists of a sub layer, a filter layer and a cover layer. First the sub layer for the slope protection was determined in Section 7.6.2.

The necessary block sizes of the cover layer were calculated using the newly available analytical design method for placed block revetments. This method is briefly described in Section 7.6.3. In order to design the slope protection, the hydraulic design conditions were derived for the main dam and both flank embankments in Section 7.6.4.

For the filter and cover layer several material options were generated as explained in Section 7.6.5. For all combinations of these materials, several slope protection alternatives were derived, having cover layer thicknesses which fulfil the stability requirement for a monsoon situation. This requirement is that no stone movement is accepted for a design significant wave height having a return period of 50 years. This was done using the newly available analytical method for placed block revetments. The resulting cover layer thicknesses for each slope protection alternative are given in Section 7.6.6.

Then a slope revetment alternative was chosen for the parts of the main dam and flank embankments, which are subject to wave attack. Subsequently, it was checked, whether the stone movements are less than 0.1 times the cover layer thickness, for a wave height of  $1.4 * H_{sig}$ . Furthermore the geotechnical micro stability of the construction was analyzed. In this way a design of the sea side slope protection was obtained for the case when no sedimentation influence would be taken into account in Section 7.6.7. The design of the slope protection including the sedimentation influence is given in Section 7.6.8.

### 7.6.2 Choice of the sub layers of the slope protection

As mentioned in the study assumptions, a clay layer, covered by a filter fabric was chosen as a sub layer for the slope protection, in order to make the comparison with the original design possible. Moreover, the choice of this sub layer was made to increase the remaining strength. This is the stability of the construction after initial failure of the cover layer. When some blocks would be lifted out of the cover layer, the clay and filter fabric can resist the wave attack for some time. The core of the dam body will not be affected immediately.

The filter fabric is necessary, because the quality of the available clay is rather poor. The clay layer was placed on the final profile at the sea side having a thickness of 0.60 meter.

### 7.6.3 General description of the analytical method for the design of the slope revetment

In Annex F, the "global method" was used to give a first estimation of the cover layer thickness. This first estimation was the basis for the calculation of the costs in the optimization procedure. For the global method the breaker index  $\xi$  had to be derived. The global method is relating this breaker index to the parameter  $H_{sig}/\Delta D$ . In this relation  $\Delta$  is the relative density under water and  $D$  is the thickness of the cover layer. The relation between  $\xi$  and  $H_{sig}/\Delta D$  is depending on the construction type and is given in ref. [12].

On the other hand, the analytical method is based on formulas, which describe the physical processes in a slope protection in detail. This method is more accurate than the global method, but the method can only be applied for slope protections having a granular filter layer.

The analytical method shows the influence of all parts of the slope protection structure. The design method can be divided into 6 parts:

- 1) Preliminary design. Using the analytical method, the preliminary design can be analyzed, whether this is stable or not. If not, the design should be adapted.
- 2) Determination of the leakage length. This is a very important factor which represents the relation between the permeabilities of the cover and filter layers.
- 3) Check on possible intrusion of sub layer material into the filter layer. In this case it should be checked whether the clay will be washed through the filter fabric.
- 4) Check on the appearance of stone movements. No movements should occur for the design significant wave height.
- 5) Check whether the stone movement is smaller than 0.1 times the cover layer thickness for a wave height of  $1.4 * H_{sig}$ .
- 6) Check on geotechnical stability of the material directly underneath the slope protection. This is also known as micro stability. The macro stability of the dam body as a whole, is analyzed in Section 7.5.2.

Here, an explanation of each of these items is given. Generally the stone movements of the cover layer of item 4) and 5) are caused by uplifting of the blocks. This failing mechanism governs the design and is present at the time of the maximum back-rush of the design wave. For this see Figure 14.

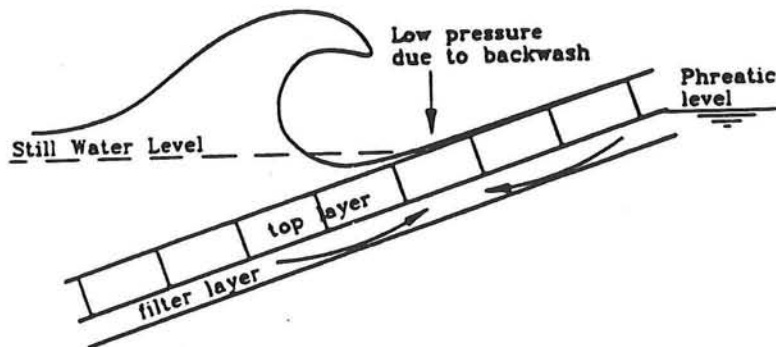


Figure 14: Loading condition, which governs the failure mechanism of the uplifting of the blocks.

The stability for this failing mechanism is depending on the following parameters:

- the block thickness  $D$ ,
- the leakage length  $\Lambda$ , which can be calculated using the following formula:

$$\Lambda = \sqrt{\frac{k b_{f1} D}{k'}}$$

in which:

$\Lambda$	= Leakage length	[ m ]
$k$	= permeability of the filter layer	[ mm/s ]
$k'$	= permeability of the cover layer	[ mm/s ]
$b$	= thickness of the filter layer	[ m ]
$D$	= thickness of the cover layer	[ m ]

- the relative density of the cover layer under water  $\Delta$ , which reads:

$$\Delta = (\rho_{\text{block}} - \rho_{\text{sea water}}) / \rho_{\text{sea water}} \quad [ - ]$$

- factors for several physical influences. These influence factors are:
  - Influence factor for transitions in the slope protection,
  - influence factor for friction between the blocks,
  - influence factor for inertia of mass, if stone movement is permissible and
  - influence factor for the flow of water from the sub layers to the cover layer, if stone movement is permissible to a certain extent.

From all these influences one influence factor (  $\Gamma$  [ - ] ) can be derived.

By introducing all these factors (  $D$ ,  $\Lambda$ ,  $\Delta$  and  $\Gamma$  ) in the design figures of ref. [12], the critical wave height can be determined. When the loading wave height is lower than the critical wave height, the slope revetment is thought to be stable. In Annex G an example of the stability analysis of the slope revetment is given using the analytical method. Furthermore, the stability of the originally applied slope revetment is analyzed in this annex too.

#### 7.6.4 Design loading conditions for the slope protection without accretion influence

For the design of the slope protection, first the hydraulic loading conditions had to be determined. In the following sections this is done for the case when the accretion influence would not be taken into account. Successively the design loading conditions are defined in Section 7.6.4.1. for the main dam, in Section 7.6.4.2 for the left and in Section 7.6.4.3 for the right flank embankment.

##### 7.6.4.1 Design conditions for the main dam

For the main dam, the water levels and wave characteristics were used as derived for the year directly after closure. Although the angle between the wave fronts and the dam axis,  $\beta$ , appeared to be about  $30^\circ$  in the design situation, the wave propagating direction is assumed to be perpendicular to the main dam axis. Accordingly, the following design parameters will be used:

$$\begin{aligned} H_{\text{sig}} &= 1.4 \text{ m} \\ T_z &= 4.6 \text{ s.} \\ \beta &= 0^\circ \\ \tan \alpha_{\text{avg}} &= 0.22 \end{aligned}$$

Here  $\alpha_{\text{avg}}$  is the mean slope angle of the sea side slope from  $2 * H_{\text{sig}}$  below SWL to SWL.

##### 7.6.4.2 Design loading conditions for the left flank embankment

After studying the bathymetric charts of ref. [7] directly downstream of the dam, the level of the fore shore in front of the left flank embankment is more or less equal to the accretion level that was reached three years after the closure of the Feni river. Moreover, it could be concluded from the bathymetric charts that the fore shore elevation in front of the left flank embankment has stayed constant.

Accordingly, wave characteristics occurring 3 years after closure should be taken into account for the design of the slope protection of the left flank embankment. The wave propagating direction was assumed to be equal to the design situation for the main dam.

The design parameters for a hydraulic situation having a return period of 50 years are given below:

$$\begin{aligned} H_{sig} &= 1.14 \text{ m} \\ T_z &= 4.7 \text{ s.} \\ \beta &= 0^\circ \\ \tan \alpha_{avg} &= 0.22 \end{aligned}$$

### 7.6.4.3 Design loading conditions for the right flank embankment

The part of the right flank embankment which is located adjacent to the regulator is severely attacked by waves. The loading conditions and slope protection of this part was determined to be equal to the main dam.

For the part of the right flank embankment whose dam axis is positioned parallel to the outlet channel, the fore shore is relatively high. For the design of the slope protection of this part two loading conditions were considered.

#### Loading case 1: South western wind direction

For the wind direction, which yields the highest wave heights, the propagating direction of the waves is almost parallel to the axis of the right flank embankment. In this case the effective slope angle  $\gamma$  can be expressed as:

$$\tan \gamma = \tan \alpha * \cos \beta$$

in which:

$\gamma$ = effective slope angle, measured perpendicular to the wave front	[ ° ]
$\alpha$ = slope angle, measured perpendicular to the dam axis	[ ° ]
$\beta$ = angle between the wave front and the axis of the flank embankment	[ ° ]

A definition sketch for these parameters is given in the Figure 15.

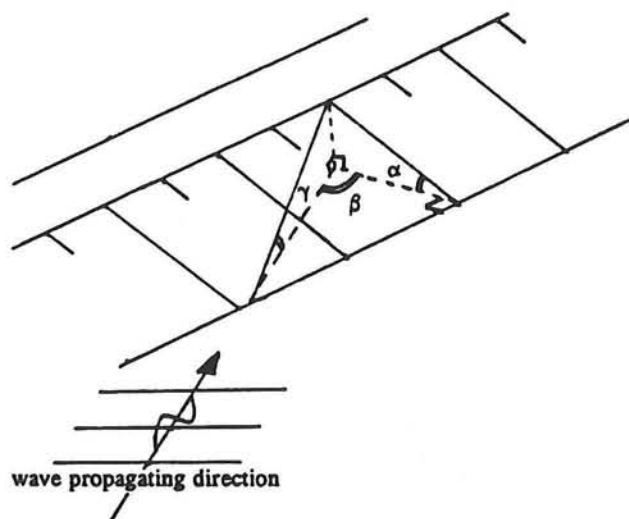


Figure 15: Definition sketch for the effective slope angle.

After running Hiswa, the resulting value for  $\beta$  appeared to be more than  $60^\circ$ . As exact figures are not known, for this loading condition,  $60^\circ$  was taken for  $\beta$ . In this way, a relatively save design was obtained. The elevation of the fore shore of the right embankment is more or less equal to the elevation of the fore shore of the main dam, 3 years after closure. Therefore, the same values as for the main dam 3 years after closure were taken into account for the remaining wave parameters.

The design wave characteristics are given below:

$$\begin{aligned} H_{sig} &= 1.14 \text{ m} \\ T_z &= 4.7 \text{ s.} \\ \beta &= 60^\circ \\ \tan \alpha_{avg} &= 0.25 \end{aligned}$$

In accordance with the above mentioned formula, this yields an effective slope angle  $\gamma$  of 1:10.

#### Loading case 2: South eastern wind direction

For a wind direction perpendicular to the axis of the right flank embankment, which is approximately south east, the resulting wave propagating direction is almost perpendicular to the axis as well. Due to the smaller fetch length in this direction, the wave heights will be lower than for case 1, but the effective slope angle will be larger. In fact  $\gamma$  will be equal to  $\alpha$  in this case.

The design parameters for this case are given below:

$$\begin{aligned} H_{sig} &= 0.93 \text{ m} \\ T_z &= 2.87 \text{ s.} \\ \beta &= 0^\circ \\ \tan \alpha_{avg} &= 0.25 \end{aligned}$$

Both loading conditions were analyzed. The governing case was taken as a basis for the design.

#### 7.6.5 Generation of alternatives for the filter and cover layers

In this section several alternatives for the slope revetment are generated. The cover layer options are described in Section 7.6.5.1. In Section 7.6.5.2 the filter layer options are determined and in Section 7.6.5.3 the filter fabric is chosen. When all the options for the various parts of the slope protection were combined, several alternatives were obtained which are described in Section 7.6.5.4.

##### 7.6.5.1 Cover layer options

In this section various options concerning the cover layer are determined. The variables which influence the design: the cover layer material, the rib sizes and the joint width are given below.

##### Cover layer material options

The most important property of the cover layer material as a resistance against uplifting is the density. When the resulting relative density under water ( $\Delta$ ) is larger, the stability is higher. Three sorts of cover layer material can be made in Bangladesh having different densities.

These are given below:

- concrete blocks with gravel aggregates;  $\Delta = 1.20$
- concrete blocks with brick aggregates;  $\Delta = 0.80$
- brick blocks;  $\Delta = 0.56$ . Brick blocks are blocks consisting of bricks with mortar in between.

These three cover layer materials were studied for the design of the slope protection.

### **Block rib size options**

Square blocks were chosen for the cover layer. When the joint width is kept constant, the rib size determines the percentage of open surface area of the cover layer and thus the permeability of the cover layer. When the rib size is decreased, the permeability of the cover layer increases and the leakage length decreases. This will result in a more stable design. Two options will be analyzed: Square blocks having a rib size of 0.25 and 0.50 meter.

### **Choice of the joint width**

Besides the block size, the joint width is influencing the cover layer permeability and thus the leaking length and the resistance against uplifting. When the joint width is chosen larger, the cover layer permeability is larger and thus the slope protection will be more stable. In practice the blocks will be placed against each other, during construction. This will result in small joint widths, which depend on the chosen cover layer material.

Furthermore, by applying small joint widths, the structure is less sensitive to vandalism. Normally, people will not be able to pull out a block then.

When concrete blocks would be used, the average joint width is estimated to be about 2 mm. The average joint width of brick blocks is larger, because of the rougher surface. The average joint width is estimated to be about 4 mm, when brick blocks are placed directly against each other. These values were measured at the dam site by the author.

### **7.6.5.2 Filter layer options**

In this section the filter layer options are analyzed. Two options were considered in this study: with or without a granular filter layer directly underneath the cover layer. For the option including a filter layer the filter material was chosen first. Subsequently the filter layer thickness was determined.

#### **Choice of filter material when a filter would be applied**

Filter materials having various gradings are available in Bangladesh. Three are mentioned below.

- chipped bricks, having a specific grain size:  $D_{50} \approx 30$  mm,
- coarse gravel, obtained from the area Sylhet in the north of Bangladesh, having a  $D_{50} = 12$  mm,
- pea gravel, also available from the Sylhet area, having a  $D_{50} = 4$  mm.

In order to increase the stability of the cover layer, the leakage length should be reduced. This is achieved by applying a filter material which is as fine as possible. In this way the permeability of the filter layer will be lower.



A restriction for the filter material is the requirement that the grain size distribution has to be chosen such that no filter material will be washed through the cover layer. The requirement reads:  $D_{n,90} \geq \text{joint width}$ . This requirement is fulfilled by all the mentioned filter materials. In general, a larger cover layer thickness is necessary when other filter materials than pea gravel would be applied. This is why pea gravel is chosen as a filter material.

Furthermore, an other possibility is not to apply a filter, but to place the blocks of the cover layer directly on the filter fabric, covering the clay layer. In this case the analytical method cannot be used any more. The global method is assumed to yield a reliable slope protection then.

### Choice of filter layer thickness

When a granular filter would be applied, the filter layer was decided to contain only one sort of material in order to facilitate the construction of the slope protection. Accordingly, the filter layer will also serve as an outfill layer to fill out the inequities of the cover layer. From the equation for the leakage length follows, that the slope protection becomes more stable when the filter layer thickness ( $b_f$ ) is reduced. The leakage length decreases then. In order to make the slope protection as stable as possible, the filter thickness should be chosen as small as possible. Since the surface of brick blocks is rougher than concrete blocks, the filter layer should be thicker for brick blocks to fill out the inequities. The filter layer thickness was chosen to be 0.05 meter for the concrete blocks and 0.10 meter for brick blocks. These are thought to be the smallest possible values, which can be constructed in practice.

#### 7.6.5.3 Choice of the filter fabric

One of the requirements of the analytical method is that no base material should be washed through the filter fabric into the filter layer. The filter fabric should therefore be geometrically stable and it should meet the following requirement:

$$O_{90} < 10 * D_{b,50} \text{ and } O_{90} < D_{b,90} \text{ and } O_{90} \leq 0.10 \text{ mm.}$$

in which:

- $O_{90}$  = characteristic mesh size of the filter fabric, [ mm ]
- $D_{b,50}$  = grain size, which is not exceeded by 50% of the base material, based on weight. [ mm ]
- $D_{b,90}$  = grain size, which is not exceeded by 90% of the base material, based on weight. [ mm ]

For the clay in the region of the Feni dam, two grain size distributions were used as obtained from ref. [11]. From these distributions the following values were estimated:  $D_{b,50} \approx 0.01$  mm and  $D_{b,90} \approx 0.03$  mm. The governing requirements appeared to be:  $O_{90} < 0.1$  mm. Therefore, a filter fabric was chosen for which  $O_{90} = 0.1$  mm. Besides, it can be concluded that the filter fabric, applied in the original design, has an  $O_{90}$  of 0.18 mm and hence does not meet this requirement!

#### 7.6.5.4 Resulting alternatives

The various alternatives are given below in Table 22.

Nr.	Cover layer material	Cover layer sizes	Filter layer
1	Concrete + gravel aggregates $\Delta = 1.20$	rib size = 0.50 m, joint width = 2 mm.	Pea gravel, $D_{n,15} = 2$ mm, thickness = 0.05 m.
2		rib size = 0.25 m, joint width = 2 mm.	Pea gravel, $D_{n,15} = 2$ mm, thickness = 0.05 m.
3		rib size = 0.50 m, joint width = 2 mm.	No filter, blocks directly on filter fabric.
4	Concrete + brick aggregates $\Delta = 0.80$	rib size = 0.50 m, joint width = 2 mm.	Pea gravel, thickness = 0.05 m.
5		rib size = 0.25 m, joint width = 2 mm.	Pea gravel, thickness = 0.05 m.
6		rib size = 0.50 m, joint width = 2 mm.	No filter, blocks directly on filter fabric.
7	Brick blocks $\Delta = 0.56$	rib size = 0.50 m, joint width = 4 mm.	Pea gravel, thickness = 0.10 m.
8		rib size = 0.25 m, joint width = 4 mm.	Pea gravel, thickness = 0.10 m.
9		rib size = 0.50 m, joint width = 4 mm.	No filter, blocks directly on filter fabric.

Table 22: Description of the alternative slope protection materials studied.

#### 7.6.6 Calculation of the cover layer thickness for the alternatives

For each alternative, the cover layer had to be derived. This was done by means of the newly available analytical method, which was generally described earlier in section 7.6.3. and more in detail in Annex G. For more information see ref. [12].

First the requirement of no stone movements caused by a design significant wave height, having a return period of 50 years was considered. For various alternative slope protection solutions, the minimum cover layer thicknesses were calculated to fulfil this requirement. From these results, a slope protection alternative was chosen for the main dam and both flank embankments.

Using the analytical method, it is only possible to check, whether a given slope protection is stable or not. The cover layer thickness,  $D$ , cannot be calculated directly. Thus for calculation of the minimum necessary cover layer thickness for the various alternatives, this value was derived by means of an iteration procedure. By systematically varying the thickness  $D$ , the minimum thickness could be derived, for which no stone movements occur for the design significant wave height. This was done for each alternative slope protection, considering the hydraulic conditions for the main dam and both flank embankments.

For each alternative the costs of the slope protection and possible filter layer per square meter were estimated, using the material rates as determined in Annex F. These costs will be used to compare the various alternatives. The results are given in Table 23. For a calculation example of the stability analysis of the slope protection, reference is made to Annex G.

Alter. nr.	main dam		left fl. emb.		right fl. emb.			
	D in m.	Costs in Tk / m <sup>2</sup>	D in m.	Costs in Tk / m <sup>2</sup>	loading case 1		loading case 2	
					D in m.	Costs in	D in m.	Costs in Tk / m <sup>2</sup>
1	0.25	640	0.25	640	0.20	520	0.20	520
2	0.20	520	0.20	520	0.15	400	0.15	400
3	0.35	840	0.35	840	0.25	600	0.25	600
4	0.35	740	0.35	740	0.30	640	0.30	640
5	0.30	640	0.30	640	0.25	540	0.25	540
6	0.55	1100	0.50	1000	0.35	700	0.35	700
7	0.65	925	0.60	860	0.45	665	0.45	665
8	0.55	795	0.45	665	0.35	535	0.35	535
9	0.75	975	0.70	910	0.50	650	0.50	650

**Table 23:** Resulting necessary cover layer thicknesses and estimated costs for the cover and filter layer.

#### 7.6.7 Design of slope protection without sedimentation influence

The slope revetment designs which were chosen for the various dam sections, when the accretion influence was not taken into account, are described below. In Section 7.6.7.1 the design of the slope protection of the main dam is given. Subsequently in Sections 7.6.7.2 and 7.6.7.3 the slope protection designs of the flank embankments are described.

##### 7.6.7.1 Design of slope protection for the main dam

Here the design of the slope revetment for the main dam without accretion influence is given. First the part of the slope which is attacked by the design waves was designed. For this Table 23 was considered. Subsequently, the slope protection in the least attacked zone below the main protection was designed.

## Main slope protection

For the design of the part of the slope protection which is attacked by the design waves the values of Table 23 are considered. When no filter layers would be used, the cover layer thickness and the costs appears to be higher than the case when a filter would be applied for all the considered material options. Furthermore, a smaller rib size yields a smaller cover layer thickness and thus lower costs. For each cover layer material option, the cheapest solution turned out to comprise a filter layer and blocks having a length of 0.25 meter.

For the main dam, the most economical solution was chosen. It is emphasized that the used material rates are just an estimation to enable a comparison.

For the part of the slope protection of the main dam, which is attacked by the design waves, the most economical slope protection was chosen resulting from the above mentioned calculations. This comprises a cover layer consisting of concrete with gravel aggregates, having a thickness of 0.20 meter. The filter layer consists of pea gravel having a  $D_{n,15}$  of 2 mm.

In Annex G it is analyzed whether the stone movements are smaller than  $0.1 * D$ . It appears that the chosen slope protection fulfils this requirement. Furthermore the geotechnical micro stability was checked as well. For this Annex G is referred to as well. It was thus concluded that the slope protection meets all the requirements.

According to ref. [12], the upper limit of this revetment should at least be higher than SWL (still water level) +  $0.5 * H_{sig}$ , or SWL +  $0.5 * z_{2\%}$  (run-up). Thus higher than  $7.69 + 0.5 * 1.41 = 8.40$  m. + PWD or higher than  $7.69 + 0.5 * 2.31$  m. = 8.85 m. + PWD. As cyclonic surges are to be expected as well, having a higher still water level, the mentioned slope protection was extended to the crest.

In ref. [12] it is advised not to apply transformations above a level of about  $H_{sig}$  to  $2 * H_{sig}$  below SWL. This is the area of the slope where the loading condition of the maximum wave back rush, which governs the design, is most severe. For safety purposes the under limit of the mentioned revetment was determined to be at  $7.69 - 2 * 1.41$  m. + PWD = 4.87  $\approx$  4.9 m. + PWD. This is below the crest level of the winter spring tide dam and thus below the transition between the two slope angles.

## Slope protection below the main slope protection

For the part of the slope below the main revetment, which is below 4.9 m. + PWD the governing loading condition had to be estimated.

The governing still water level is assumed to be 5.0 m. + PWD than, which yields a depth in front of the dam of about 5.0 meters. Then the level of the maximum wave back-rush is more or less positioned at the concerned part of the slope. When Table 6 of section 7.3.2.2 was considered, the corresponding return period for this water level was assumed to be less than one year. Again a joined probability between the waves and the water level is assumed.

Considering Table 12 of section 7.4.5.1, which represents 5 years of wind observation, the wind speed which is prevailing for about 1 hour per year on an average is about 20 m/s. Consequently, the wind speed is less than 20 m/s for the considered return period, which is less than one year. Here a wind speed of 15 m/s was taken into account.

In accordance with ref. [11], the wind direction having the highest annual probability of occurrence is a southern direction. This situation was considered, having a fetch length is about 3 km. From figures in ref. [12], which can be used to estimate the wave growth, the peak wave period is assumed to be 2.5 seconds for a wind velocity of 15 m/s, a depth of about 5 meters and a fetch length of 3 km. The wave height is estimated to be about 0.6 meter then. These figures yield a breaker index of 1.0 .

For the concerned part of the slope brick blocks were chosen as a cover layer material. Two alternatives were considered; with or without a filter layer. The resulting minimum cover layer thicknesses and costs for the cover and filter layer are given in the Table 24, using the analytical method.

	Cover layer thickness (m)	Estimated costs (Tk / m <sup>2</sup> )
Brick blocks on a filter layer	0.20	335
Brick blocks directly on geotextile	0.30	390

**Table 24:** Resulting minimum cover layer thickness for two slope protection alternatives.

From this table it can be concluded that the costs are a little bit lower for the alternative including the filter layer. As a filter layer had been chosen for the main slope protection previously, a filter was chosen for this part of the slope as well in order to facilitate the construction of the slope protection.

The resulting slope protection below the main slope protection comprises a brick block cover layer having a rib size of 0.25 meter and a thickness of 0.20 meter. The filter layer is 0.10 meter thick and consists of pea gravel. For this structure, the stone movements for a wave height of  $1.4 * H_{sig}$  are less than  $0.1 * 0.20 \text{ m.} = 2 \text{ cm.}$  The requirement for geotechnical micro stability is fulfilled as well.

This revetment was chosen between the main revetment and the toe structure. This toe structure is positioned at a level of about 1.2 m. + PWD. The same toe structure was chosen as applied in the original design. For completeness sake, it is mentioned once again that the protection of the crest is no subject of this study.

#### 7.6.7.2 Design of slope protection for the left flank embankment

For the main revetment of the left flank embankment the resulting cover layer thicknesses of Table 23 were considered. The costs appeared to be equal to the main dam for both concrete options. As the brick block option is not cheaper, concrete blocks with gravel aggregates including a filter layer were chosen.

For the left flank embankment, reduced wave heights were introduced, due to a higher fore shore. It appeared that the necessary block thickness does not decrease for this situation compared to the main dam. This is mainly caused by the fact that the positive effect of the wave height reduction is equal to the negative effect of the breaker index increase. The breaker index increases namely, when the wave height decreases and the wave period stays the same.

The chosen slope protection of the left flank embankment on top of the sub layers was determined to comprise the following items for the area of the most severe wave attack. The cover layer consists of concrete blocks with gravel aggregates, having a length of 0.25 meter and a thickness of 0.20 meter. The filter layer, whose thickness measures 0.05 meter, contains pea gravel.

This slope protection was checked on dynamic stability for a wave height of  $1.4 * H_{sig}$ . Then the movement is less than  $0.1 * 0.20 \text{ m.} = 2 \text{ cm.}$

The level of the toe structure is at 5.00 m. + PWD. As this level is about the same level as the under limit of the main revetment, the mentioned slope protection is applied for the whole slope.

### 7.6.7.3 Design of slope protection for the Right flank embankment

Again, the slope protection of the right flank embankment can be divided into two parts. With regard to the part parallel to the outlet channel, the resulting cover layer thicknesses turned out to be the same for both considered loading conditions which are mentioned in Section 6.6.4.3. The solution was chosen, for which the costs are minimal. The resulting slope protection comprises a cover layer consisting of concrete blocks with gravel aggregates, having a length of 0.25 meter and a thickness of 0.15 meter. Then the filter layer consists of pea gravel, which has a thickness of 0.05 meter.

For this solution the stone movement is less than  $0.1 * 0.15 \text{ m.} = 1.5 \text{ cm}$  for a wave height of  $1.4 * H_{sig}$ . Afterwards the geotechnical micro stability was checked.

Since the level of the toe structure is about 5.0 m. + PWD, the mentioned revetment is chosen for the whole slope.

As mentioned earlier in this report, the slope protection of the part adjacent to the regulator was determined to be equal to the main dam.

### 7.6.8 Design of slope protection including sedimentation influence

Now the case is considered, when the sedimentation process in front of the dam after closure of the Feni river could have been predicted accurately at the time the original design was made. For this case the slope protection was designed as well. From Table 14 of section 7.4.5.3 it can be seen that the wave period almost stays the same and that the significant wave heights decrease in the course of the years after the closure. Due to the elevation of the fore shore, the wave height is decreased by breaking.

The situation three years after closure was considered. This situation yields the same loading condition as used for the left flank embankment, when no sedimentation influence was taken into account. See for this section 7.5.3. Using these loading conditions the same calculations for the cover layer thickness could be carried out, which resulted in the same values as calculated for the left flank embankment.

Accordingly, the same design as for the slope protection of the main dam was achieved. So, although the wave height is reduced, the necessary slope protection stays the same. The cause of this effect is that the reduction of the wave height results in an increase of the breaker index. The effect of the breaker index increase is approximately equal to the effect of the wave height reduction and subsequently, the cover layer thickness appears to be the same. This was also mentioned in section 7.6.7.2.

In the first year after the closure of the Feni river, the slope protection disappeared under the accreted land, to a level of approximately 3 meters + PWD. It is therefore justified and attractive to apply a relatively cheap slope protection for this part of the slope. It was determined to apply bricks, having a thickness of 0.10 meter as a cover layer up to a level of 3.0 meter + PWD. Because of this thin cover layer, the probability of damage to the revetment is relatively higher, during the first year after closure. This design therefore requires a frequent monitoring and damage repair during the first year.

## **8      INFLUENCE OF IMPROVED DESIGN METHODS AND MORPHOLOGICAL CHANGES**

### **8.1    INTRODUCTION**

In this chapter the influence is analyzed of applying better design methods, which have become available since the year in which the design was originally made: 1983. The influence of the application of numerical computer models for the assessment of hydraulic boundary conditions is analyzed in Section 8.2. In contrast with the originally used wave run-up formula, the recent formula to calculate the wave run-up takes the wave steepness into account. The impact of this new formula is analyzed in Section 8.3. In Section 8.3 the application of an economic optimization procedure is compared to the application of the original design criteria to derive the geometric dam profile. The most important improvement of the design methods with respect to the Feni dam design, is the fact that the analytical design method to design the slope protection consisting of a placed block revetment became available recently. In Section 8.5 the slope protection which was designed using this method is compared to the original design. Moreover, in the same section the stability of the originally applied slope revetment is analyzed using the analytical method. Finally, it is examined in Section 8.6 what would be the amount of cost savings when the morphological process, caused by the construction of a hydraulic structure, could be anticipated accurately. The influence of a hypothetical method to predict the accretion process is analyzed in this section.

### **8.2    INFLUENCE OF THE APPLICATION OF NUMERICAL MODELS**

In 1983, 2-dimensional computer models were available to simulate the hydraulic situation. However these models were not easily accessible and computations took very much time. Accordingly no probability distribution for water levels during cyclone conditions was derived. The only way to do this was to analyze the gauge readings in the area, which comprised only about 10 years of record. This was probably the reason why no distinction between monsoon and cyclone conditions was made for the original design. By means of the newly available 2-dimensional numerical computer models it is possible to generate the maximum water levels during cyclone conditions in the area, using among others meteorological information of cyclones. However, the set-up of the model required a lot of time, partly because of the fact that the computer program DUCHES is not very user friendly.

With regard to the wave climate assessment, no wave observation has ever been carried out in the area of the Feni dam. For the original design, the wave climate near the dam had to be estimated by means of making rough schematizations of the bathymetry and using theoretical relations. For a return period of 50 years, this resulted in a wave height of 1.7 meters and a significant wave period of 7.0 seconds for incoming waves from the ocean. This was thought to be the governing situation. For waves generated locally, the estimated significant wave height was 1.4 m and the significant wave period was 4.8 seconds.

Nowadays, the wave climate can be estimated more accurately by means of numerical wave hindcast models. The wave climate can be computed for a dense grid. The bathymetry can be introduced more in detail and thus the computational results for a certain wind field will be more accurate. The resulting waves near the Feni dam, generated at the ocean, appeared to be negligible. For the locally generated waves, a wave height of 1.4 meter and a significant period of 5.3 seconds were found.

From the results of the numerical model it can be seen that the governing situation is the wave climate generated by local winds. This is in contrast with the original design, where the incoming waves from the ocean were thought to be governing. However, the wave climate, for locally generated waves estimated in the original design corresponds well to the design conditions arrived at for the redesign.

From the Hiswa results it can be concluded, that a wave height of 1.7 meter only occurs during cyclone conditions (see figure 14 and 15 of section 7.4). The accompanying significant wave period is estimated to be about 6.0 seconds. It can thus be concluded that the wave climate, used for the original design will probably not occur in reality. The parameters used as a basis for the original design yield a wave steepness which is too small. This subsequently causes a breaker index, which is overestimated.

### 8.3 INFLUENCE OF WAVE RUN-UP FORMULAS

For completeness sake the wave run-up formula, used in the original design, is given here again. The formula reads:

$$z_{2\%} = 8 * f * H_{sig} * \tan \alpha * \cos \beta$$

in which:

$z_{2\%}$	= wave run-up exceeded by 2% of the waves	[ m ]
$f$	= friction coefficient, which was determined to be 0.95 for concrete blocks.	[ - ]
$H_{sig}$	= significant wave height at the foot of the dam slope	[ m ]
$\alpha$	= slope angle	[ ° ]
$\beta$	= angle between the mean propagating direction of the waves and the line perpendicular to the dam axis.	[ ° ]

For the water levels and wave conditions used in the original design, the wave run-up was calculated in section 6.5 to be 1.86 meter.

Since 1983 new methods to calculate the wave run-up have become available. The formulas read according to ref. [12]:

$$\begin{aligned} z_{2\%} &= 1.5 * H_{sig} * \gamma_b * \gamma_r * \gamma_\beta * \xi & \text{for } \xi < 2.0 \\ z_{2\%} &= 3.0 * H_{sig} * \gamma_b * \gamma_r * \gamma_\beta * \xi & \text{for } \xi \geq 2.0 \end{aligned}$$

in which:

$\gamma_b, \gamma_r, \gamma_\beta$	= reduction factors with respect to influence of a berm, surface roughness and oblique wave attack	[ - ]
$\xi$	= breaker index, see section 1.1.3 of Annex F	

When these new formulas would be applied on the original design for the original hydraulic boundary conditions and the original design criterion, the run-up could be calculated.

The friction coefficient corresponds to  $\gamma_r$ . Thus for  $\gamma_r$  a value of 0.95 is introduced. The reduction factor with respect to the influence of oblique wave attack  $\gamma_\beta$  corresponds to the factor  $\cos \beta$  in the original formula. As  $\beta$  is about 30° for the factor  $\gamma_\beta$  a value of 0.87 is introduced. The factor  $\gamma_b$  is assumed to be 1.0.



For  $H_{sig} = 1.7$  m,  $T_{sig} \approx T_p = 7.0$  seconds and  $\tan \alpha = 1/6$ , the breaker index yields:  $\xi = 1.12$ . All these values yield a wave run-up of  $1.5 * 1.7 * 1.0 * 0.95 * 0.87 * 1.12 = 2.36$  meter. This is 0.50 meter higher than the wave run-up resulting from the originally used formula! This is due to the fact that in the new formula the wave run-up is influenced by the wave steepness. (through the breaker index). For a wave steepness of 0.035, the factor  $1.5 * \xi$  yields the factor  $8 * \tan \alpha$  and the formulas are equal. As the wave steepness is about 0.022 for the originally used wave climate, the run-up will be higher, because of a larger breaker index.

When the values of the reduction factors would be introduced, which are advised nowadays, all the reduction factors yield the value 1.0, in accordance with ref. [12]. This results in a wave run-up of  $1.5 * 1.7 * 1.0 * 1.12 = 2.86$  meter. When the crest level of the dam would be calculated using the advanced wave run-up method, using the same wave characteristics and design criteria as used for the original design, the crest level would be selected 1.0 meters higher. However, the wave characteristics used for the original design do not correspond to reality, as explained in section 8.1.

#### **8.4 INFLUENCE OF OPTIMIZATION METHOD FOR THE GEOMETRIC DESIGN**

For the original design, the crest level was derived by means of applying only the wave overtopping criterion, using a water level distribution, in which 2 cyclonic surges were present. In the present study and contrary to the original design, an economic optimization procedure was used. When this method to derive the geometric dam profile was applied, the crest level appeared to be 10.60 meter + PWD, including the geotechnical settlement, whereas the crest level of the original design was determined to be 10.96 meter + PWD. This is a difference of about 0.4 meter. Since the resulting slope is steeper than the original design, the profile of the redesign turned out to be more economical. Compared to the original design, the cost savings by applying the newly obtained dam profile can be divided into two parts: Cost reduction due to (1) a reduced amount of earth fill and (2) a reduced surface area for the slope protection. The cost reduction could be calculated, using the same unit rates as used for the original design.

The reduction in earth fill, due to a steeper sea side slope and a lower crest level was estimated to be about 74,000 m<sup>3</sup> for the main dam. For a unit rate of 100 Tk per m<sup>3</sup> this corresponds to 7.4 million taka's. For this reference is made to Annex H.

The reduction of the slope protection surface area was estimated to be about 6,300 m<sup>2</sup>. According to ref. [3], the average unit rate for the whole slope protection is 800 Tk/m<sup>2</sup>. Thus the cost reduction for the slope protection becomes:  $6,300 \text{ m}^2 * 800 \text{ Tk/m}^2 \approx 5.0$  million taka's. In total the cost reduction caused by the reduced geometric profile obtained by applying the economic optimization procedure is about 12.5 million taka's. With regard to the total base costs for the main dam this corresponds to a cost reduction of only 2.5 % !

#### **8.5 INFLUENCE OF ADVANCED DESIGN METHOD FOR PLACED BLOCK REVETMENTS**

The method, which was used to design the slope protection for the original design, was based on the Hudson formula. For this formula, reference is made to section 6.6.2. Originally this formula was developed for the design of the slope protection consisting of rip-rap, which contains dumped boulders and stones. In this formula a damage factor was used. By means of changing this value, the formula could be adapted to various sorts of materials and to various degrees of expected damage.

Thanks to research, the formula could be adapted for the use of designing a slope protection comprising placed block revetments. For this purpose the damage factor appeared to be 8.0 . Then the necessary block weight can be derived for which 1% damage is expected, in-dependent of the type of filter layer.

The behaviour of placed block revetments is different from the behaviour of rip-rap under several hydraulic conditions. Nevertheless, this formula was used in 1983, mainly because of the fact that there were no other methods available to design placed block revetments at that time. By means of the Hudson formula the minimum stone weight was calculated to be 1260 N for the main dam. From this the stone thickness and rib size were chosen assuming the practical relation that the block thickness is 0.5 times the rib size.

By means of the newly available analytical method, the influence of the relation between the permeabilities of the filter and cover layer can be analyzed. This is done by means of the leakage length. By means of the analytical method, the minimum block thickness can be derived then, in stead of the block weight by using the Hudson formula. In contrast to the Hudson formula, the damage to the slope protection is thought to be zero for the design condition when the analytical method is used.

Using the new method, by means of which the slope protection can be considered more in detail, the stability of the original slope protection could be checked, using the same hydraulic boundary conditions. This was done in Annex G.

First, the filter fabric appeared to be geometrically unstable; the characteristic mesh size of the geotextile turned out to be too large. In this way, clay, which serves as a base for the slope protection, may wash through the filter fabric. Possibly this will ultimately lead to failure of the slope protection. As the exact properties of the clay are not known, no conclusions should be drawn from this.

Furthermore, it was concluded that the slope protection applied for the original design is not stable at all for the considered design criterion. This is mainly caused by the fact that the leakage length is rather large.

Even for a monsoon return period of 5 years, the slope protection turned out to be unstable, when the newly available design method was used! This can be considered as a rather unexpected conclusion. Accordingly, the probability of failure of the slope protection by the lifting of blocks out of the revetment is higher than 0.2 per year! This failure mode has already occurred, among others during the moderate cyclone of 1985 and apparently also during the 1991 cyclone. Because of their southern track, these cyclones must have caused a seaward directed wind at the Feni dam, implying heavy wave attack at the reservoir side slope. A number of blocks were lifted out of the slope protection at the reservoir side as was observed during a visit after the cyclone occurred.

Hypothetically, the slope protection could be made stable for hydraulic situations having a return period of 50 years, by applying one of the following modifications:

- An increased cover layer thickness of 0.45 meter in stead of 0.25 meter,
- A filter layer comprising pea gravel ( $D_{n,15} = 2$  mm), whose permeability is less, which results in a smaller leakage length,
- A filter layer thickness reduction. This modification should be applied in combination with other modifications, because when only this reduction is considered, a filter thickness of about 0.01 meter should be applied to make the structure stable again. This would be impossible in practice.

The average costs of the slope protection could be calculated per surface area, by analyzing Table H.3 of Annex H. The total slope protection costs for the main dam were estimated to be 55.8 million taka's for a surface area of about 80,700 m<sup>2</sup> (see Annex H). This yields an average costs per m<sup>2</sup> of approximately 690 taka's. Since the average costs per square meter of the original slope protection were about 800 tk, the cost reduction due to the application of the analytical method could be estimated to be about 110 taka's per m<sup>2</sup>. For the redesign, this means a reduction of 110 Tk/m<sup>2</sup> \* 80.700 m<sup>2</sup> = 8.9 million taka's, which is approximately 1.8 % relative to the total base construction costs of the main dam. This small value is mainly caused by the fact that the present slope protection is not overestimated. In fact it is unstable.

When no accretion influence would be taken into account, the total base construction costs for the redesign of the main dam would amount to about 482 million taka's, whereas these costs were about 504 million taka's for the original design. This means a reduction of about 22 million taka's, which was equivalent to about 0.6 million US Dollars in 1985. This is only 4.2 % of the original design base construction costs! This cost reduction can thus be divided into two causes: A reduction of about 2.5 % due to the decrease of the crest level and a reduction of about 1.8% due to the application of a different slope protection. Again it is emphasized that the calculation of the costs is based on an estimation of the unit rates of the various materials. Because of this the comparison of the costs, which is mentioned above is only indicative.

## **8.6 INFLUENCE OF A HYPOTHETICAL METHOD TO PREDICT THE SEDIMENTATION PROCESS**

As explained before, the accretion process influences the geometric dam design. From section 7.5.5 the resulting crest level appeared to be 0.20 meter lower for the redesign, when the accretion influence would be taken into account. After analyzing the resulting costs for the main dam in Table H.3 of Annex H, this crest level reduction causes a reduction of the earthfill of about 19,000 m<sup>3</sup>, which corresponds to 1.9 million taka's, which is about 0.4 % of the total base costs for the main dam.

Besides a reduction of the earthfill amount, the decrease of the crest level causes a decrease of the slope protection costs as well. This cost reduction amounts to about 2.3 million taka's, of which 1.2 million taka's is induced by applying a cheaper slope protection below the level, which will be accreted in the first year after closure.

Altogether, the influence of an anticipation of the accretion amounts to only 4.5 million taka's, which is about 1.0 % of the total base costs of the main dam.

This small influence is mainly caused by the fact that a cheaper slope protection appeared to be unstable. This is caused by the following effect:

The wave height decreases for about 20% due to the accretion of land downstream of the Feni dam, during the first 3 years after closure. However, the wave period stays the same. This can be seen among others, when the Table 16 of section 7.4.6.4 is considered. This causes a reduction of the wave steepness and therefore an increase of the breaker index. As mentioned before in this report, the positive effect of the wave height reduction is approximately equal to the negative effect of the increase of the breaker index.

The calculation of the overtopping amount of sea water is the basis for the optimization procedure to design the geometric dam profile. A larger breaker index yields a larger overtopping amount, when the wave heights stay the same. When additionally the wave height decreases, the increase of the overtopping amount is reduced.

Accordingly, the net influence of the accretion process for the optimization procedure is relatively small. The same considerations are valid for the design of the slope protection, using the analytical method. Consequently, the influence of the anticipation of the accretion process is more or less zero for the slope protection!

## 9 FINAL CONCLUSIONS

- By means of an application of a numerical storm surge model, it is possible to derive a water level distribution for cyclone conditions. This enables a distinction between monsoon and cyclone conditions. For an accurate representation of the water level the model should be calibrated well for the point of interest. This will generally require a lot of time and reliable hydraulic and meteorological observations.
- By means of a numerical wave hindcast model, the wave climate can be estimated more accurately. When the roughly estimated governing wave climate in front of the dam was analyzed for the original design, it appeared that it is not likely that this wave climate occurs in reality.
- The main difference between the advanced and original method to derive the wave run-up is the fact that the breaker index is not taken into account in the original formula. The advanced method is thought to describe the wave run-up effect better. For the original design, the original formula yields a wave run-up, which is a considerable underestimation, compared to the advanced method.
- The use of an optimization method for the design of the geometric dam profile for cyclone conditions yields a lower crest level and a steeper sea side slope angle, compared to the original design. The cost reduction due to the application of the optimization method is estimated to be 2.5 %, which is a rather small influence.
- By means of the newly available analytical method to design placed block revetments, the slope protection of the original design turns out to be unstable. Even for a relatively small return period of 5 years. This means that the estimated probability of failure of the slope protection by uplifting of several blocks out of the cover layer is higher than 0.2 per year. Furthermore, the mesh size of the original filter fabric appeared not to be sufficiently small. Accordingly, the redesign of the slope protection is just 1.8 % more economical with respect to the total base costs of the original design.
- If the accretion process in front of the dam could have been anticipated accurately, the geometric dam profile and the slope protection could have been designed more economically. The estimated reduction of the costs appears to be only about 1 % of the total base costs. This small influence is caused by the fact that the positive effect of the wave height reduction is more or less equal to the negative effect of the breaker index increase.
- Summarizing, when the advanced design methods are applied, having become available since 1983, and when the accretion process downstream of the Feni dam could be anticipated accurately, the total base construction costs turned out to be reduced by about 5% . (2.5% + 1.8% + 1.0%)

At last some salient figures resulting from this study are drawn up in the following Table 25.

## General figures

Reservoir storage at normal operating level	5.8 * 10 <sup>7</sup> m <sup>3</sup>
Total dam length	3,265 meters

## Hydraulic conditions for a return period of 50 years

Original design	Design water level (m + PWD) <sup>1</sup>	8.52	
	Design significant wave height (m) <sup>2</sup>	1.70	
	Design wave period (s) <sup>3</sup>	7.0	
Condition		Monsoon	Cyclone
Redesign excl. accretion	Design water level (m + PWD) <sup>1</sup>	7.69	9.75
	Design significant wave height (m) <sup>2</sup>	1.41	2.26
	Design wave period (s) <sup>3</sup>	4.6	6.6
Redesign incl. accretion	Design water level (m + PWD) <sup>1</sup>	7.69	9.75
	Design significant wave height (m) <sup>2</sup>	1.14	1.94
	Design wave period (s) <sup>3</sup>	4.6	6.6

## Original design features

Dam section		Main dam	Right fl. emb.	Left fl. emb.
Geometric profile	Upper slope angle	1 : 6	1 : 4	1 : 6
	Crest level (m. + PWD)	10.96	9.46	9.46
Main slope revetment	Relative density of cover layer Δ	1.20	0.56	0.80
	Cover layer thickness (m)	0.25	0.25	0.25
	Block rib sizes (m)	0.50	0.50	0.50
	Filter grain size (mm)	30	4	30

## Features of redesign excluding accretion influence

Dam section		Main dam	Right fl. emb.	Left fl. emb.
Geometric profile	Upper slope angle	1 : 5	1 : 4	1 : 5
	Crest level (m. + PWD)	10.60	9.10	9.10
Main slope revetment	Relative density of cover layer Δ	1.20	1.20	1.20
	Cover layer thickness (m)	0.20	0.20	0.15
	Block rib sizes (m)	0.25	0.25	0.25
	Filter grain size (mm)	4	4	4

## Features of redesign including accretion influence

Dam section		Main dam	Right fl. emb.	Left fl. emb.
Geometric profile	Upper slope angle	1 : 5	1 : 4	1 : 5
	Crest level (m. + PWD)	10.40	8.90	8.90
Main slope revetment	Relative density of cover layer Δ	1.20	1.20	1.20
	Cover layer thickness (m)	0.20	0.20	0.15
	Block rib sizes (m)	0.25	0.25	0.25
	Filter grain size (mm)	4	4	4

**Table 25:** Some salient figures resulting from this study

## 10 REFERENCES

- [1] **Hydrographer of the Navy,**  
Admiralty Tide Tables and Tidal Stream tables 1992, Volume 2 Atlantic and Indian Oceans, 1991
- [2] **Department of Hydrography, BIWTA**  
Bangladesh Tide Tables, Dhaka, Bangladesh, 1987
- [3] **Haskoning/MIP Design Cell/BWDB**  
Feni River Closure Dam Final Design Report, September 1983
- [4] **IECO/MIP Design Cell/BWDB**  
Feni River Closure Dam, Design report, including supplement A, June 1981
- [5] **Kampsax International A/A/BCEOM/Danish Hydraulic Institute/Development Design Consultants Ltd./BWDB**  
Cyclone Protection Project II - FAP 7, Feasibility and Design Studies, Draft Project Preparation Report, Appendix C: Embankment design, February 1992
- [6] **D. K. Barua**  
Land Reclamation Project, Some considerations on the selection of the height of empoldering level in the newly accreted south-eastern deltaic region of Bangladesh, Chittagong, March 1990
- [7] **M. Shuhabuddin, Bangladesh University of Engineering and Technology**  
Study of the Siltation process below a closure dam: a case study of the Muhuri closure, May 1988
- [8] **N. Booij, Delft University of Technology Department of Civil Engineering group of Fluid Mechanics**  
User Manual for the Program Duchess, Delft university computer program for 2-dimensional horizontal estuary and sea surges, March 1990
- [9] **N. Booij & L.H. Holthuijzen, Delft University of Technology department of Civil Engineering**  
Hiswa User Manual, Prediction of stationary short crested waves in shallow water with ambient currents, March 1992
- [10] **Kampsax International A/S/BCEOM/Danish Hydraulic Institute/Development Design Consultants Ltd./BWDB**  
Cyclone Protection Project II - FAP 7, Feasibility and Design Studies, Draft Project Preparation Report, Appendix A: Hydraulic studies, February 1992
- [11] **Euroconsult/Delft Hydraulics/Haskoning/Bangladesh Consultants Team/Ministry of Transport and Public Works/Soil Mechanics Laboratory Delft**  
Land Reclamation Project, Final Report Feasibility Study on the Sandwip Cross-dam Development Scheme, Volume III, Annex C: The Sandwip cross-dam, March 1987

- [12] **CUR Gouda/TAW**  
Rapport 155, Handboek voor dimensionering van gezette taludbekledingen (language: Dutch), March 1992
- [13] **Haskoning**  
Biseis v. 1.0, Stability program for circular slip surfaces, May 1989
- [14] **Committee of Experts on Earthquake Hazard Minimization**  
Seismic zoning of Bangladesh and Outline of a code for earthquake Resistant Design of Structure, Geological Survey of Bangladesh, Final Report, 1979
- [15] **Flood Plan Coordination Organization, Ministry of Irrigation, Water Development and Flood Control**  
Bangladesh Action Plan for Flood Control, FAP, Guidelines for project assessment, Dhaka, July 1991
- [16] **Haskoning/Delft Hydraulics/Bangladesh Engineering and Technical Services**  
Meghna River Bank Protection Short Term Study, Final Report, Volume III, Annex C: Geotechnical investigations, February 1992
- [17] **Hydrographer of the Navy**  
Admiralty charts and publications, Chart no. 859, Raimangal River to Elephant Point, Taunton, June 1991
- [18] **Hydrographer of the Navy**  
Admiralty charts and publications, Chart no. 829, Bay of Bengal - Northern Part, Taunton, January 1992
- [19] **Delft Hydraulics/Euroconsult**  
Land Reclamation Project, Second interim report, December 1983
- [20] **E.W. Schwiderski, Naval Surface Weapons Center**  
Global Ocean Tides, Atlas of Tidal Charts and Maps Part II - IX:  
The semidiurnal principle lunar tide ( $M_2$ ), December 1979  
The semidiurnal principle solar tide ( $S_2$ ), March 1981  
The diurnal luni-solar declination tide ( $K_1$ ), May 1981  
The diurnal principle lunar tide ( $O_1$ ), May 1981  
The semidiurnal elliptical lunar tide ( $N_2$ ), May 1981  
The diurnal principle solar tide ( $P_1$ ), May 1981  
The semidiurnal luni-solar declination tide ( $K_2$ ), June 1981  
The diurnal elliptical lunar tide ( $Q_1$ ), June 1981
- [21] **W.D. Eysink**  
Land Reclamation Project, Report no. 15, Basic considerations on the morphology and land accretion potentials in the estuary of the lower Meghna river, December 1983
- [22] **Digital Hydraulics Holland B.V.**  
Dolphin - B1, User Manual, April 1993
- [23] **Delft Hydraulics/Euroconsult**  
Land Reclamation Project, Third Interim Report 1983-1987, March 1988



- [24] **MIP Design Cell-II, BWDB, Dhaka**  
Muhuri Irrigation Project, Report on the Redesign of the Feni River Closure Dam, Part I, June 1982
- [25] **M.M. Vierhout & J.T.L. Yap, Haskoning**  
Land & Water International 59/1987, Optimization of Polder Embankment Design Height in Agricultural Areas, 1987
- [26] **FAO**  
Water Quality for Irrigation, Irrigation and Drainage Paper no. 29, Food and Agriculture Organisation of the United Nations, Rome, 1976
- [27] **IECO**  
Muhuri Irrigation Project, Operation & Maintenance Manual for Project Major Works, March 1983
- [28] **W.W. Massie**  
Coastal Engineering (F11A), Volume I Introduction, Delft University of Technology, Department of Civil Engineering, Hydraulic and Geotechnical Engineering Group, January 1986
- [29] **Rijkswaterstaat, Directie Sluizen & Stuwten Hoofdafdeling Waterbouw, Vakgroep Waterloopkunde en Grondmechanica**  
Waterbouw, rekenregels voor waterbouwkundig ontwerpen, Utrecht the Netherlands, May 1990, Dutch language



**ANNEX A**

**DISTRIBUTION ANALYSIS DURING MONSOON CONDITIONS**

**TABLE OF CONTENTS**

A.1	<u>DISTRIBUTION ANALYSIS SONAPUR STATION</u> . . . . .	A - 3
A.2	<u>MONSOON DISTRIBUTION FOR AZIMPUR STATION</u> . . . . .	A - 6



## ANNEX A DISTRIBUTION ANALYSIS DURING MONSOON CONDITIONS

### A.1 DISTRIBUTION ANALYSIS SONAPUR STATION

In order to analyze whether the water level readings of Azimpur station, which were used for the original design, are reliable, the probability distribution at Sonapur station was derived. For the location of the gauge stations, reference is made to Figure 10 of section 7.3.2. First the monthly means were calculated for each month, during which water level readings are available. Because of the fact that Sonapur station is located at the reservoir side of the Feni Dam, data after closure have not been used. From these monthly means the annual mean values could be derived. It turned out to be more convenient to calculate this for a year starting at April 1st and ending at March 31st. In theory the annual means should be more or less the same for different years. When considering the figures in Table A.1, the annual means of the years 1958-1959 and 1968-1969 appear to be considerably lower than the other annual mean values. As there is no reasonable explanation for this deviation, these data are thought to be rather unreliable and were therefore skipped. For the remaining years, the maximum water levels were derived which were observed during these years. The annual mean and extreme values of the water level are given in following Table A.1.

Year (April - March)	Annual mean (m. + PWD)	Annual max. (m. + PWD)
1958 - 1959	1.256 -> skip	--
1968 - 1969	2.084 -> skip	--
1970 - 1971	2.541	6.46
1971 - 1972	2.648	5.91
1972 - 1973	2.421	6.05
1973 - 1974	2.974	6.61
1974 - 1975	3.068	7.85
1975 - 1976	2.817	5.79
1976 - 1977	2.961	6.72
1977 - 1978	2.700	6.11
1982 - 1983	2.261	5.40
1983 - 1984	2.505	5.76
1984 - 1985	2.681	5.86
1985 - 1986	No tidal influence	--

Table A.1: Annual means and extremes for Sonapur station.

Subsequently, the annual maximum water level observations were ranked by magnitude using a rank number,  $m$ , which is 1 for the largest extreme water level. Then for every value the probability of being equalled or exceeded could be calculated out of the observations as follows:

$$p \{ \text{water level} \geq \text{annual extreme} \} = m/(n+1)$$

= plotting position for the concerned annual extreme.

in which:

$$m = \text{rank number and} \quad [-]$$

$$n = \text{total number of years of record.} \quad [-]$$

In Table A.2 the plotting position derived from the observations are given.

Rank	1	2	3	4	5	6	7	8	9	10	11
Water level + PWD	7.85	6.72	6.61	6.46	6.11	6.05	5.91	5.86	5.79	5.76	5.40
plotting position	0.083	0.167	0.250	0.333	0.417	0.500	0.583	0.667	0.750	0.833	0.917

**Table A.2:** The plotting positions, derived from the ordered annual extremes.

As only 11 years of observation are available, a theoretical distribution for the probability of exceedance should be applied in order to calculate the water levels for small exceedance frequencies. A generally used theoretical distribution for the probability of the water level  $x$  to be equalled or exceeded in one year is the Gumbel distribution for extreme values, which reads:

$$p \{ \text{water level} \geq x \} = 1 - e^{-e^{-A \cdot x + B}} = 1 - e^{-e^{-y}}$$

in which:

$$A, B = \text{coefficients} \quad [-]$$

$$y = \text{so-called reduced or standard variable} \quad [-]$$

In order to let the theoretical distribution correspond to a straight line, this distribution was transformed as follows:

$$-\ln(-\ln(1-p \{ \text{water level} \geq x \})) = y$$

The same transformation for the plotting positions yielded:

$$-\ln(-\ln(1-\text{plotting position})) = -\ln(-\ln(1-m/(n+1)))$$

A linear regression method was applied to obtain the relation between the theoretical probability of exceedance and the water level, by fitting a straight line through the transformed plotting positions. In Figure A.1 the transformed plotting positions and the theoretical distribution is plotted.

The theoretical distribution appears to be:

$$p \{ \text{water level} \geq x \} = 1 - e^{-e^{-1.46 \cdot x + 8.59}}$$

**Probabilities of exceedance  
Sonapur station (incl. cyclonic surges)**

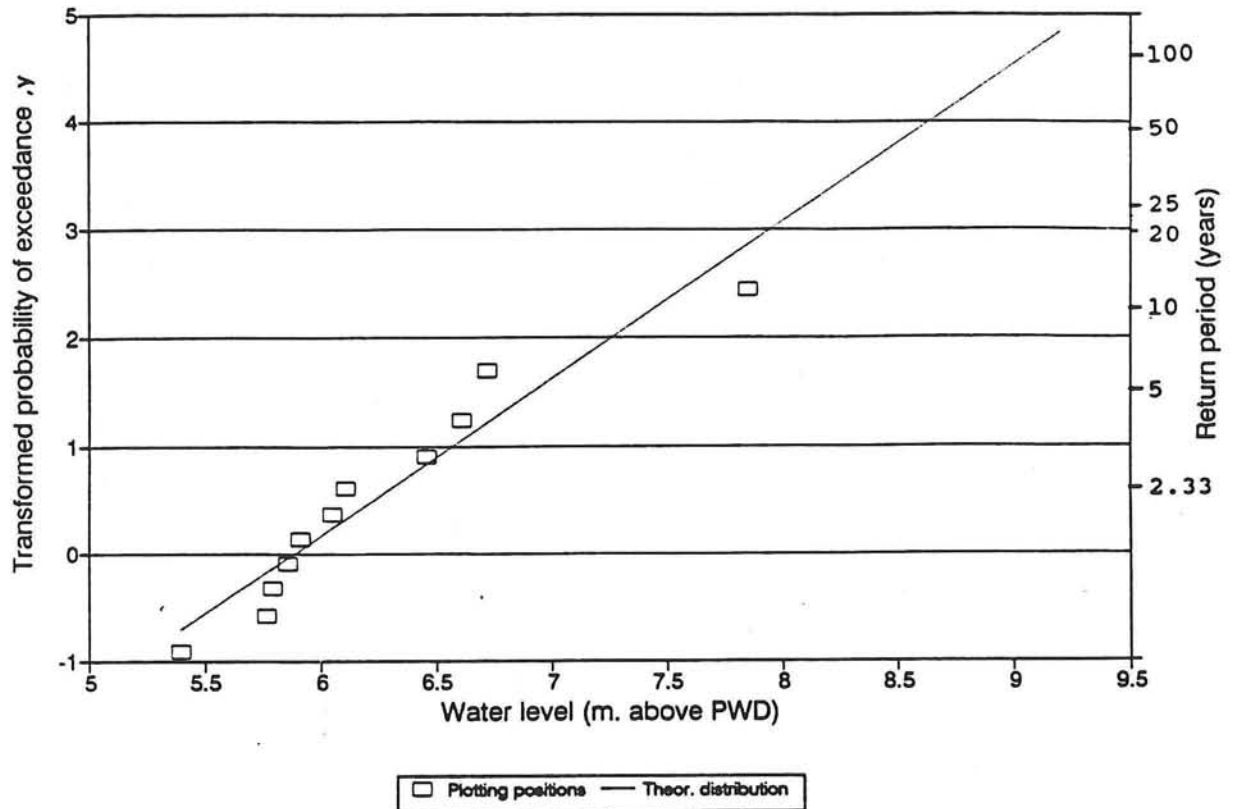


**Figure A.1:** Probability distribution for Sonapur station.

Due to the limited period of observation, which comprises only 11 years, the accuracy of the derived theoretical distribution is rather small, when Figure A.1 is considered. Here it can be seen that the difference between some plotting positions and the theoretical distribution is relatively large. The water levels at Sonapur station for several return periods are given in Table A.3.

Return periods (years)	2.33	5	10	20	25	50	100
Water levels Sonapur (m + PWD)	6.28	6.92	7.43	7.92	8.08	8.56	9.04
Water levels Azimpur (m. + PWD) original distribution	6.48	7.05	7.51	7.95	8.08	8.52	8.94

**Table A.3:** Water levels for return periods using the theoretical distribution for Sonapur, compared with the ones used on the original design. In meters above PWD.

In spite of the inaccuracies, it can be concluded that the correspondance of the two distributions is rather good. Because of this, the observations which the original design is based on, are thought to be rather reliable.

## A.2 MONSOON DISTRIBUTION FOR AZIMPUR STATION

For the years of which data are available, from 1957 till 1977, the annual means were calculated. For this see Table A.4. From this table it is obvious that from 1969 onwards, the annual means are structurally higher than the annual means before this year. Probably the reference level was shifted at that time. As explained in Section 6.3 of the main report, only data from 1958-1967 were used, like the original design.

Year	Annual mean m. + PWD	Annual max. m. + PWD	Year	Annual mean m. + PWD	Annual max. m. + PWD
1957	1.779	4.52	1968	2.008	5.65
1958	2.365	6.38	1969	2.450	6.23
1959	2.313	6.44	1970	2.534	6.38
1960	2.234	6.71	1971	2.623	5.95
1961	2.390	6.47	1972	2.579	6.19
1962	2.206	6.13	1973	2.795	6.22
1963	1.979	5.89	1974	3.078	8.14
1964	2.187	6.56	1975	2.788	5.80
1965	2.063	6.10	1976	3.033	6.71
1966	1.971	5.55	1977	2.764	6.01
1967	1.971	5.49			

**Table A.4:** Annual means and extremes for Azimpur station.

In order to determine the probability distribution during monsoon conditions, the cyclonic surges had to be filtered out of the used records. The cyclones occurring during that period were analyzed, using the cyclone record obtained from the Bangladesh Meteorological Department. In Table A.5 the properties of the two cyclones, which caused monthly extreme water levels, which were also equal to the annual maximum level, are described. For an explanation of the cyclone phenomenon Section 3.5 of the main report is referred to.

year	month	point of landfall	max. wind speed (km/h)	pressure drop (mBar)	Cyclonic surge (m. + PWD)	Ann.max. excl.cyc. (m. + PWD)
1961	May	Noakhali, near Feni	113	20	7.08	6.47
1966	Oct.	Sandwip island	139	31	7.78	5.55

**Table A.5:** Description of cyclones during which the observed monthly maximum water level is equal to the annual maximum.



The annual extremes for these two years had to be replaced by the maxima of the remaining months in the concerned year. Then the observations are assumed to correspond to monsoon conditions. In the same way as described for Sonapur station, a new theoretical Gumbel distribution for monsoon conditions could be determined, which was used for design purposes of the Feni River Closure Dam. This reads:

$$p \{ \text{water level} \geq x \} = 1 - e^{-e^{-2.25 \cdot x + 13.37}}$$

Finally the water levels for various return periods were calculated. The results are given in Table A.6.

Return periods (years)	2.33	5	10	20	25	50	100
Water level (m + PWD)	6.21	6.62	6.95	7.27	7.37	7.69	8.00

**Table A.6:** Water levels for various return periods for the Feni Dam. Monsoon conditions.

From this table it can be seen that the water level is 7.69 meters for a return period of 50 years. This is 0.83 meters lower than the water level for the same return period, when the original design distribution would be considered. This difference can be ascribed to the omittance of the cyclonic surges.

In the Figure A.2 the theoretical distribution and the plotting positions are plotted.

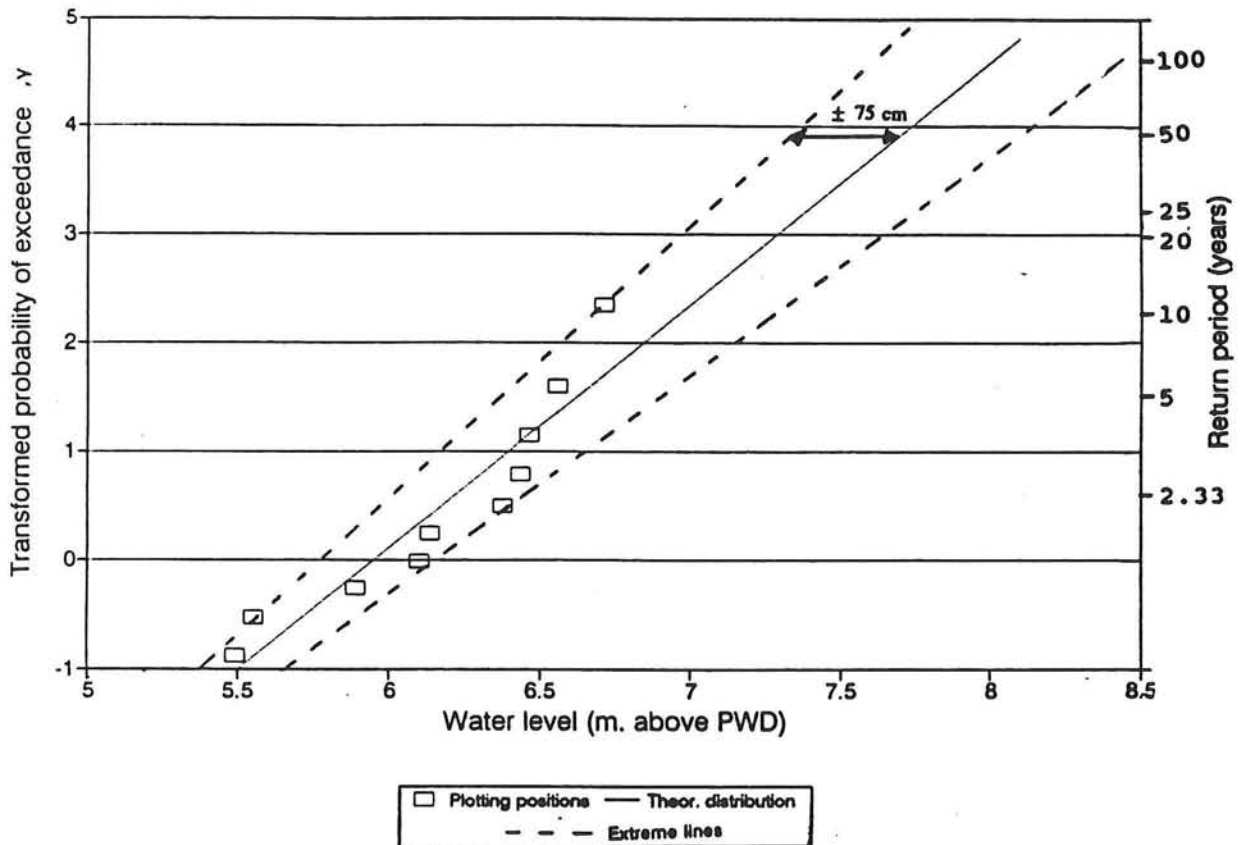


**Figure A.2:** Probability distribution for the Feni dam during monsoon conditions.

From this figure it can be concluded that the accuracy of this distribution for high return periods is not large, due to the limited period of observation. For a return period of 50 years for example the error was estimated to be about 75 cm. However, as no other data are available, these figures were used as a basis for the redesign.

## ANNEX B

### THE SET-UP OF A NUMERICAL STORM SURGE MODEL

#### TABLE OF CONTENTS

B.1	<u>MODEL SCHEMATIZATION</u> .....	B - 3
B.2	<u>GENERAL SET-UP OF THE STORM SURGE MODEL</u> .....	B - 4
	B.2.1 MODEL AREA .....	B - 4
	B.2.2 GRID SPACING .....	B - 5
	B.2.3 TIME STEP .....	B - 5
B.3	<u>INPUT PARAMETERS</u> .....	B - 5
	B.3.1 BOTTOM FRICTION .....	B - 5
	B.3.2 BATHYMETRY AND TOPOGRAPHY .....	B - 6
	B.3.3 TIDE GENERATION AT THE SOUTHERN MODEL BOUNDARY ...	B - 6
	B.3.3.1 Diurnal and semi-diurnal constituents .....	B - 6
	B.3.3.2 Fortnightly constituent .....	B - 10
	B.3.3.3 Derivation of mean sea level .....	B - 10
	B.3.4 THE RIVER DISCHARGES .....	B - 11



## **ANNEX B THE SET-UP OF A NUMERICAL STORM SURGE MODEL**

### **B.1 MODEL SCHEMATIZATION**

In order to construct a numerical model, schematizations of reality have to be made. The main schematizations are drawn up below:

#### **Discretization**

First of all, Duchess is a mathematical model, which means that it discretizes reality by means of transforming properties, which are continue in nature, to grid points.

#### **Tidal schematisation**

Only the eight main tidal constituents with periods of about one day and half a day were introduced in the model as a boundary condition at the southern boundary. In reality the tide comprises more tidal constituents.

#### **Seasonal change**

In reality, the monthly seasonal change values vary over the model area for a certain month of the year. The seasonal change was schematized to be constant over the model area.

#### **Tidal bore**

Due to the relatively coarse computational grid, this hydraulic jump cannot be simulated properly by Duchess. As a matter of fact this is not important, because only extreme water levels were considered, not the variation of the water levels in the time.

#### **Water density differences**

This effect cannot be dealt with by Duchess. The MSL change caused by the variation of the water density differences cannot be generated. The water density in the model area is assumed to be constant. The time related variation of MSL had to be introduced by means of the boundary conditions.

#### **Morphological changes**

The bathymetry in the lower Meghna estuary is subject to rather big changes in a period of several years. In the greater part of the model area, the bathymetry is assumed to be constant for the life time of the Feni River Closure dam. So here only one set of bathymetry charts were used. For the area near the Feni Dam however, these bottom changes were measured well after construction of the dam. For the present study, the calculated water levels are assumed not to be influenced by the sedimentation process, because the wave length of the tidal wave is much larger than the size of the sedimentated area in front of the dam.

## Ocean currents

In reality, water currents due to tide and ocean currents cause water velocities at the southern boundary, which are not equal to zero. The sensitivity of the water levels near the Feni Dam for currents at the southern boundary is assumed to be negligible.

## B.2 GENERAL SET-UP OF THE STORM SURGE MODEL

In this section the general set-up of the model is given. The model area is defined and illustrated in Section B.2.1. The discretisations in place and time are given in the subsequent sections. In Section B.2.2 the mesh size is given and the time step is defined in Section B.2.3.

### B.2.1 MODEL AREA

The southern boundary had to be chosen so far away from the coast that the water depths are sufficiently large to assume that the bottom does not influence the water movement any more by means of bottom friction. Furthermore, at this depth, the wind set-up is relatively small. It is assumed that this is the case if the depth is more than 1000 meters below mean sea level. As a result, it was determined that the southern boundary is located at  $19^{\circ}48'$  latitude north, approximately 350 kilometres south of the Feni Dam. The eastern, western and northern boundaries successively comprise the coast of India, Bangladesh and Burma. Figure B.1 is referred to for the location of the model area.

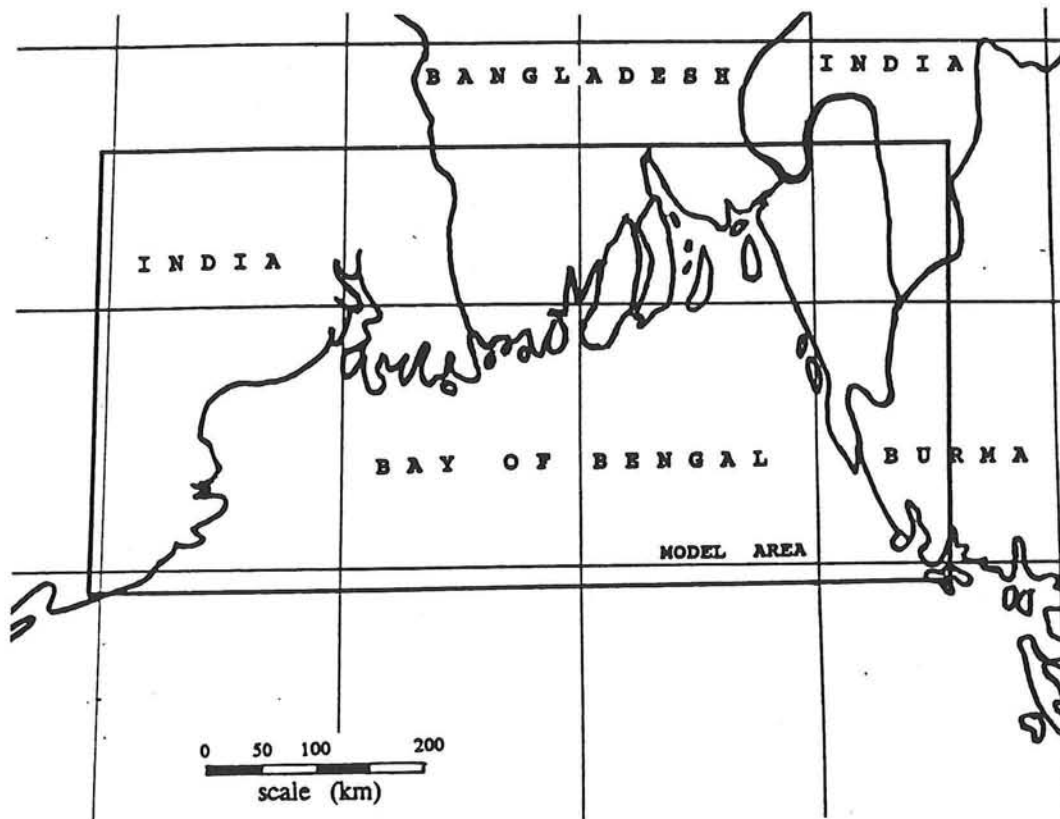


Figure B.1: Model area of the 2 dimensional storm surge model

### B.2.2 GRID SPACING

Duchess demands that the total amount of grid points is less than 10.000, with regard to the available memory space and computational time. With this restriction, a grid spacing of 5500 meters was applied. In this way the mesh size is as small as possible and a rather good representation of reality could be achieved.

### B.2.3 TIME STEP

The model is implicit, so in general no instabilities will occur. In order to get a sufficiently accurate computation, this time step was chosen in such way that the Courant number is less than 10. This Courant number reads:

$$C = \sqrt{g * h} * \frac{\Delta t}{\Delta x}$$

In which:

C	= the Courant number,	[ - ]
g	= the gravitational acceleration,	[ m/s <sup>2</sup> ]
h	= maximum water depth,	[ m ]
Δ t	= time step,	[ s ]
Δ x	= mesh size	[ m ]

This is why the time step was determined to be 450 seconds, because the maximum water depth in the model area is approximately 1400 meters. Here probably a larger time step could be used, because the point of interest is located in relatively shallow water. Yet, the mentioned time step was applied, because the total computational time appeared to be sufficiently small already.

## B.3 INPUT PARAMETERS

In this section it is described how the various input parameters to be introduced in the model were obtained. The successively treated parameters are: The bottom friction, the bathymetry and topography, the tide at the southern boundary and the river discharges.

### B.3.1 BOTTOM FRICTION

The value for the bottom friction has not been surveyed in the model area at all. For the parameter "Fr", which has to be introduced in Duchess, the following relation is valid:

$$Fr = g/C^2,$$

in which,

g	= acceleration of gravity	[ m/s <sup>2</sup> ]
C	= Chezy coefficient	[ m <sup>0.5</sup> /s ]

The parameter "Fr" was determined to be the main calibration parameter of the model. How the calibration procedure was carried out is described later.

### **B.3.2 BATHYMETRY AND TOPOGRAPHY**

In order to generate water level variations and currents in the model area it is necessary to introduce the bottom levels in each grid point in the mathematical model. Thus, a bottom file had to be constructed in which the values for every grid point are given. The bottom levels were introduced in the model with reference to MSL. The bottom depths were derived from several sources.

- 1) For the largest part of the model area, south of the line 22°30' latitude, the depth have been obtained from British Admiralty Charts (ref. [17] and [18]). Here depths are given relative to CD and had to be transformed to MSL.
- 2) North of this line, in the neighbourhood of the Feni Dam, soundings were used, that were obtained from the Land Reclamation Project in 1985 (ref. [19]). Here depths are given below PWD.

For an explanation of the used datums, Chapter 4 of the main report is referred to. At every grid point the bottom depth relative to CD or PWD had to be determined and introduced in the bottom file. After this procedure, factors to transform these values to MSL had to be derived for every grid point in the model area. These factors were derived by interpolation between the tidal stations, for which the relations between the various datums are known. In this way a file comprising transformation factors for every grid point was achieved. By means of adding this file to the original bottom file, the bathymetry was obtained relative to MSL. In Figure B.2 the contour lines of the bathymetry file are given. As there are certain depth inaccuracies, this parameter was used as a calibration parameter for the model, to a certain extent. In the area of interest the topography had to be introduced by means of the mentioned bottom file. The topography comprises the land levels above MSL. During high cyclonic storm surges, when dry land in the coastal zone may start to inundate, the hydraulic situation will also depend on the topography. As the topography is not known accurately, this parameter could be used for calibration purposes as well.

### **B.3.3 TIDE GENERATION AT THE SOUTHERN MODEL BOUNDARY**

The tide to be introduced at the southern boundary comprises diurnal, semi-diurnal and fortnightly constituents. These are described in Sections B.3.3.1 and B.3.3.2. Finally the derivation of the MSL is given in Section B.3.3.3.

#### **B.3.3.1 Diurnal and semi-diurnal constituents**

In order to obtain the parameters, which comprise the amplitude and the phase of the diurnal and semi diurnal constituents at the southern boundary for a certain time, two methods could be used: The Simplified Harmonic Method using the British Admiralty Tide Tables and the Schwiderski method.



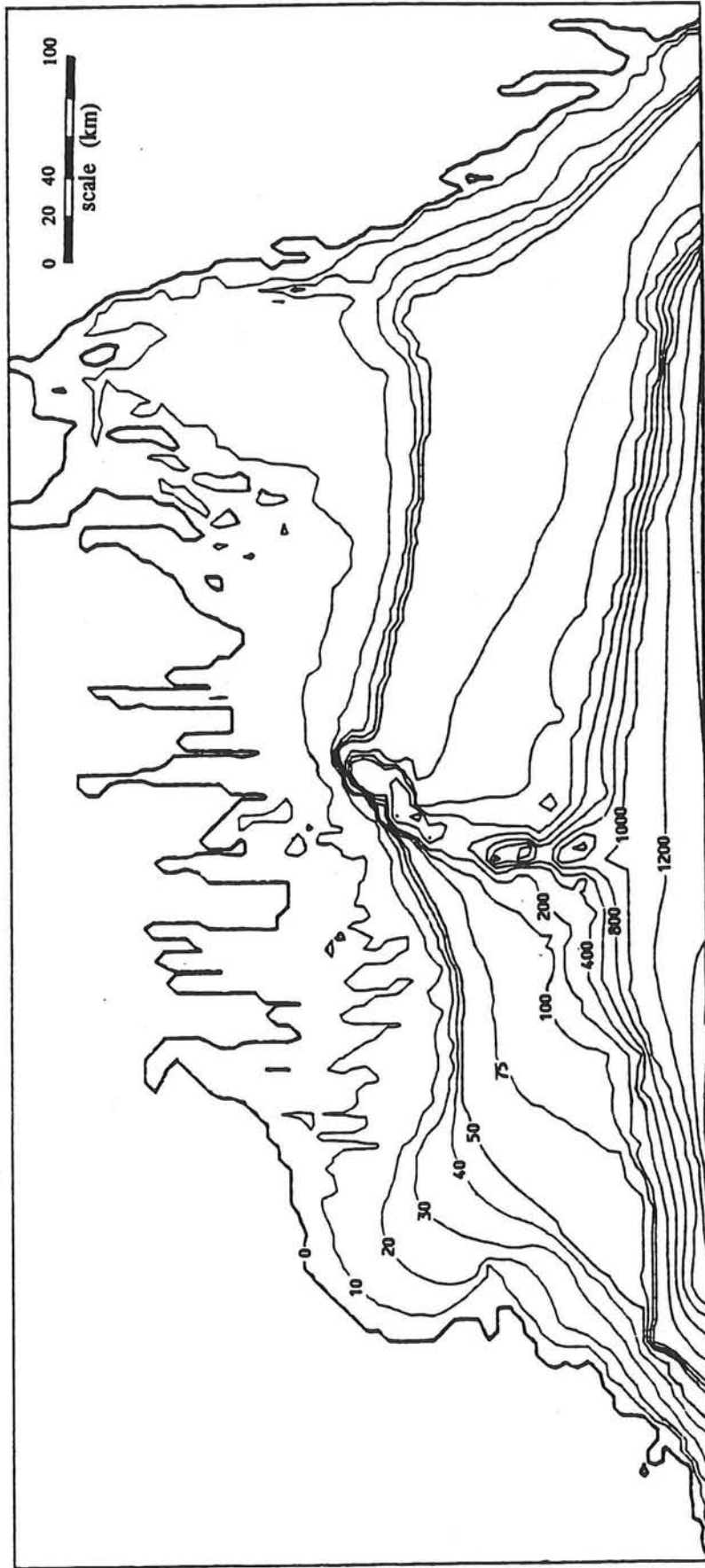


Figure B.2: Bathymetry of the model area in meters below MSL

## Simplified Harmonic Method

In the British Admiralty Tide Tables (ref. [1]) amplitudes of the four main tidal constituents can be found for several gauge stations along the coast of India, Bangladesh and Burma. In order to obtain the right phase for each constituent at a certain time when the simulation starts, the so-called Simplified Harmonic Method has to be used. The parameters of the tidal constituents would have to be interpolated over a distance of about 750 km. between a tidal gauge station along the east coast of India and a station along the coast of Burma in order to get the tidal input parameters along the southern boundary of the model area.

## Schiderski's tidal prediction method:

In 1978 Schwiderski introduced a unique hydrodynamic interpolation technique to compute partial global ocean tides by means of a hydrodynamic model. In this way it was possible to construct the eight main tidal constituents any where in the open oceans. The resulting tidal amplitudes and phases were tabulated as a  $1^\circ \times 1^\circ$  grid system, covering the whole oceanic globe. Interpolation would have to take place between the known values of the mentioned grid system over a distance of about 100 kilometres. Then the boundary conditions at the southern boundary could be obtained. See Figure B.3.

Schwiderski claims that the accuracy of his method is less than 5 cm. This is less than the acquired accuracy using the Simplified Harmonic Method, explained in the British Admiralty Tide Tables, where only 4 constituents are considered. The application of Schwiderski's method is also more advisable because of the higher accuracy reached through interpolation over a smaller area. It was thus determined to use Schwiderski's method.

In general, the methodology to derive the southern boundary condition is described below. For the mentioned Schwiderski-grid points, the values for the amplitude ( $\xi$ ) and the Greenwich phase ( $\delta$ ) are given per constituent. Using the formulas which vary per constituent, the astronomical argument ( $\chi$ ) can be calculated for a specific time in a certain year. For more detailed information reference is made to ref. [20]. The general formula for the tidal elevation reads:

$\zeta = \xi * \cos (\sigma * t + \chi - \delta)$ , in which:

$\zeta$ = tidal elevation at the southern boundary,	[ m ]
$\xi$ = tide amplitude,	[ m ]
$\sigma$ = tide frequency,	[ s <sup>-1</sup> ]
$t$ = Bangladesh Standard Time (BST),	[ s ]
$\chi$ = astronomical argument and	[ ° ]
$\delta$ = Greenwich phase.	[ ° ]

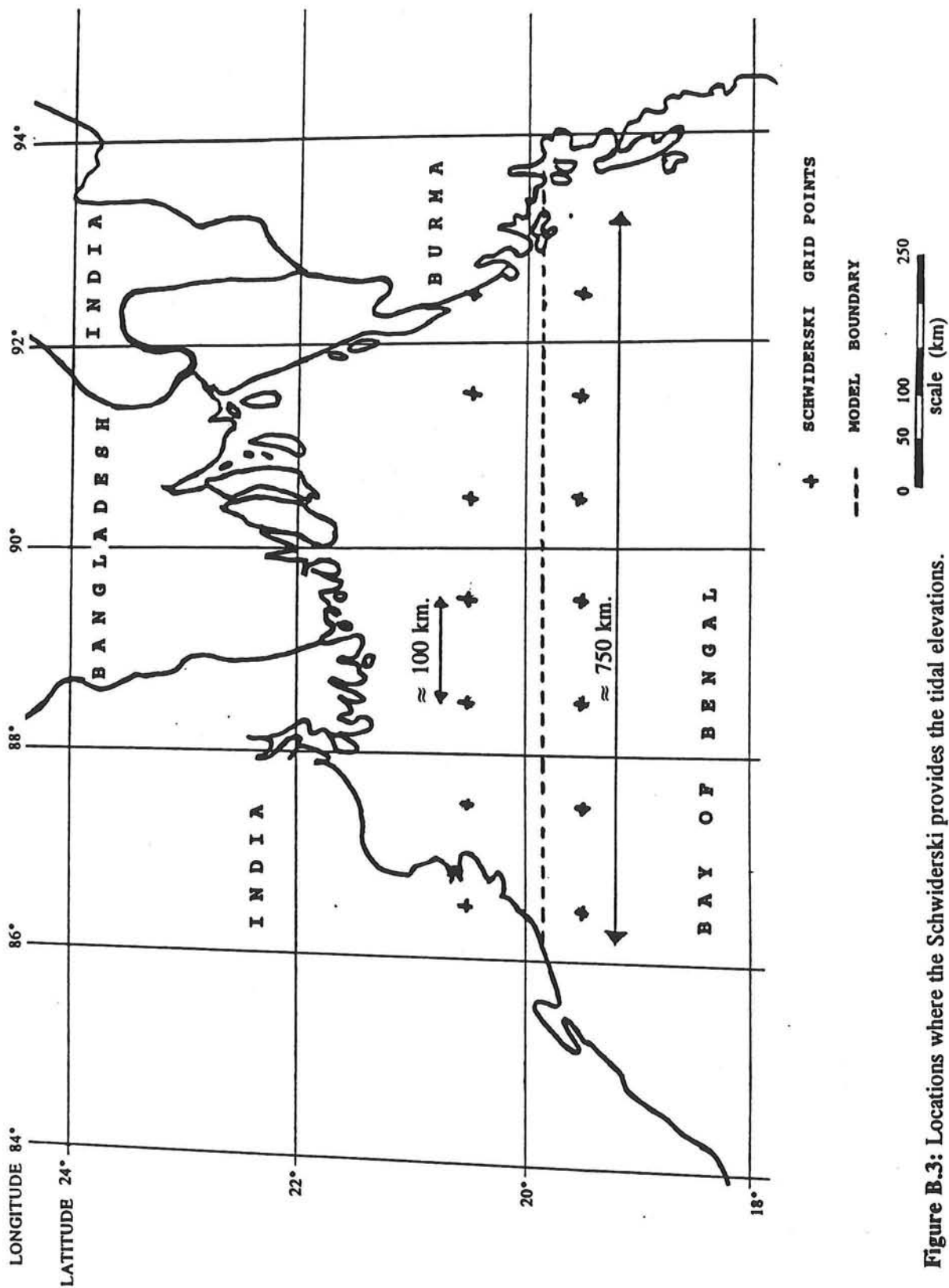


Figure B.3: Locations where the Schwidorski provides the tidal elevations.

### B.3.3.2 Fortnightly constituent

Due to shallow water effects, the tidal constituent having a period of 14 days is important in the northern part of the Bay of Bengal. In some stations this component results in a MSL change of more than 20 cm. This fortnightly constituent was not introduced in the southern boundary condition. As this shallow water effect is not constant over the model area, the resulting water level values near each gauge station have to be corrected separately after computation, by means of a correction factor. These correction factors, obtained from the the British Admiralty Tide Tables (ref. [1]), depend on the number of days after spring tide and are given in Table B.1. For the location of the mentioned gauge stations, see Figure 5 of section 4.3 of the main report.

No. of days after spring	Correction of M.S.L. (m.) for gauge stations		
	Char Changa	Sandwip	Chittagong
0	+ 0.18	+ 0.06	+ 0.13
1	+ 0.16	+ 0.05	+ 0.12
2	+ 0.11	+ 0.04	+ 0.08
3	+ 0.04	+ 0.01	+ 0.03
4	- 0.04	- 0.01	- 0.03
5	- 0.11	- 0.04	- 0.08
6	- 0.16	- 0.05	- 0.12
7	- 0.18	- 0.06	- 0.13

Table B.1: MSL corrections due to fortnightly component.

### B.3.3.3 Derivation of mean sea level

Due to the seasonal influences, the time related MSL variations throughout the year appear to be rather large. In some gauge stations the MSL may be 0.30 m. higher in summer than in winter. Therefore, this variation has to be taken into account in the model. In ref. [1] the monthly variations of MSL are tabled for all the gauge stations along the coast. As the place related MSL variation appears to be rather small over the model area for a certain month, the MSL was assumed to be constant over the area and one mean value was introduced. This was done by adjusting the mean value of the tidal constituents at the southern boundary. The concerned correction factors were obtained from ref. [1] and are given in Table B.2.

Month	January	February	March	April	May	June
Factor	-0.3	-0.4	-0.4	-0.3	-0.1	+0.2
Month	July	August	September	October	November	December
Factor	+0.4	+0.5	+0.4	+0.2	+0.0	-0.2

Table B.2: Correction factors to take into account the seasonal change of MSL.

### B.3.4 THE RIVER DISCHARGES

As mentioned before, the discharge of the three main rivers in the area, which confluence in the lower Meghna, influence the water movement in the northern part of the Bay of Bengal.

As the discharge varies widely during a year, the mean monthly discharge during the simulated month is chosen for introduction in the numerical model. The values to be introduced in the model are given in Table B.3, according to ref. [21].

Month	January	February	March	April	May	June
Discharge (m <sup>3</sup> /s)	8,900	7,600	7,600	10,100	21,900	40,800
Month	July	August	September	October	November	December
Discharge (m <sup>3</sup> /s)	65,500	91,200	79,700	45,900	20,600	11,800

**Table B.3:** Mean monthly discharges of the lower Meghna



## ANNEX C

### MODEL CALIBRATION

#### TABLE OF CONTENTS

C.1	<u>INTRODUCTION</u> .....	C - 3
C.2	<u>CALIBRATION WITHOUT WIND AND AIR PRESSURE INFLUENCE</u> .....	C - 3
C.2.1	METHODOLOGY .....	C - 3
C.2.1.1	Depth adjustment .....	C - 3
C.2.1.2	Bottom friction adjustment .....	C - 4
C.2.2	CALIBRATION RESULTS WITHOUT WIND AND AIR PRESSURE INFLUENCE .....	C - 5
C.3	<u>CALIBRATION OF THE CYCLONE GENERATING MODEL</u> .....	C - 10
C.4	<u>CALIBRATION AND VERIFICATION OF THE MODEL COMPLEX INCLUDING CYCLONES</u> .....	C - 10
C.4.1	CHOICE OF CYCLONES FOR CALIBRATION AND VERIFICATION .	C - 10
C.4.2	CALIBRATION USING THE 1985 CYCLONE .....	C - 11
C.4.3	VERIFICATION OF THE MODEL USING THE 1991 CYCLONE. ....	C - 14
C.4.4	VERIFICATION OF THE MODEL USING THE 1981 CYCLONE ....	C - 15
C.4.5	CALIBRATION OF THE AREA NORTH OF CHITTAGONG .....	C - 15
C.4.6	CONCLUSIONS .....	C - 17





## ANNEX C MODEL CALIBRATION

### C.1 INTRODUCTION

Due to the model schematizations and the fact that some input parameters are not known, the calculations of the first computer run will generally not correspond to the measured values. The model has to be calibrated. That means that uncertain input variables have to be modified in such manner that the computed values more or less correspond to the real values. In that way a numerical model is achieved that is able to simulate reality in a reasonable way.

First the model was calibrated by adapting the depth and friction values, without taking the wind and air pressure influences into account. After this, the model complex, including wind velocities and air pressures, was calibrated by adapting the wind friction parameter. All this is explained in next sections.

### C.2 CALIBRATION WITHOUT WIND AND AIR PRESSURE INFLUENCE

#### C.2.1 METHODOLOGY

For the calibration procedure without wind effects the computational results had to be compared to water levels, occurring in reality when the wind set-up is excluded. This is why tidal predictions are used in which fortnightly and seasonal effects are included and wind effects are excluded. The model had to be moderated until the computed water levels would be more or less equal to the tidal predictions at five gauge stations near the Feni River Closure Dam. These gauge stations are from west to east: Hiron Point, Char Changa, Sandwip, Khal no.10 (Chittagong) and Cox's Bazar. For the location of these gauge stations, Figure 5 of section 4.3 of the main report is referred to.

For calibration the period from May 17th till May 21st in 1991 was considered, which is a period in between spring and neap tide and during the pre-monsoon. This season is one of the periods of interest, because cyclones tend to occur during the pre- and post-monsoon.

##### C.2.1.1 Depth adjustment

First the depth was adjusted. It is obvious that the tidal phase will vary with the depth, because of the fact that the propagation speed of a tidal wave can be written as follows:

$$c_{\text{tide}} = \sqrt{g * d}$$

in which:

$$g = 9.81$$

$$d = \text{water depth}$$

$$[ \text{m}^3/\text{s} ]$$

$$[ \text{m} ]$$

In theory the phase will increase when the depth is increased. The depth was modified until the resulting tidal phase corresponded well to the tidal predictions. Modification limits were defined for this calibration procedure. The depth values could be modified as long as the modification is less than the error caused by the inaccuracy of the soundings and the error of reading the bathymetric chart.

These limits were determined to be approximately 10% plus or minus the values on the bathymetric charts. Furthermore, the tidal range changes as well, when the depth is varied. This is because of the fact that the depth appears, among others, in the friction term in the equation of motion. This term reads:

$$\text{Friction term} = Fr * \frac{|Q| * Q}{d^2} = \frac{g}{C^2} * \frac{|Q| * Q}{d^2}$$

in which:

Fr = friction factor	[ - ]
Q = current	[ m <sup>2</sup> /s ]
d = water depth	[ m ]
C = Chezy coefficient	[ m <sup>1/2</sup> /s ]

In general it can be stated that the friction term will decrease, when the depth is increased. This causes a higher tidal range near the coast. All this was demonstrated by the model runs.

### C.2.1.2 Bottom friction adjustment

When the depth values had been derived, the bottom friction could be modified. When the friction is decreased, this will result in an increase of the tidal amplitude. The modification of the friction was carried out for separate parts of the model area by changing the factor "Fr" of the above mentioned friction term in the equation of motion.

First the model area was divided into several parts, corresponding to the location of the 5 stations. The size and the friction value of the various parts of the model area were adjusted by trial and error. The calibration procedure was stopped, when the difference between the calculated and predicted water level was less than the maximum error caused by inaccuracies of the input variables. This part of the study turned out to take a lot of time. The following types of inaccuracies can be considered:

#### Numerical accuracy

The order of the numerical accuracy is second order in space and time. An extra run was executed with a time step of 150 seconds. The differences between the calculated values of this run and the run with a time step of 450 seconds appeared to be in the order of 1 mm., which is relatively small.

#### Tide at southern boundary

According to Schwiderski the maximum error of the amplitudes of the various tide constituents is 5 cm. The error of omitting the other tide components with minor amplitudes was estimated to be 5 cm as well. In this case, the relative error is defined as the total error divided by the average amplitude at the southern boundary ( $\approx 1.5$  meters). In this way the relative accuracy of the tide input is about  $(0.05 + 0.05) / 1.5 \approx 7\%$ . Due to an accuracy of 7% at the southern boundary, the resulting accuracy of the calculated water level near the northern boundary was assumed to be 7% as well.

#### River discharge

When running Duchess with a river discharge which was 20 % higher than the mean value during the concerned month, the water level appeared to be more or less insensitive to this change. The accuracy of this input parameter appeared to be small. In reality, the MSL is mainly influenced by salinity differences, which cannot be represented by Duchess.

## Mean sea level

Due to seasonal influences, the MSL varies. This variation was schematized to be the same all over the model area. This introduced an error of about 0.1 m. Furthermore, the values given in the British Admiralty Tide Tables are mean values and do not necessarily repeat themselves exactly from year to year. This causes an error of about 0.1 meter. The total error, caused by this item is accordingly  $0.1 + 0.1 = 0.2$  m. The relative error is defined as the total error divided by the average amplitude in the considered area near the Feni Dam ( $\approx 4$  meters). This is approximately 5 % .

In this case it was assumed, that the required accuracy would be obtained, when the difference between the calculated and the predicted maximum water levels would be less than about 7% of the mean tidal range in the area.

### C.2.2 CALIBRATION RESULTS WITHOUT WIND AND AIR PRESSURE INFLUENCE

The situation near the tidal stations Hiron Point, Char Changa, Chittagong and Cox's Bazar could be calibrated with an error, which is less than the required accuracy, rather easily. For the gauge station on Sandwip Island, it is very difficult to reach the minimum accuracy. The water levels near this station are highly influenced by the friction factors in the neighbouring areas. Eventually, it was found out that the water levels near Sandwip correspond well to the predicted values, when the friction factor is kept low in the biggest part of the model area. The errors finally obtained near the several gauge stations are given in Table C.1. The results were considered to be sufficiently accurate. However, the applied friction factors are very low and they probably do not occur in reality. For the resulting friction values, reference is made to Figure C.6. The low friction values can be justified, because these are supposed to correct the schematization errors.

Gauge station	A: Error of HW	B: Tidal range	Rel. accuracy (A/B *100 %)
Hiron Point	0.06 m.	1.59 m.	4 %
Char Changa	0.14 m.	1.95 m.	7 %
Sandwip	0.22 m.	3.22 m.	7 %
Khal no.10	0.18 m.	2.87 m.	6 %
Cox's Bazar	0.12 m.	1.94 m.	6 %

Table C.1: Calculation of the relative accuracy obtained after calibration.

In the following Figures C.1 - C.5 the results of the calibration are plotted.

- Figure C.1: Results of calibration for Hiron Point.
- Figure C.2: Results of calibration for Char Changa.
- Figure C.3: Results of calibration for Sandwip.
- Figure C.4: Results of calibration for Khal no. 10.
- Figure C.5: Results of calibration for Cox's Bazar.
- Figure C.6: Map of introduced friction values in the model.

Final calibration without wind effects  
Hiron Point

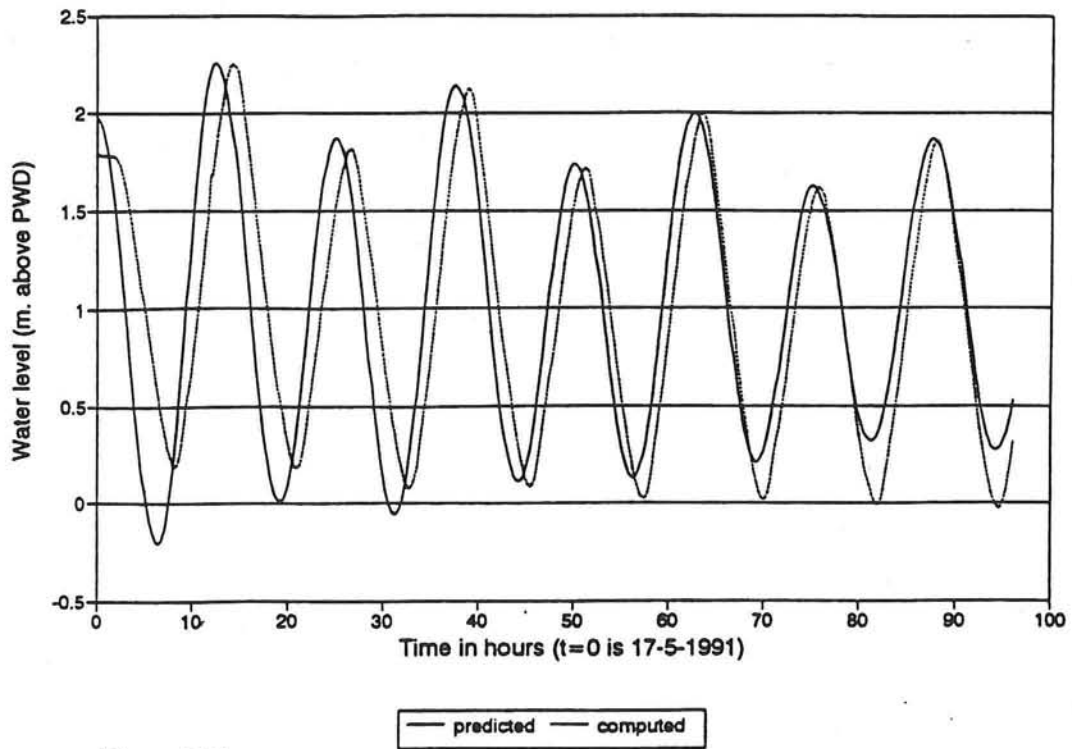


Figure C.1

Final calibration without wind effects  
Char Changa

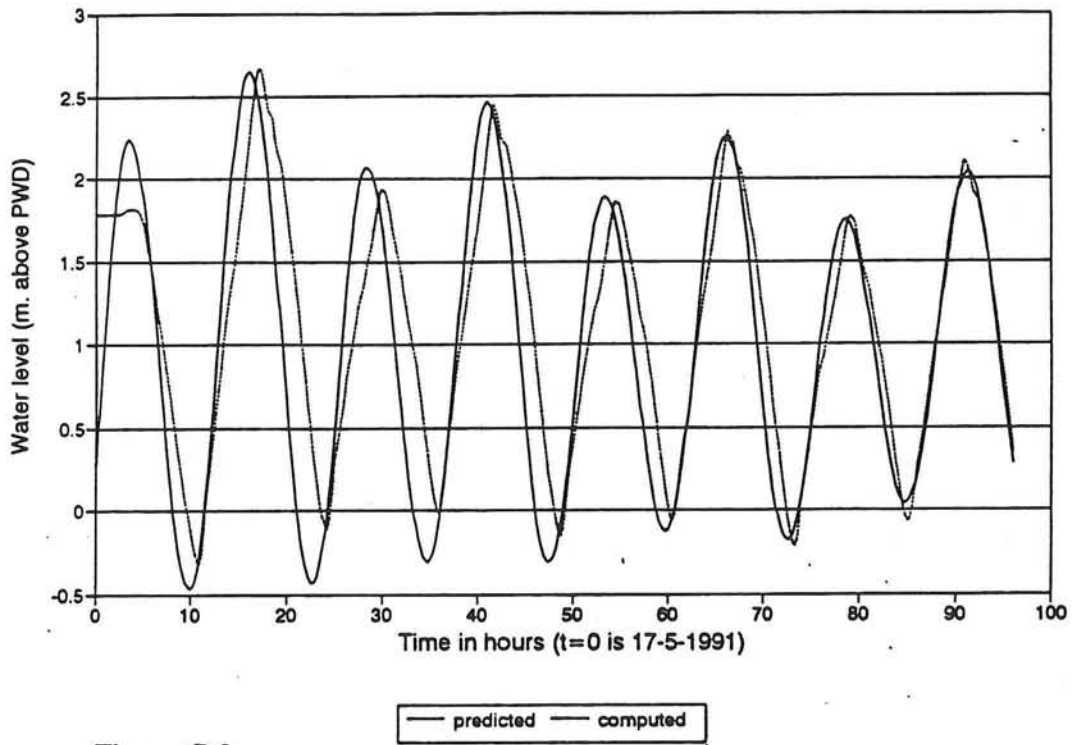


Figure C.2

Final calibration without wind effects  
Sandwip

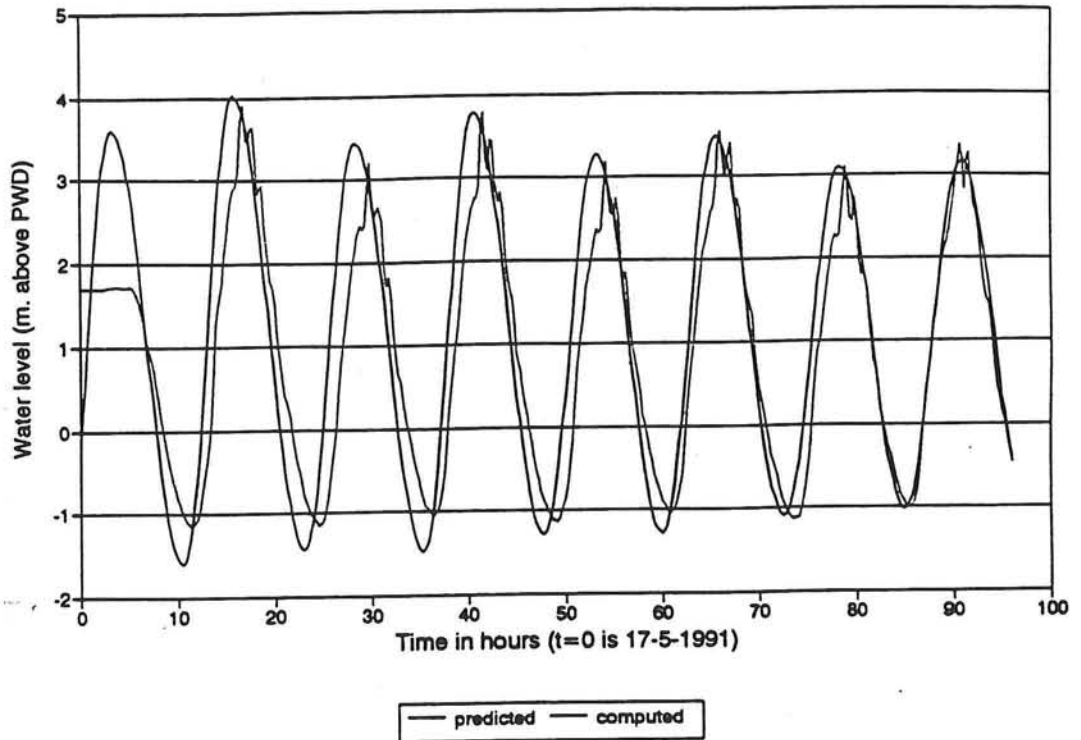


Figure C.3

Final calibration without wind effects  
Khal no. 10

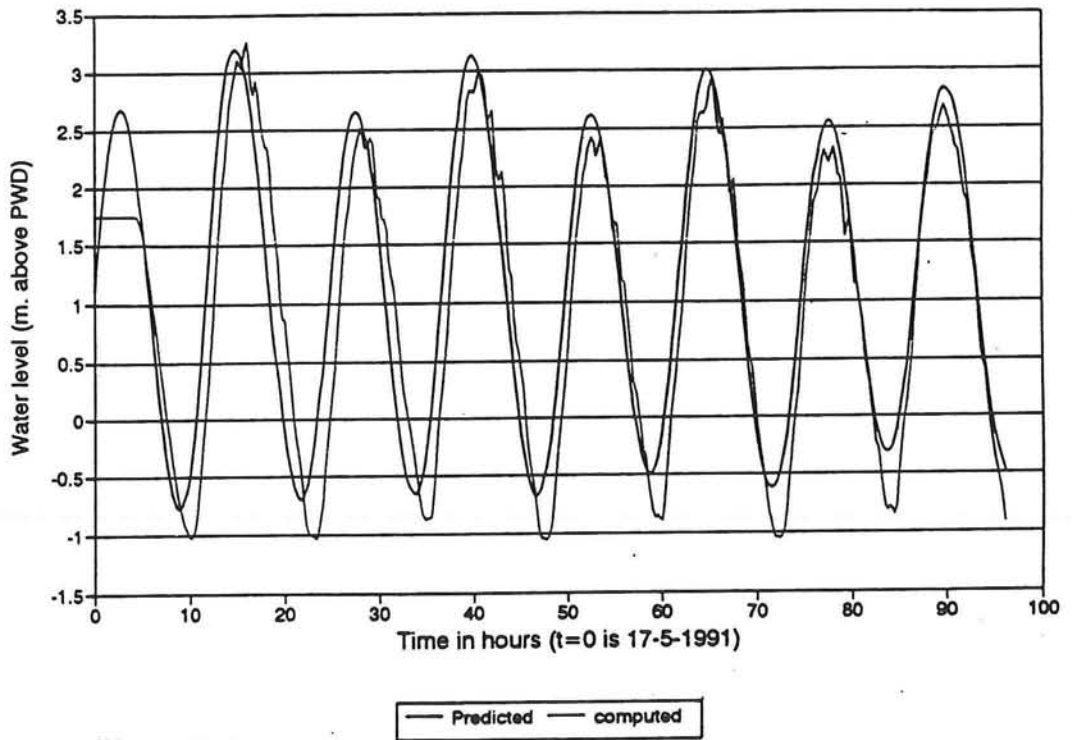


Figure C.4

Final calibration without wind effects  
Cox's Bazar

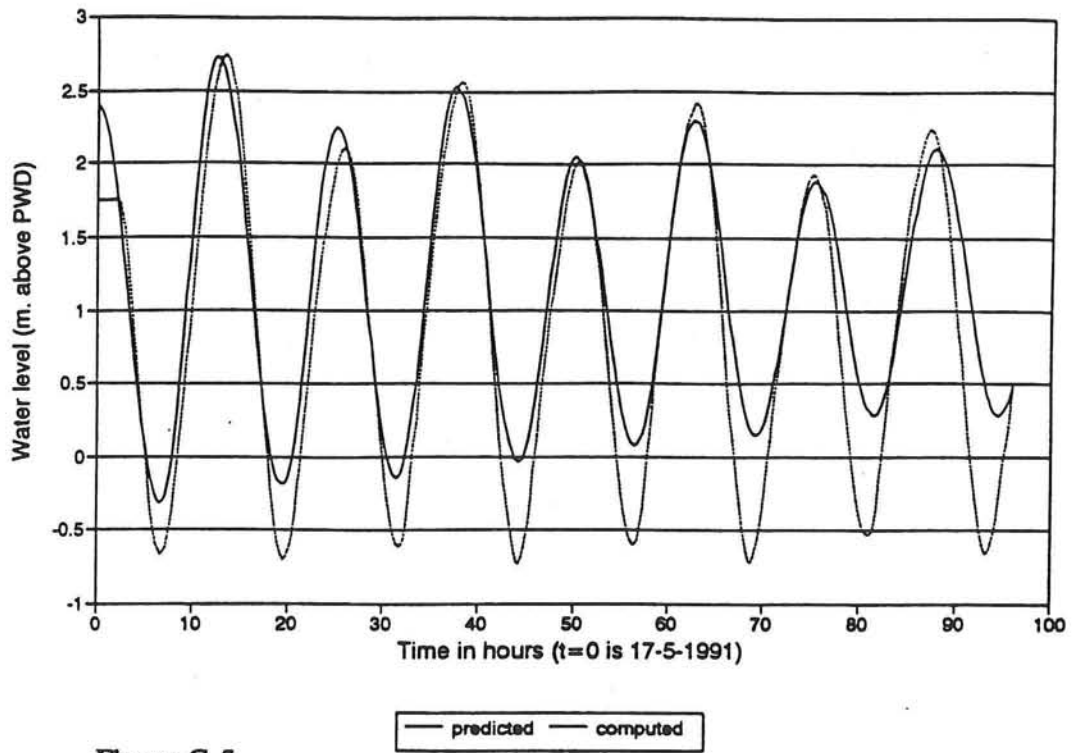


Figure C.5

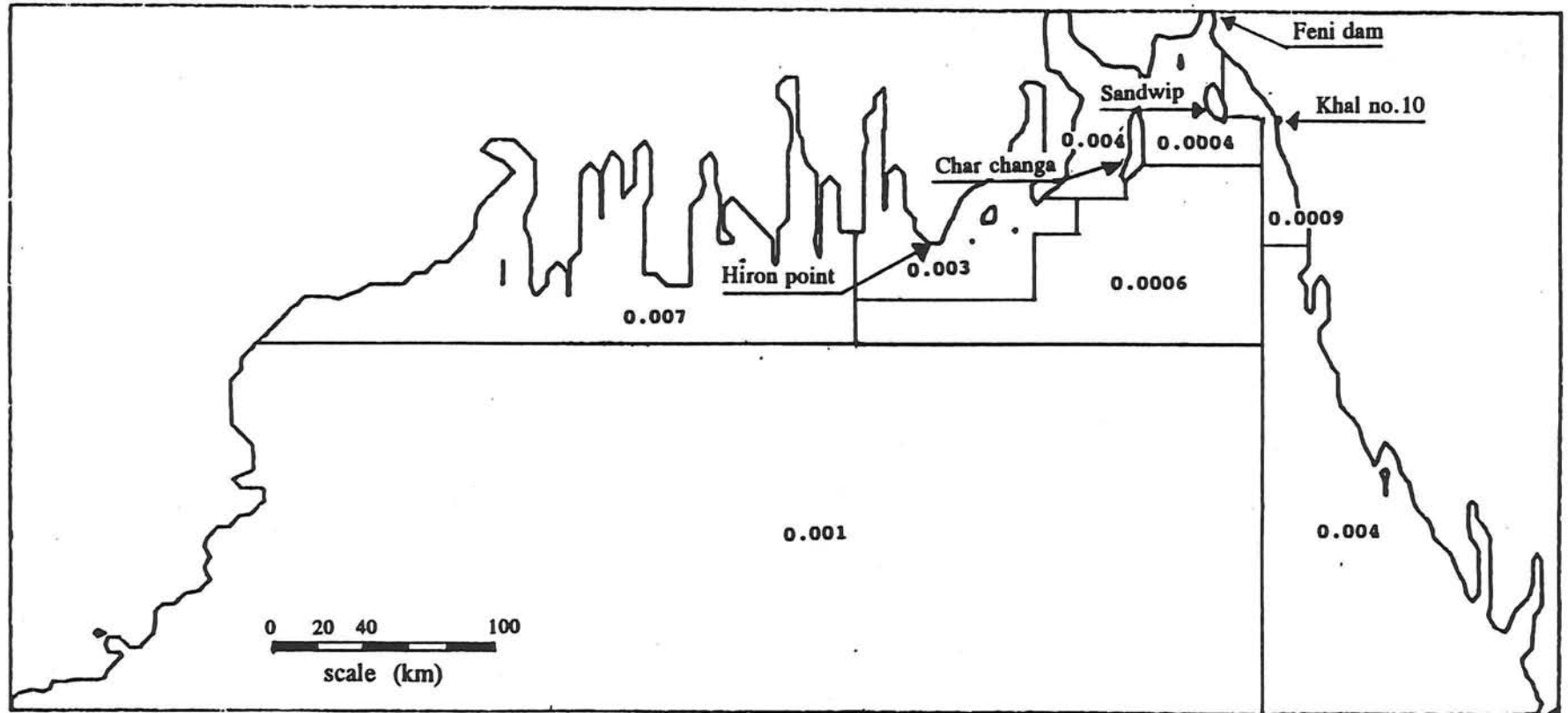


Figure C.6: Map of introduced values for the friction factor "Fr".

### **C.3 CALIBRATION OF THE CYCLONE GENERATING MODEL**

Duchess requires input files for the introduction of wind velocities and air pressures, which influence the water levels at distinct time steps.

For the introduction of dynamic and non uniform wind fields, such as cyclones, a cyclone generating model was used. For an explanation of this model, ref. [22] is referred to.

For each cyclone that would be simulated, the observed radius to maximum wind speed ( $R_{max}$ ) and the pressure drop ( $\Delta p$ ) were introduced for various points of time. By means of these parameters the cyclone generating model calculates the values for the air pressure for each grid point of the model area and for each cyclone time step. These values are scribed to an air pressure input file. The wind velocities at a level of 10 meters above the MSL were calculated from the mentioned pressure field. This is done by means of a factor  $R_{edg}$ . The calculated wind velocities are scribed to an input file as well.

In order to accomplish a cyclone generating model that is representing reality well, this model had to be calibrated. Here,  $R_{edg}$  is used as a calibration variable to adapt the calculated maximum wind speeds in a cyclone to the observed maximum wind speed. In general, the maximum wind velocities were recorded during the simulated cyclone.

It can be justified that the parameter  $R_{edg}$  is used for calibration purposes. First, errors due to the observation of maximum wind speed are to be expected. For example, the location where the cyclone reaches its maximum velocity, is mostly not equal to the location where the measuring equipment is located. Furthermore, in the cyclone model the cyclone phenomenon is schematized as a perfectly round shape, which is not in accordance with nature. In this way it seems reasonable to use the factor  $R_{edg}$  as a calibration variable. The resulting values for  $R_{edg}$  are given in the following sections.

### **C.4 CALIBRATION AND VERIFICATION OF THE MODEL COMPLEX INCLUDING CYCLONES**

#### **C.4.1 CHOICE OF CYCLONES FOR CALIBRATION AND VERIFICATION**

The main requirement for this procedure is that cyclones are needed of which all the following properties are known: the cyclone track, the pressure drop ( $\Delta p$ ), the radius of maximum wind speed ( $R_{max}$ ) and the maximum wind speed ( $V_{max}$ ). Moreover, reliable water level observations should be available in the lower Meghna estuary. In the last 10 years the following cyclones meet these requirements: The cyclones of December 1981, May 1985 and April 1991. For the explanation of the mentioned cyclone properties Section 3.5 of the main report is referred to. For the location of the gauge stations, see Figure 5 of Section 4.2 of the main report.

#### **1981 cyclone**

At December 11th early in the morning the storm, which had a severe cyclone intensity, crossed the coast near Hiron Point, which is located at approximately 250 km west of the Feni Dam area. The maximum wind velocity was estimated to be 130 km per hour, the radius to the maximum wind speed was approximately 50 km and the maximum pressure drop was 27 millibar. During the cyclone, water level readings are available for the gauge stations Char Changa, Sandwip and Sadarghat (Chittagong).



### 1985 cyclone

This cyclone was classified as a severe cyclonic storm with a core of hurricane intensity. During May 23 to 25th it travelled through the Bay of Bengal, hitting the coast of Bangladesh near Chittagong. The radius of maximum wind speed was estimated to be approximately 60 km with maximum wind velocities of up to 166 km per hour. Observations during this cyclone were carried out for two stations in the neighbourhood of the Feni dam, Char Changa and Sadarghat.

### 1991 cyclone

On the 25th of April at the Indian Ocean a deep depression turned into a cyclonic storm that moved in north eastern direction and crossed the coast approximately 30 km north of Chittagong. This cyclone can be described as a super cyclone, that 138.000 people did not survive. The maximum wind speed observed at Sandwip was 225 km per hour. The actual maximum wind speed could have been higher, because the wind measuring device was blown away after this velocity was recorded. The radius to the maximum wind speed was 75 km and a maximum pressure drop of approximately 70 to 75 millibars was observed. Along the coast opposite to Sandwip Island, observations of the extreme water levels are available. For the cyclone tracks, Figure C.7 is referred to.

Other cyclones, from 1977 onwards, were studied for the Cyclone Protection Project II (ref. [10]). Accurate properties of these cyclones are not available. This is why these cyclones could not be used for calibration. For a design of the Feni dam, it is important that cyclones that result in a large water elevation near the dam site, correspond to reality. This condition is valid for the 1985 cyclone, which was accordingly taken for calibration of the model complex. As a verification, the situation during the cyclone of 1991 having approximately the same track was simulated. Finally it was analyzed, whether the model represents reality well for a situation during a cyclone, that crossed the coast relatively far away from the dam site: the 1981 cyclone.

#### C.4.2 CALIBRATION USING THE 1985 CYCLONE

The model including wind and pressure effects was calibrated, using the 1985 cyclone. After calibrating the cyclone generating model for this cyclone, the factor  $R_{edg}$  appeared to be 1.5. The most important possibility for calibrating the model including a cyclonic wind and pressure field is to adjust the factor representing the wind shear stress. This is the only component in the 3 basic hydraulic equations, which describes the influence of wind velocities on the water movement. This component reads:

$$\underline{W} = CWF * |w| * \underline{w},$$

in which:

$\underline{W}$	= the wind shear stress, divided by the water density,	[ m <sup>2</sup> /s <sup>2</sup> ]
$\underline{w}$	= vector representing the wind velocity at 10 meters above MSL,	[ m/s ]
$ w $	= absolute magnitude of the wind velocity,	[ m/s ]
CWF	= wind friction factor.	[ - ]

In order to calibrate the model for cyclonic storms, the water level set-up induced by wind and air pressure fields had to be adapted to the observations by modifying the wind friction factor "CWF".

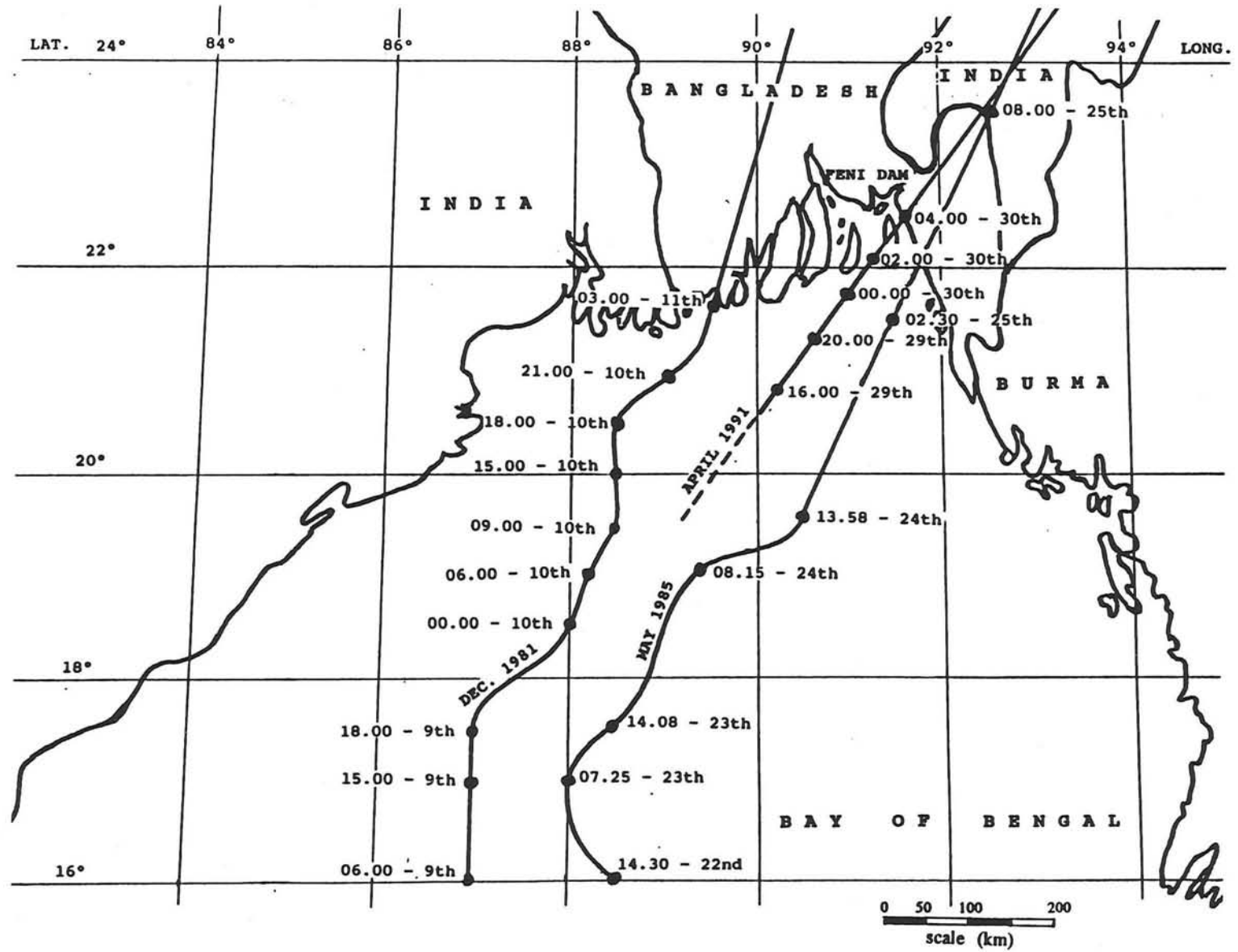


Figure C.7: Tracks of the 1981, 1985 and 1991 cyclones

During this cyclone, observations are only available for the gauge stations Sadarghat and Char Changa. As Sadarghat is located a few kilometres inland, the water level cannot be simulated well here. The observations at Sadarghat station had to be transformed to values for Khal no.10, along the coast near Chittagong. For this transformation a relation between the two stations was used, which had been derived for the Cyclone Protection Project II in ref. [5]. In this report it was concluded, that the extreme water level at Sadarghat is approximately 0.30 meters higher than Khal no.10 during cyclone conditions. For the calibration procedure mainly the maximum values were considered, not the exact variation of the water level in time. In Table C.2 some computational results are given.

CWF	Gauge station	Calc. water level (m. +PWD)	Observed Water level (m. +PWD)	Difference (in m.)
0.0019	Khal no.10	3.760	3.38	+ 0.38
	Char Changa	3.328	3.84	- 0.51
0.0017	Khal no.10	3.531	3.38	+ 0.15
	Char Changa	3.090	3.84	- 0.75
0.0016	Khal no.10	3.477	3.38	+ 0.10
	Char Changa	3.010	3.84	- 0.83
0.0015	Khal no.10	3.367	3.38	+ 0.01
	Char Changa	2.937	3.84	- 0.90

**Table C.2:** Results of the calibration using the 1985 cyclone.

The computed water level in Khal no.10 is substantially higher than in Char Changa, while the observed water level is lower. This is a structural error. Probably the topography above MSL near Char Changa has to be modified in such way that the calculated maximum water levels become higher here.

The water levels near the dam site are mainly influenced by the hydraulic situation in the two channels bordering Sandwip Island: Sandwip and Hatia Channel. This is why the water level variations in Bhola Channel, west of Char Changa station, is assumed not to influence the water level near the dam. As a result, Char Changa station was not considered any more.

Finally, for the wind friction factor a value of 0.0015 was chosen, regarding the situation near Khal no.10.

In Figure C.8 the computed and observed water level variation are given.

**Water levels during 1985 cyclone**  
**Calculated and observed at Khal no.10**

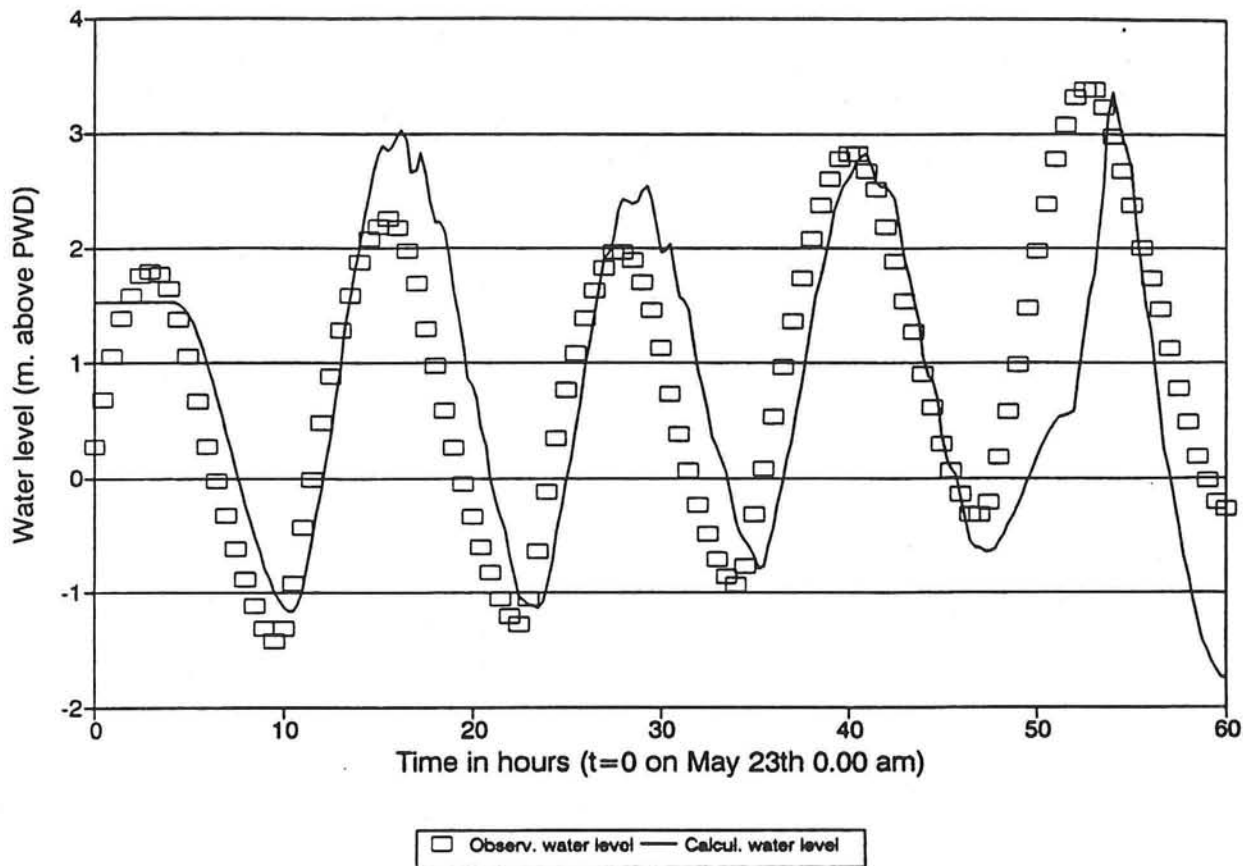


**Figure C.8:** Final calibration for Khal no. 10 using CWF = 0.0015.

**C.4.3 VERIFICATION OF THE MODEL USING THE 1991 CYCLONE.**

For the wind friction factor of 0.0015, the model had to be verified using a second cyclone with approximately the same track as the 1985 cyclone: the "killer-cyclone" of 1991. The used data of observations comprised only extreme water levels during the passage of the cyclone at several locations along the coast of the Sandwip Channel (between Sandwip and the Chittagong main land). Even the maximum water levels near the Feni dam were available. For the present verification only the observation at Chittagong (Khal no.10) was used. In Table C.3 the observed and computed water levels are compared.

Computed water level (m. +PWD)	MSF component (meters)	Cal. water level inc. MSF (+ PWD)	Obs. max. water level (m. + PWD)
7.85	+ 0.13	7.98	8.0

**Table C.3:** Comparison between computed and observed maximum water levels at Khal no.10

Although the accuracy and reliability of the observations during the 1991 cyclone are not very high, the difference appears to be very small.

#### C.4.4 VERIFICATION OF THE MODEL USING THE 1981 CYCLONE

Then the hydraulic situation during the 1981 cyclone was analyzed. In Table C.4 the computational results are given for a wind friction factors of 0.0015.

CWF	Gauge station	calc. max (m + PWD)	MSF comp.	calc. max incl. MSF (m+PWD)	Obs. max. (m. +PWD)	diff.
0.0015	Sandwip	4.487	+0.13	4.62	4.27	+0.35
	Khal no.10	3.670	+0.06	3.73	2.85	+0.88

**Table C.4:** Comparison between computed and observed maximum water levels during the 1981 cyclone.

It was determined before, that the gauge station Char Changa would not be considered any more. For Khal no.10 the resulting water levels do not correspond to the observed values. The computed water levels are considerably higher here. A possible explanation for this is that the area influenced by a cyclone is smaller in reality than simulated in a numerical model.

#### C.4.5 CALIBRATION OF THE AREA NORTH OF CHITTAGONG

In order to simulate the water level near the Feni dam, the situation was considered in Sandwip Channel, which borders the closure dam. For calibration of this region the cyclone of April 1991 was used. During this cyclone, observations of the maximum water levels for the whole coast of the Chittagong main land were obtained from ref. [10].

For calibration of the Sandwip Channel, the topography, the friction and bathymetry variables were used as calibration parameters, because these have not yet been modified during calibration of the tide simulation in this area.

The concerned locations of available observations during the 1991 cyclone are given in Figure C.9.

Four situations of the bathymetry and topography were considered:

- 1) The initial situation,
- 2) Depth reduction of Sandwip Channel with approximately 2 meters, taking the initial situation as a starting point.
- 3) Depth increase of Sandwip Channel with regard to the initial situation.
- 4) Modification of the topography north of Chittagong by reducing the land level in such manner that a large area will be flooded during a cyclonic storm surge.

After computing the water levels for the various situations, Table C.5 could be drawn up.

It was found out that the friction change did not influence the water level in the concerned region.

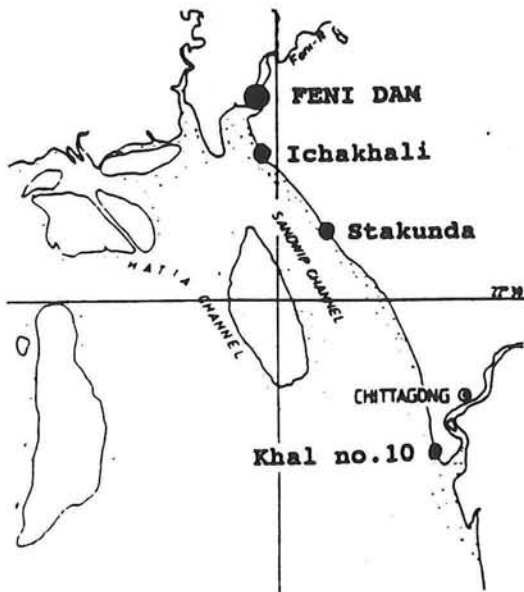


Figure C.9: Locations where maximum water levels were observed.

Situation	Water levels (m. + PWD)		
	Khal no.10	Stakunda	Ichakhali
1	7.98	9.72	10.25
2	7.60	9.57	10.21
3	7.70	9.85	10.32
4	7.61	9.44	10.23
Observed	8.0	7.7	6.0

Table C.5: Observed and computed maximum water levels during 1991 cyclone along the coast of the Sandwip Channel.

Decreasing the depth of Sandwip Channel using situation 2, resulted in lower water levels in this channel. This can be explained to be caused by the enlargement of the friction term in the basic equation of motion.

Considering the third situation with an increased depth of the Sandwip Channel, the opposite thing happened.

In general it can be stated that lower land levels result in a larger storage area and thus in lower water levels. This can be confirmed comparing the fourth situation to the third.

In all the situations the computed water level is more than 4 meters higher than the observed ones near Ichakhali, which is located near the Feni River Closure Dam. It thus appears to be impossible to simulate reliable extreme water levels near the Feni dam using the present Duchess model.

#### C.4.6 CONCLUSIONS.

After calibrating the model the wind friction factor appears to be 0.0015. When the simulation of the 1991 cyclone is considered, the model appears to reflect reality well near Chittagong for this wind friction value. The point of landfall of this cyclone is relatively close to the Feni dam. For the simulation of the 1981 cyclone, which crossed the Bangladeshi coast relatively far from the Feni dam, the model overestimates the extreme water levels. Cyclones crossing the coast far from the dam appear to yield a lower extreme water level near the Feni dam than cyclones in the dam area itself. Thus, for design purposes, an accurate representation of the 1981 cyclone is not necessary. As a result, the model is thought to generate reliable extreme water levels, when only cyclones in the eastern lower Meghna estuary are considered.

For the area north of Chittagong, it turns out to be very difficult to simulate reality well. The extreme water levels generated near the dam do not correspond to the observed ones. This could be ascribed to the inaccuracy of the observations. But the main cause of this probably is that this area can not be represented well by a model having a relatively large mesh size of 5.5 km. By means of a nest, a mesh refinement could be applied. This nest is a smaller model within the general model, having a smaller mesh size, which obtains its boundary conditions from the results of the general model. This nesting procedure has not been carried out, because of the lack of available time and reliable detailed input parameters. Consequently, the model was assumed to generate reliable extreme water levels for Chittagong, when only cyclones hitting the coast of the lower Meghna estuary are considered.

In order to obtain the extreme water levels near the Feni dam, the generated extremes near Chittagong had to be transformed to the Feni dam. This procedure is explained more in detail in Annex D.





## ANNEX D

### DERIVATION OF WATER LEVEL DISTRIBUTION FOR CYCLONE CONDITIONS

#### TABLE OF CONTENTS

D.1	<u>GENERAL METHODOLOGY</u> .....	D - 3
D.2	<u>SCHEMATIZATION OF INPUT VARIABLES</u> .....	D - 3
D.2.1	INTRODUCTION .....	D - 3
D.2.2	RIVER DISCHARGE SCHEMATIZATION .....	D - 3
D.2.3	SCHEMATIZATION OF MSL .....	D - 4
D.2.4	SCHEMATIZATION OF CYCLONE TRACK .....	D - 5
D.2.5	SCHEMATISATION OF CYCLONE STRENGTH .....	D - 8
D.2.5.1	Methodology .....	D - 8
D.2.5.2	Probability analysis of maximum wind speeds during cyclones .....	D - 9
D.2.5.3	Relation between maximum wind speed and pressure drop	D - 11
D.2.5.4	Relation between maximum wind speed and radius .....	D - 12
D.2.5.5	Results of schematization of cyclone strength .....	D - 12
D.2.6	TIDE SCHEMATIZATION .....	D - 12
D.3	<u>DERIVATION OF WATER LEVEL PROBABILITY DISTRIBUTION FOR CHITTAGONG DURING CYCLONES</u> .....	D - 14
D.4	<u>DERIVATION OF WATER LEVEL PROBABILITY DISTRIBUTION FOR THE FENI DAM DURING CYCLONES</u> .....	D - 15
D.4.1	MONSOON RELATION BETWEEN CHITTAGONG AND THE FENI DAM .....	D - 15
D.4.2	WATER LEVEL REDUCTION DUE TO INUNDATION .....	D - 16
D.4.3	RESULTING WATER LEVEL DISTRIBUTION FOR THE FENI DAM	D - 19



## **ANNEX D DERIVATION OF WATER LEVEL DISTRIBUTION FOR CYCLONE CONDITIONS**

### **D.1 GENERAL METHODOLOGY**

The objective of this annex is to derive a probability distribution for water levels during cyclone conditions near the Feni dam using meteorologic records from 1900 onwards. The idea was to construct several synthetic situations from these records, for which the maximum water level near Chittagong could be computed. Subsequently, these water levels were transformed to the Feni dam, among others by monsoon relations between the two locations.

For each synthetic situation the probability of occurrence could be estimated using the historic meteorological record. Out of the water levels and the probabilities of occurrence the probability distribution could be estimated for the water levels during cyclone conditions near the Feni dam.

### **D.2 SCHEMATIZATION OF INPUT VARIABLES**

#### **D.2.1 INTRODUCTION**

First the various synthetic situations have to be generated. This was done by determining the synthetic values for each parameter that influences the water variation. The main properties that influence the water level are:

- River discharge
- Mean sea level
- Cyclone track
- Cyclone strength
- Tidal situation

The explanation how this was done is given in the following sections for each parameter successively.

#### **D.2.2 RIVER DISCHARGE SCHEMATIZATION**

First the sensitivity of the water levels near Chittagong for the variation of the river discharge is studied. For the simulation of the 1985 cyclone, the introduced discharge during the month of May is 21900 m<sup>3</sup>/s, according to the river discharge data (ref. [23]). After increasing this river discharge with 20%, the extreme water level near Chittagong increased only by 1 cm.

In order to determine the river discharge to be introduced for the synthetic situations only one value was used, because of the small river discharge sensitivity. For each month of the year, the probability of occurrence of a cyclone could be estimated from the historic cyclone record. In this way, a weighted average could be derived for the whole year, using the mean monthly river discharge values. This is done in Table D.1.

This weighted average was used for the synthetic situations.

Month	A: Mean discharge (m <sup>3</sup> /s)	B: Probability of cyclone occurrence per year	A * B (in m <sup>3</sup> /s)
January	8,900	0	0
February	7,600	0	0
March	7,600	0	0
April	10,100	0.059	596
May	21,900	0.275	6,023
June	40,800	0.020	816
July	65,500	0	0
August	91,200	0.020	1,824
September	79,700	0.039	3,108
October	45,900	0.275	12,623
November	20,600	0.216	4,450
December	11,800	0,098	1,156
Weighted average		$\Sigma (A * B)$	30,600 m <sup>3</sup> /s

Table D.1: Calculation of the river discharge for the schematic situations.

### D.2.3 SCHEMATIZATION OF MSL

The mean sea level is subject to seasonal changes, caused by varying density differences in the area. The MSL was schematized to be constant over the model area. In order to derive the monthly mean sea level, a factor, representing the seasonal change had to be added to the yearly mean sea level values. These factors are average values, which were provided by the British Admiralty (ref. [1]). For this Annex B, Section 4.3.3 is referred to. The monthly mean sea level had to be introduced in the model by means of modifying the mean values of the tide at the southern boundary. The factor for the seasonal change used for the synthetic situations was derived by means of calculating the weighted average, like the river discharge. See Table D.2. The calculated factor for the seasonal change turned out to be about 2 cm, which could be rounded off to zero. Thus, during the representation of the synthetic situations, no modification of the mean sea level due to seasonal influences was introduced in the model.

Month	A: Probability of cyclone occurrence per year	B: Factor for seasonal change, (m. + MSL)	A * B
January	0	- 0.3	0
February	0	- 0.4	0
March	0	- 0.4	0
April	0.275	- 0.3	- 0.0177
May	0.020	- 0.1	- 0.0275
June	0.020	+ 0.2	+ 0.0040
July	0	+ 0.4	0
August	0.020	+ 0.5	+ 0.0100
September	0.039	+ 0.4	+ 0.0160
October	0.275	+ 0.2	+ 0.0550
November	0.216	0.0	0
December	0.098	- 0.2	- 0.0196
Weighted average (m. + MSL)		$\Sigma (A * B)$	+ 0.0197

Table D.2: Results of the calculation of seasonal change used for schematization

#### D.2.4 SCHEMATIZATION OF CYCLONE TRACK

In order to schematize the cyclone track, first the relation between the extreme water level near Chittagong and the position of the cyclone track had to be analyzed. For this, several computer runs were performed for several cyclone tracks, each of which passing Chittagong at a different distance to the east or to the west. The values of the pressure drop and the radius to maximum wind speed were taken equal to the 1985 cyclone. Then a figure could be drawn, representing the relation between the maximum water level near Chittagong and the distance over which the cyclone track is shifted. See Figure D.1.

From this figure it is clear that the largest extreme water levels occur near Chittagong, when the cyclone is passing Chittagong to the west at a distance of about 60 km. In this situation the wind speed is maximum near Chittagong and the wind is directed to the coast, which causes a high wind set-up. On the other hand, when the cyclone is passing Chittagong to the east, the extreme water level near Chittagong is relatively low, due to the wind, which is directed offshore. It can thus be concluded that the maximum water level attained at a location near the coast is very much depending on the wind direction and wind speed at the time the cyclone is passing this location. The effect of the air pressure drop, which is concentrated near the cyclones eye appears to be relatively small. Considering Figure D.1, it can be concluded that the sensitivity of the extreme water level for changing the track is considerably large.

For the generation of the synthetic situations, two schematic cyclone tracks were considered. Occurring cyclones in the eastern lower Meghna estuary, which pass Chittagong at a distance of 60 to 120 kilometres were schematized to track 1, at 90 km. west of Chittagong. Cyclones passing Chittagong at less than 60 kilometres were schematized to track 2 at 30 km. west of Chittagong.

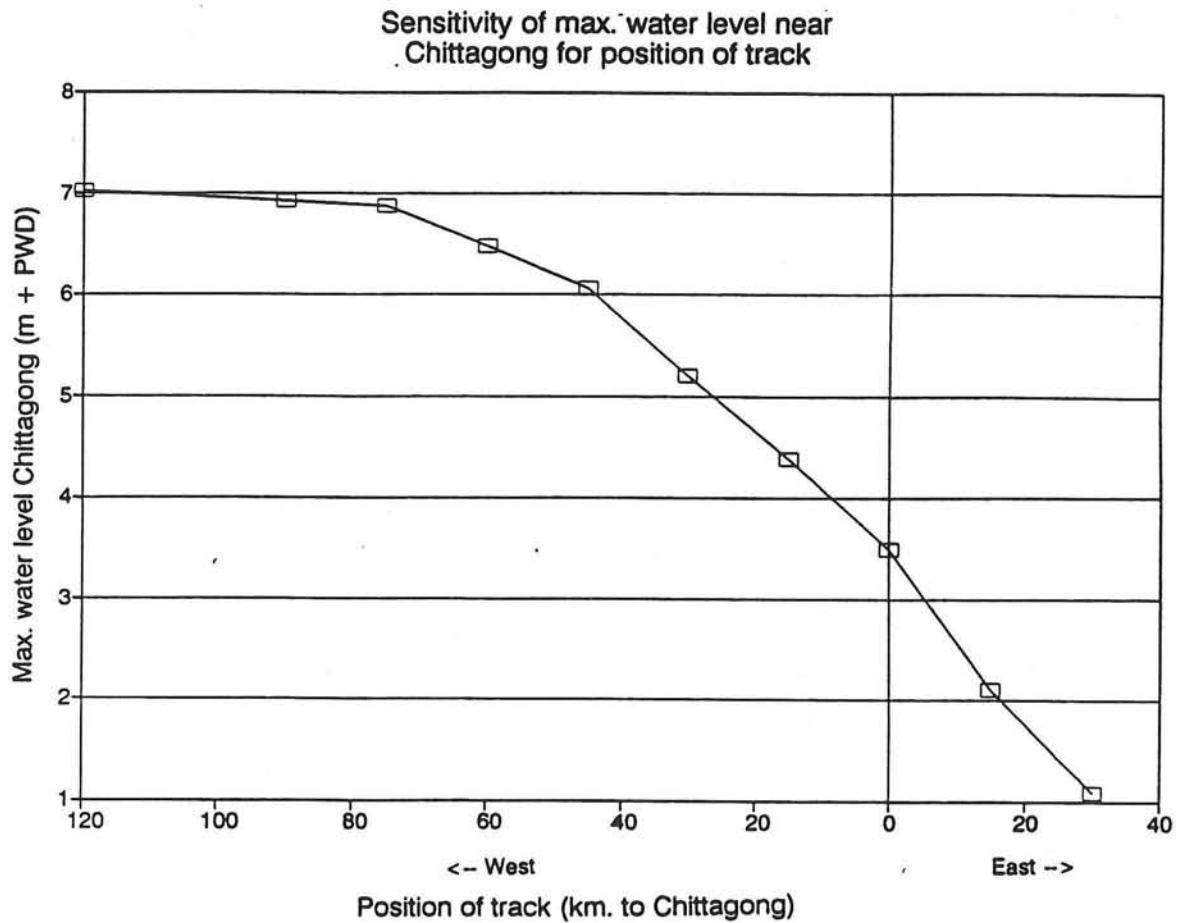


**Figure D.1:** Sensitivity of maximum water level near Chittagong for position of the cyclone track.

For construction of the synthetic tracks the following assumptions were made:

- The track is a straight line.
- At the start of the model runs, the location of the eye was determined at a location on the ocean, where generally depressions turn into cyclonic storms. This location is the same for both tracks.
- The cyclone passes Chittagong at the west side 50 hours after starting the computation. In this way the average propagation speed is comparable to real cyclones.
- The termination of the computation is 60 hours after the starting time. At this time the location of the cyclone track is determined by extrapolation of the cyclone tracks.

For the schematic tracks, reference is made to Figure D.2

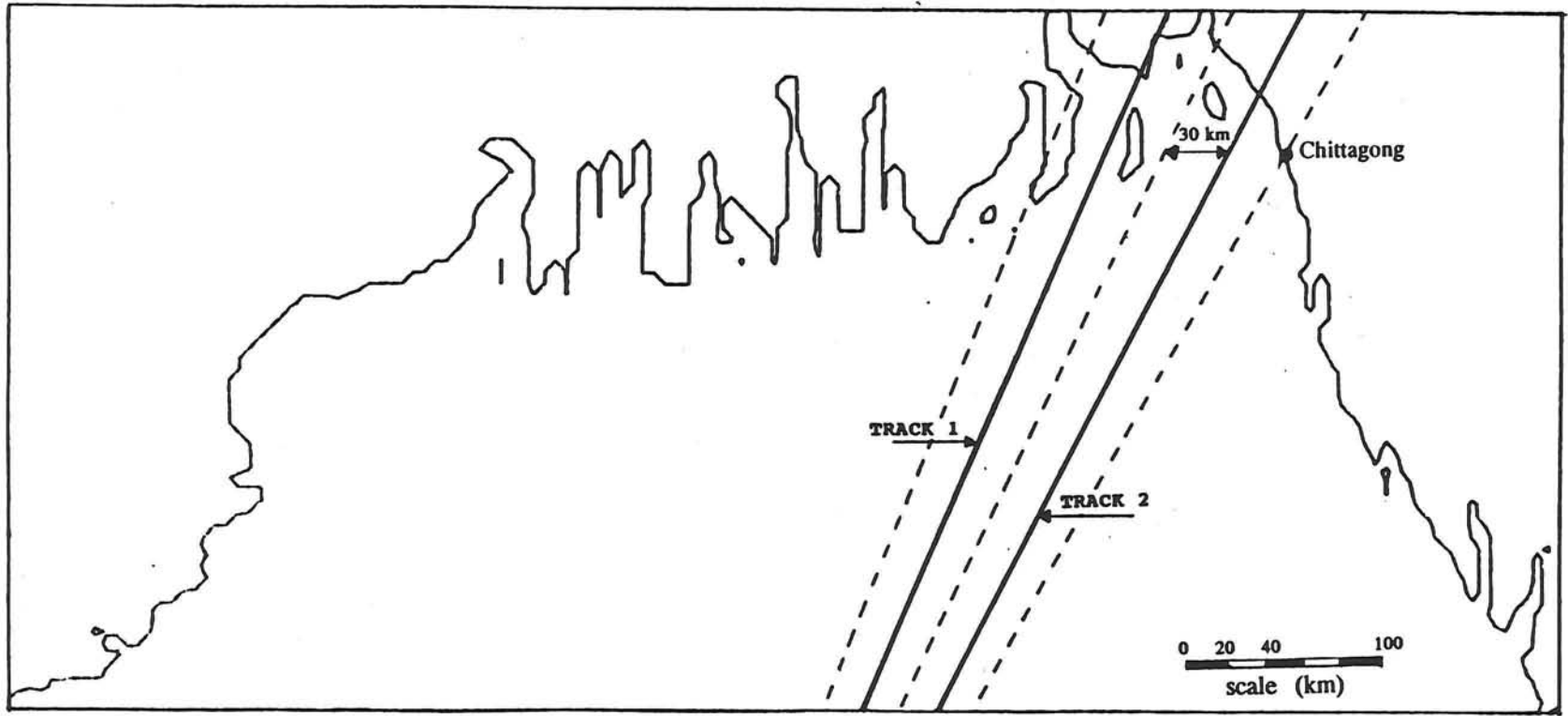


Figure D.2: Schematic cyclone tracks.

For both schematic tracks, the probabilities of occurrence could not be derived from the historic meteorological record. These probabilities were assumed to be the same, which is the half of the probability that a cyclone hits the coast in the eastern lower Meghna estuary. This last mentioned probability can be calculated from historic data.

## D.2.5 SCHEMATISATION OF CYCLONE STRENGTH

### D.2.5.1 Methodology

The cyclone strength mainly depends on:

- Radius to maximum wind speed ( $R_{max}$ )
- Pressure drop ( $\Delta p$ )
- Maximum wind speed ( $V_{max}$ )

For an explanation of these parameters, reference is made to section 3.4 of the main report. First a sensitivity analysis for these parameters was performed.

#### Radius sensitivity

In order to analyze the sensitivity of the water level for a radius change, this variable was increased with 10 % . The results are given in Table D.3.

Max. water level for original radius (m. + PWD)	Max. water level for 10% increased radius (+PWD)	Difference (m.)
3.37	3.34	- 0.03

Table D.3: Influence of radius change.

In general the influence of changing the radius on the calculated water levels appeared to be rather small.

#### Pressure drop sensitivity

For a sensitivity analysis of the pressure drop, this parameter was reduced by 10% , compared to the 1985 cyclone situation. This was realized by reducing the pressure drop in the input file of the cyclone generating model. Furthermore, the factor  $R_{edg}$  had to be modified in such a way that the maximum wind speed remains the same. The results are given in Table D.4.

Max. water level for original pressure drop (m. + PWD)	Max. water level for 10% pres. drop change (+PWD)	Difference in max. water level.
3.37 m.	3.35 m	- 0.02 m

Table D.4: Influence of pressure drop change.



From the sensitivity analysis it was concluded that the influence of the pressure drop on the water level is not big.

### Wind speed sensitivity

For the sensitivity analysis for variations of maximum wind velocities, the maximum wind velocity was increased by 10 % . For this, the factor Redg in the cyclone generating model was modified. The results are given in Table D.5.

Max. water level for original wind speed (m. + PWD)	Max. water level for 10% higher wind speeds (+PWD)	Difference (m.)
3.37	3.47	0.10

**Table D.5:** Influence of increase of maximum wind speeds

In general, the maximum wind speed appeared to govern the water level more than the other parameters. This is why first the maximum wind velocities were divided into several intervals, each representing a certain synthetic cyclone strength.

From the cyclone record, the maximum wind speed and the accompanying pressure drop of each cyclone which crossed the coast of Bangladesh since 1900 was obtained. Then a relation between the maximum wind velocity in a cyclone and its pressure drop was derived using these historic cyclones. Subsequently, the pressure drop, which is most likely to correspond to the different synthetic wind velocity intervals was thought to be the pressure drop resulting from this relation. In the same way a relation between the maximum wind velocity in a cyclone and its radius could be derived from the historic meteorological record. The  $R_{max}$ 's, which are most likely to accompany the various synthetic wind speed intervals were obtained, using the relation mentioned. In this way the properties for the various synthetic cyclone strengths were determined.

#### D.2.5.2 Probability analysis of maximum wind speeds during cyclones

In order to derive the probability that a cyclone has a maximum wind speed within a certain wind speed interval, the probability distribution of the maximum wind speed during a cyclone had to be derived.

First it was assumed that this probability distribution corresponds to a Gumbel distribution, because of the fact that extreme wind speeds were considered here. Whether this is true or not had to be examined. The derivation of the probability distribution is comparable to the probability analysis, which is described in Annex A.

For all the historic cyclones for which the maximum wind speed is known, the plotting positions for these extreme wind velocities were calculated. Subsequently, a straight line was fitted through these plotting positions by means of a linear regression method. From this a Gumbel distribution was derived, representing the probability of exceedance of maximum wind speeds during cyclones.

This Gumbel distribution reads (see Figure D.3):

$$p \{ \text{max. wind speed} \geq x \mid \text{cyclone} \} = 1 - e^{-e^{-0.027 \cdot x + 2.72}}$$

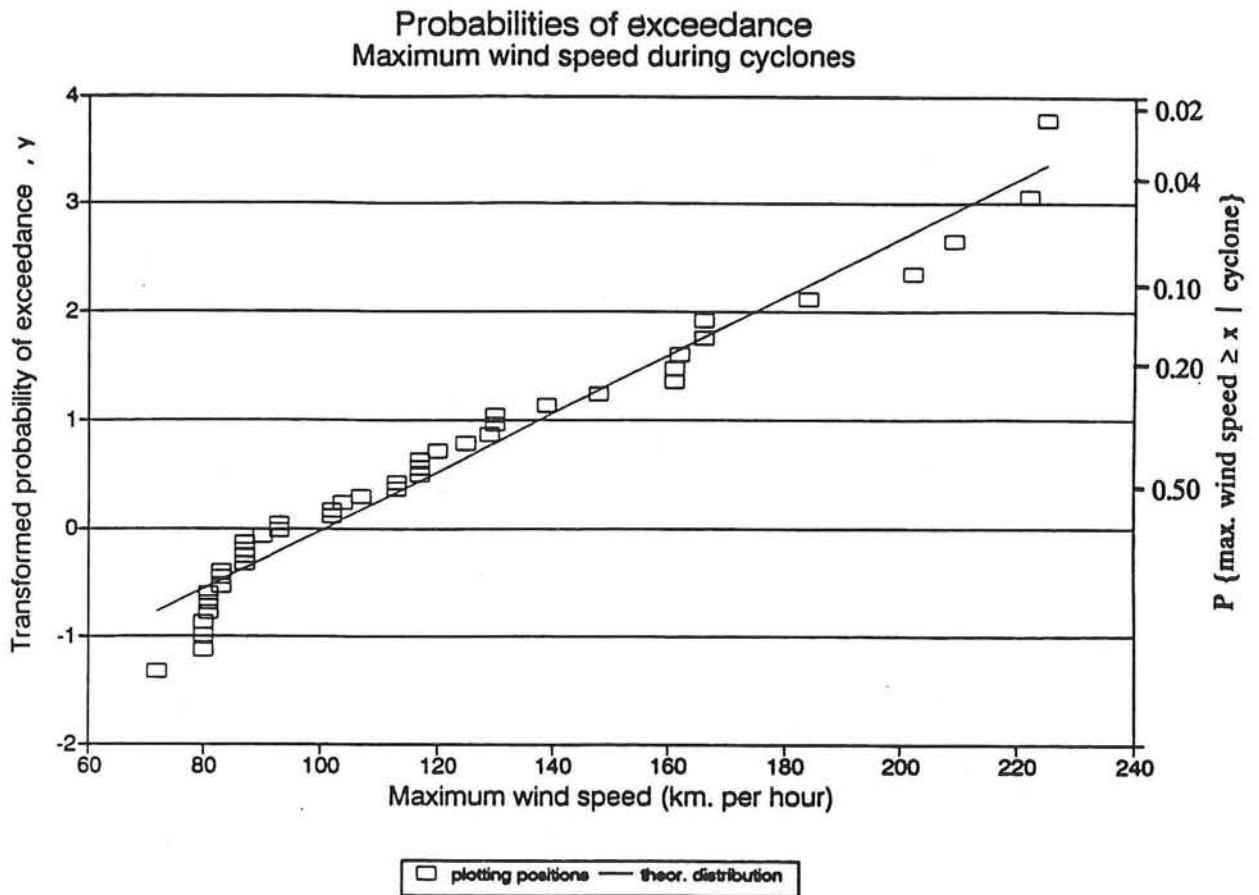


**Figure D.3:** Probability distribution of maximum wind speeds when cyclones occur.

The probability distribution of maximum wind speeds in cyclones appeared to fit a Gumbel distribution well. The cyclone strength was schematized in such a way that the wind velocity was divided into 5 intervals with a width of 32 km. per hour each. In this way, the maximum deviation from the mean wind velocity per interval is 16 km/h. The maximum wind speed intervals and their probability of occurrence, according to the derived Gumbel distribution are given in Table D.6. Here the parameter  $P(x)$  was used.  $P(x)$  is defined as  $p \{ \text{max. wind speed} \geq x \mid \text{cyclone} \}$

Interval	Probability of occurrence	V(mean)
$V \text{ max} \leq 102 \text{ km/h}$	$1.0 - P(102) = 1.0 - 0.620 = 0.380$	86 km/h
$102 \leq V \text{ max} \leq 134 \text{ km/h}$	$P(102) - P(134) = 0.620 - 0.335 = 0.285$	118 km/h
$134 \leq V \text{ max} \leq 166 \text{ km/h}$	$P(134) - P(166) = 0.335 - 0.158 = 0.177$	150 km/h
$166 \leq V \text{ max} \leq 198 \text{ km/h}$	$P(166) - P(198) = 0.158 - 0.070 = 0.088$	182 km/h
$198 \leq V \text{ max}$	$P(198) = 0.070$	214 km/h

**Table D.6:** Intervals of maximum wind speed during cyclones.

### D.2.5.3 Relation between maximum wind speed and pressure drop

In order to determine the corresponding pressure drop for each interval of maximum wind speed, the relation between this pressure drop and the maximum wind speed was derived from the historic meteorological records. From the year 1942 onwards, observations of the maximum pressure drop have been carried out for cyclones in Bangladesh. For each cyclone after this date, the concerned relation is plotted in Figure D.4.

From the Bangladesh Meteorological Department the following equation was obtained, that is plotted in the figure as well.

$$V_{\max} = 26.67 * \sqrt{\Delta p}$$

in which:

$$\begin{aligned} V_{\max} &= \text{maximum wind speed} && [ \text{m/s} ] \\ \Delta p &= \text{pressure drop} && [ \text{mbar} ] \end{aligned}$$

Regarding this figure it can be concluded that there is a distinct relation between the mentioned variables. As the theoretical equation, derived from the BMD, appears to fit the historic observations approximately, this relation was used here as well.

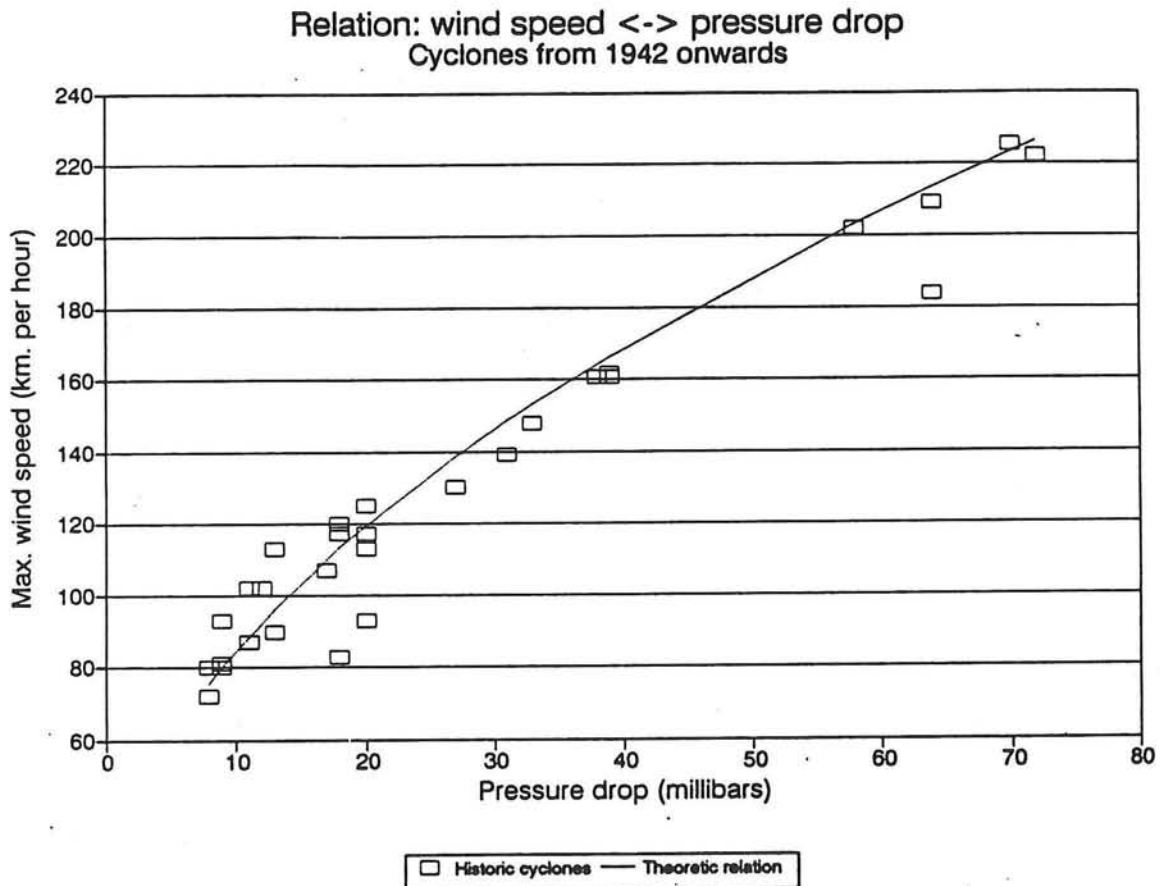


Figure D.4: Relation between maximum wind speed and the pressure drop in cyclones.

#### D.2.5.4 Relation between maximum wind speed and radius

Before satellite pictures were introduced, the radius of the various cyclones was observed only roughly. For each interval of maximum wind speed the mean radius could be calculated. This is done in Table D.7.

Interval V(max) (km)	Number of occurrences			Mean Radius
	50 < R ≤ 60	60 < R ≤ 70	R > 70 km	
V(max) ≤ 102	12	2	0	56
102 < V(max) ≤ 134	0	7	0	60
134 < V(max) ≤ 166	0	4	3	70
166 < V(max) ≤ 198	0	0	1	74
V(max) > 198	0	0	4	74

Table D.7: Relation between wind speed intervals and radius to maximum wind speed.

#### D.2.5.5 Results of schematization of cyclone strength

In this way 5 synthetic cyclones were obtained. For each situation, the factor  $R_{edg}$  of the cyclone generating model had to be modified in such a way, that the pressure drop and the accompanying radius to maximum wind speed yielded the right maximum wind speed. The resulting values of the different variables for each synthetic situation are given in Table D.8.

Situation	Wind speed (km/h)	Pressure drop (millibars)	Radius (km)	Redg factor	Probability of occurrence
1	86	13	56	1.16	0.380
2	118	20	60	1.28	0.285
3	150	30	60	1.32	0.177
4	182	47	74	1.27	0.088
5	214	62	74	1.29	0.070

Table D.8: Parameters for the 5 schematic cyclone strengths.

#### D.2.6 TIDE SCHEMATIZATION

The maximum cyclonic storm surge generally occurs at the time when the cyclone hits the coast. For Chittagong, this is assumed to happen when the cyclone is passing at 50 hours after starting the computations. The tidal amplitudes were schematized to the situations neap and spring tide. Furthermore, the tidal variation during one tidal cycle was schematized to only two situations: high water and low water. This is illustrated in Figure D.5.

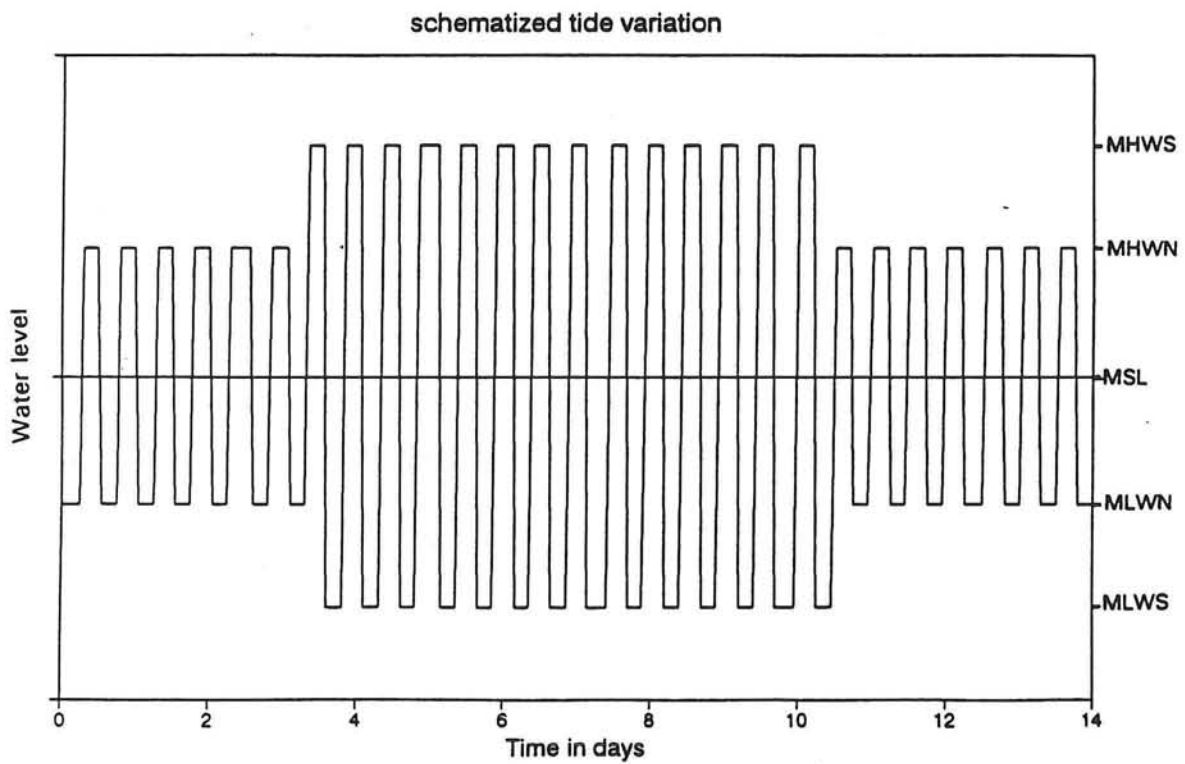
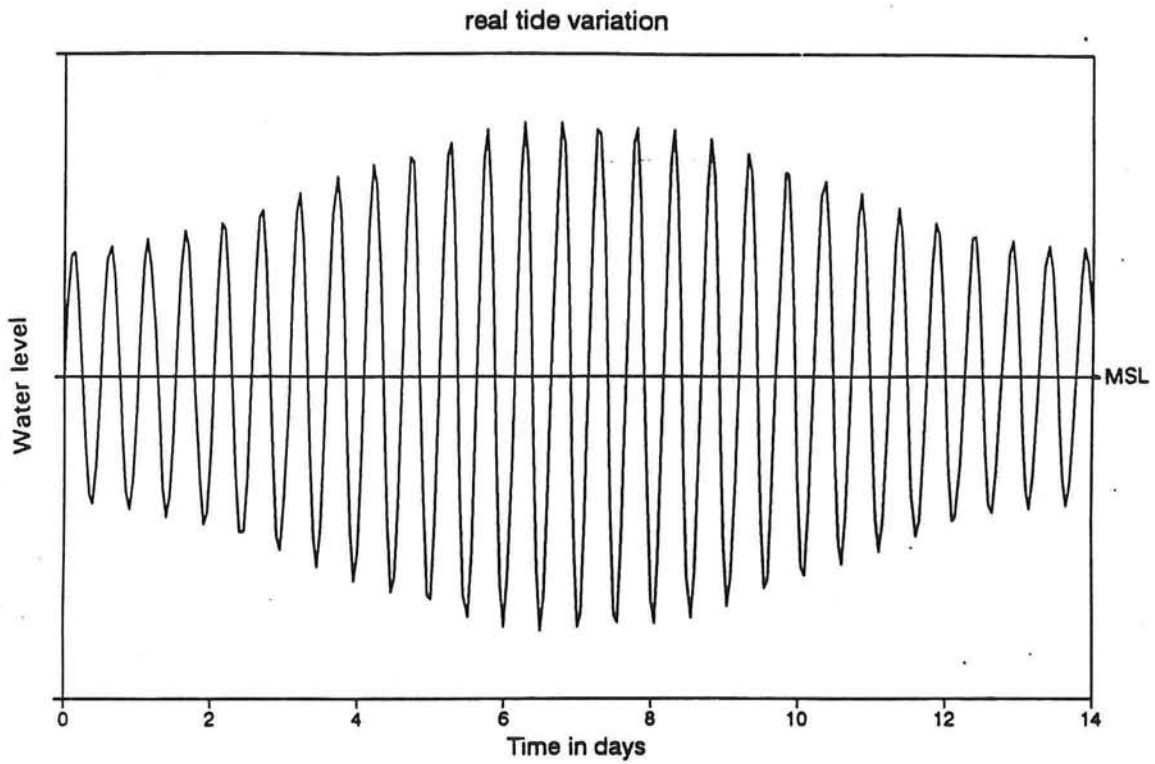


**Figure D.5:** Schematization of tide.

Accordingly, 4 tidal situations were considered at the time that a cyclone is passing Chittagong: MHWS, MLWS, MHWN and MLWN (Mean High Water Spring, etc). These tidal situations had to be generated by modifying the tidal input at the southern boundary. The probabilities of occurrence of each tidal situation are thought to be the same, thus: 0.25.

### **D.3 DERIVATION OF WATER LEVEL PROBABILITY DISTRIBUTION FOR CHITTAGONG DURING CYCLONES**

By applying all the mentioned schematizations, various synthetic situations could be achieved.

- In total:
- 1 schematic river discharge,
  - 1 schematic mean sea level,
  - 2 schematic cyclone tracks,
  - 5 schematic cyclone strengths and
  - 4 schematic tidal situations have been defined.

This yields  $1 * 1 * 2 * 5 * 4 = 40$  synthetic situations. The various variables were assumed to be statistically independent. For each synthetic situation the probability of occurrence could be derived by multiplying the probabilities of occurrence of each variable.

In this way a maximum water level near Chittagong could be computed for each situation, using the calibrated Duchess model.

By ranking the 40 achieved values and the accompanying probabilities of occurrence, the cumulative probability of exceedance was calculated for each computed extreme water level. After transforming these exceedance frequencies to a Gumbel scale, the relation between the probability of exceedance and the water levels could be plotted. Then a straight line was fitted through these points. This line represents the theoretical probability distribution. See Figure D.6.

The probability distribution for water levels near Chittagong during cyclonic conditions reads:

$$p \{ \text{water level} \geq x \} = 1 - e^{-e^{-0.59 * x + 0.60}}$$

In Table D.9 the water levels for various return periods are given.

Return period, years	5	10	20	25	50	100	200
water level (+PWD)	3.55	4.82	6.04	6.42	7.61	8.79	9.97

**Table D.9:** Water levels for various return periods during cyclonic conditions for Chittagong.

From Figure D.6 it can be concluded that the probability distribution for cyclonic water levels more or less corresponds to a Gumbel distribution.

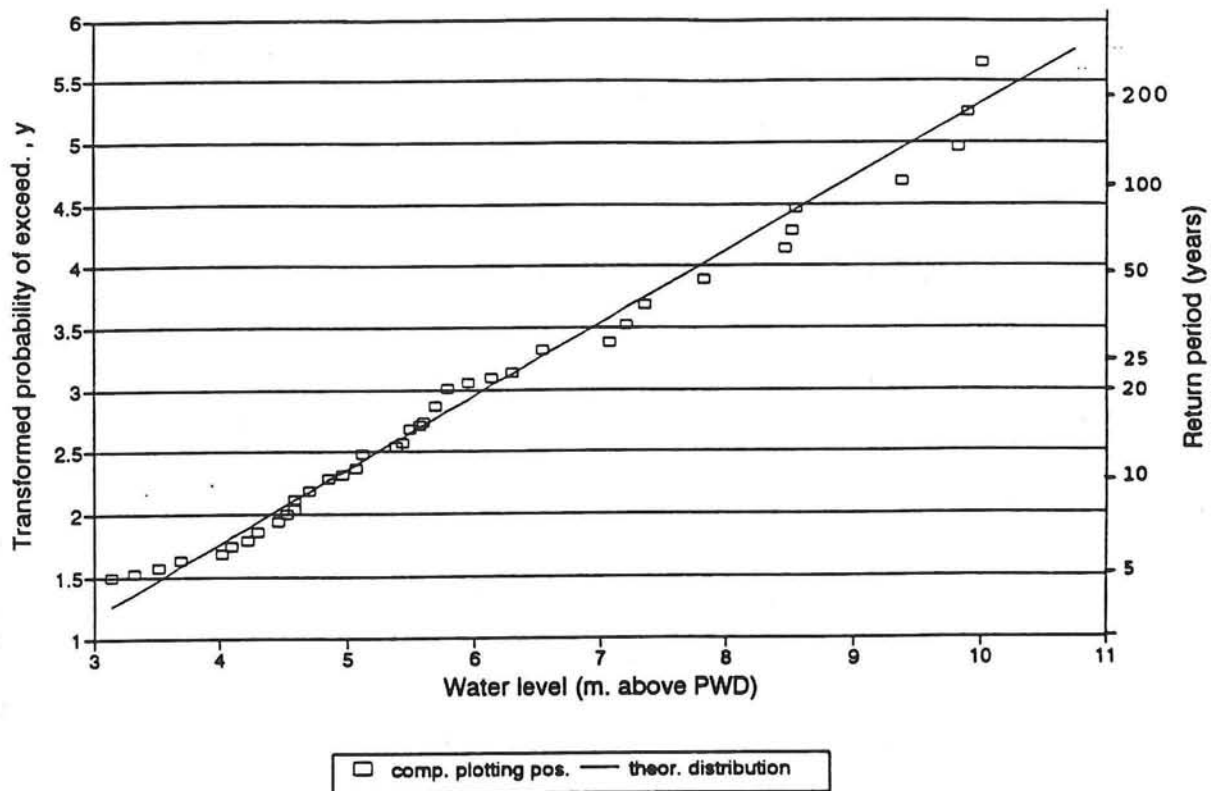


Figure D.6: Probability distribution during cyclone conditions for Chittagong.

#### D.4 DERIVATION OF WATER LEVEL PROBABILITY DISTRIBUTION FOR THE FENI DAM DURING CYCLONES

In this chapter it is described how the probability distribution for cyclone water levels near the Feni dam was derived using the distribution near Chittagong. When the coastal embankments are assumed to have an unlimited crest level, no water will overtop the embankment. For this situation the water levels during cyclone conditions were derived using the monsoon relation between Chittagong and the Feni dam. This procedure is described in Section D.4.1. This water level is thought to be lower in reality due to the limited crest levels of the coastal embankments. In Section D.4.2 the reduction of the water levels near the Feni dam caused by inundation of the hinter land is estimated using rough schematizations. Finally the water level distribution for cyclone conditions near the Feni dam to be used for the redesign is derived in Section D.4.3.

##### D.4.1 MONSOON RELATION BETWEEN CHITTAGONG AND THE FENI DAM

From ref. [5] the water levels for various return periods during monsoon conditions were derived for Khal no. 10, which is located near Chittagong. The accompanying distribution reads:

$$p \{ \text{water level} \geq x \} = 1 - e^{-e^{-2.54 \cdot x + 8.46}}$$

The probability distribution for water levels near the Feni River Closure Dam during monsoon conditions was derived in chapter 2 of Annex A. The distribution is repeated here:

$$p \{ \text{water level} \geq x \} = 1 - e^{-e^{-2.25 \cdot x + 13.37}}$$

Out of these two monsoon distributions a relation between the water levels at the two locations could be derived. For a certain return period the difference between the water levels at both locations during monsoon conditions is assumed to be equal to the difference between the water levels during cyclone conditions.

For various return periods the difference between the water levels near Khal no. 10 and the Feni dam could be computed during monsoon conditions. For the same return period, this difference was added to the water level during cyclone conditions near Khal no. 10. The result is the water level during cyclone conditions for the same return period near the Feni dam. This is done in Table D.10.

Return period (years)	5	10	20	25	50	100
A: Water level (m + PWD) cyclone conditions Chittagong	3.55	4.82	6.04	6.42	7.61	8.79
B: Water level (m + PWD) monsoon conditions Chittagong	3.92	4.21	4.50	4.59	4.86	5.14
C: Water level (m + PWD) monsoon conditions Feni dam	6.62	6.95	7.27	7.37	7.69	8.00
C-B+A: Water level (m + PWD) cyclone conditions Feni dam derived from monsoon relation	6.25	7.56	8.81	9.20	10.44	11.65

**Table D.10:** Calculation of water levels for various return periods for cyclone conditions near the Feni dam, derived from monsoon relations between Chittagong and the Feni dam.

#### D.4.2 WATER LEVEL REDUCTION DUE TO INUNDATION

The monsoon relation can be queried however. When the water level rises higher than the crest level of the coastal embankments, land will be flooded. Caused by the topography, which is more mountainous near Chittagong than near the Feni dam, relatively more land will be flooded near the Feni dam. Probably, this will result in a lower water level near the Feni dam than calculated out of the monsoon relation between the two locations. In order to estimate the water level reduction because of inundation of dry land, the Duchess model cannot be used, because this numerical model could not be calibrated well in the concerned area. Furthermore, it is doubted, whether the hydraulic situation near the embankments, can be simulated accurately using Duchess. These embankments behave like free fall weirs, during the overtopping period. As a first estimation of the water level reduction, the following method was applied:

First an area was defined near the dam and was schematized as shown in Figure D.7.



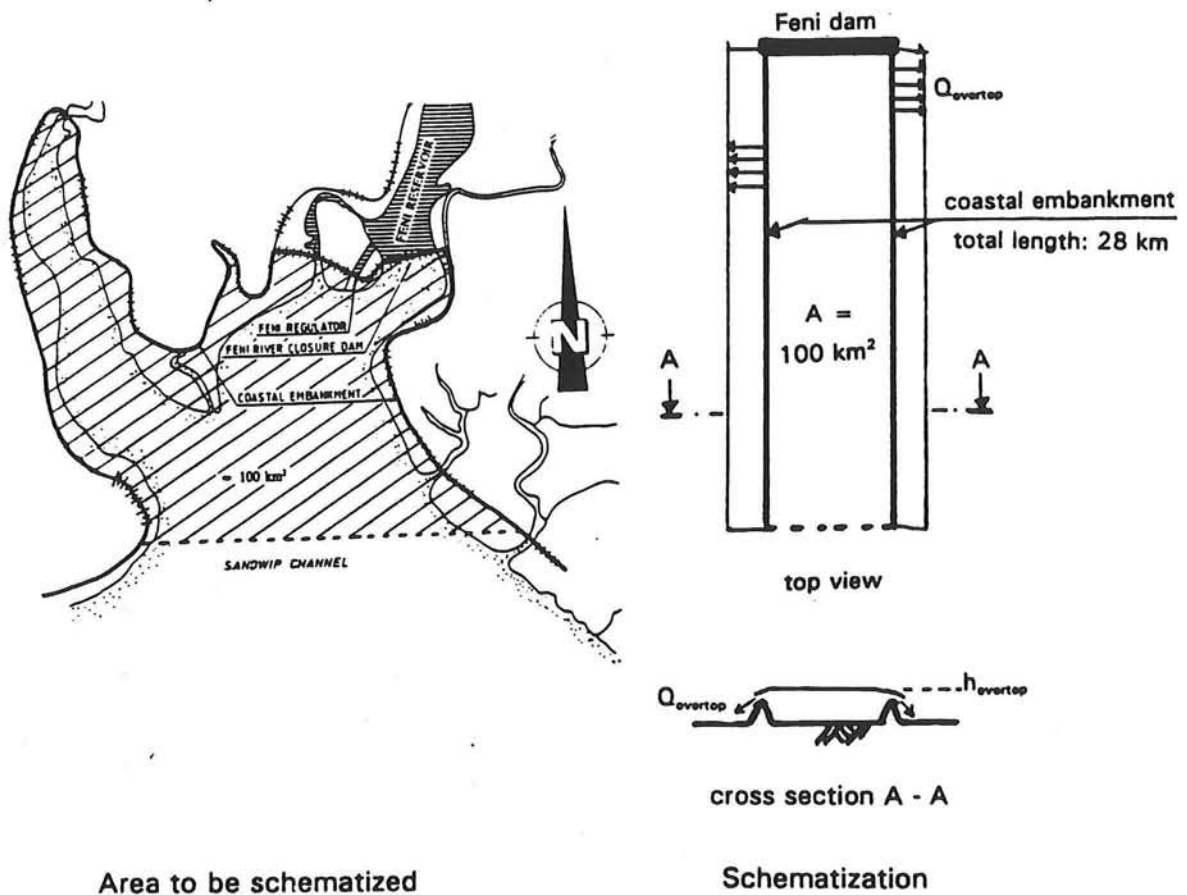


**Figure D.7:** Schematized area near the Feni River Closure Dam for the calculation of the water level reduction due to inundation of the hinterland.

As a starting point, the situation was considered, when the embankments are sufficiently high to prevent inundation of dry land. In this situation the water level in this area is assumed to be equal to the water level, calculated using the monsoon relation between the Feni dam and Chittagong. The variation of this water level is schematized as a half sinus curve, whose maximum corresponds to the calculated extreme water level. The period was determined to be 12 hours. So, for the water level variation, the following equation was used:

$$h_{\text{theor}}(t) = h_{\text{max}} * \sin \left( \frac{2 * \pi}{12 * 3600} * t \right)$$

in which:

$$\begin{aligned} h_{\text{theor}}(t) &= \text{water level variation with unlimited crest levels of the coastal embankments [ m ]} \\ h_{\text{max}} &= \text{theoretical extreme water level calculated out of the monsoon relation. [ m ]} \\ t &= \text{time [ s ]} \end{aligned}$$

As the length of the schematized area  $\approx 10$  km is much smaller than the tidal wave length, the water level in the area can be considered horizontal and the following equation of continuity can be drawn up:

$$Q_{\text{south}}(t) = A * \frac{dh_{\text{theor}}(t)}{dt}$$

in which:

$$\begin{aligned} Q_{\text{south}}(t) &= \text{discharge through the southern boundary of the schematized area} && [ \text{m}^3/\text{s} ] \\ A &= \text{surface area of the schematized region} = 100 * 10^6 \text{ m}^2 && [ \text{m}^2 ] \end{aligned}$$

The time related discharge at the southern boundary could be derived, when no land would be flooded. In reality the embankments have a limited height. For water levels higher than the crest levels, water will flow out of the schematized area into the polders, which will yield a water level reduction.

In order to estimate the water level variation when dry land would be inundated, the following assumptions were made:

- The water level is horizontal in the schematized area,
- The discharge through the southern boundary of the schematized area during inundation of land is assumed to be equal to the discharge for unlimited crest levels =  $Q_{\text{south}}(t)$ .
- The water flow over the coastal embankments during overtopping is assumed to be critical. Thus the embankments are assumed to behave like free fall weirs.

Now the continuity equation can be rewritten:

$$Q_{\text{south}}(t) - Q_{\text{overtop}}(t) = A * \frac{dh_{\text{overtop}}(t)}{dt}$$

in which:

$$\begin{aligned} Q_{\text{overtop}}(t) &= \text{overtopping discharge over the coastal embankments} && [ \text{m}^3/\text{s} ] \\ h_{\text{overtop}}(t) &= \text{time related water level when water is overtopping the embankments} && [ \text{m} ] \end{aligned}$$

After discretization this equation becomes:

$$h_{\text{overtop}}(t + \Delta t) = h_{\text{overtop}}(t) + \frac{Q_{\text{south}}(t) - Q_{\text{overtop}}(t)}{A} * \Delta t$$

in which:  $\Delta t$  = time step

[ s ]

The overtopping discharge could be calculated using the equation for a free fall weir. This becomes:

$$Q_{\text{overtop}}(t) = m * \frac{2}{3} * \sqrt{\frac{2}{3} * g * \Delta h(t)^3} * L_{\text{embank}}$$

in which:

$$\begin{aligned} m &= \text{discharge coefficient, here assumed to be 1.0} && [ - ] \\ g &= \text{acceleration of gravity, here 9.81} && [ \text{m/s}^2 ] \\ \Delta h(t) &= \text{water level above embankment crest level} = h_{\text{overtop}}(t) - \text{crest level} && [ \text{m} ] \\ L_{\text{embank}} &= \text{total length of the coastal embankment in the schematic area} = 28 * 10^3 \text{ m} && [ \text{m} ] \end{aligned}$$

Using a time step  $\Delta t = 300$  seconds and the existing embankment crest level of 7.6 m. + PWD, the time related water level variation for this schematic situation could be derived by iteration using the following initial conditions:

$$Q_{\text{overtop}}(0) = Q_{\text{south}}(0) \text{ and}$$

$$h_{\text{overtop}}(0) = \text{MSL} = 1.0 \text{ m. + PWD.}$$

In this way, the extreme water level could be derived in the schematic situation, when the hinterland is inundated for the theoretic extreme water level, calculated using the monsoon relation. This is done for various theoretical water levels by means of a spread sheet computer program in the Table D.11.

$h_{\text{theor, max}}$ (m. + PWD)	8.0	9.0	10.0	11.0	12.0	13.0
$h_{\text{overtop, max}}$ (m. + PWD)	7.98	8.45	8.76	9.00	9.21	9.39

**Table D.11:** Reduced water levels due to overtopping for various water levels in the hypothetical case of coastal embankments having unlimited crest levels.

#### D.4.3 RESULTING WATER LEVEL DISTRIBUTION FOR THE FENI DAM

These results are a very rough estimation of the water level reduction due to inundation of dry land. For these calculations only the equation of continuity was considered. The equation of motion was neglected. In the two situations where the coastal embankments have either unlimited or limited crest levels, the discharge through the southern boundary was assumed to be the same. In reality, next to the equation of continuity, more hydraulic processes will occur.

The schematic area is thought to be relatively small compared to the area influenced by a cyclonic storm surge. Accordingly, outside this schematic area, where the depths are larger, the water level is thought to be relatively insensitive to the loss of water due to overtopping. Initially, a hydraulic gradient will develop from the insensitive water level outside the schematic area to the reduced water level near the embankments. This will cause a larger incoming discharge in the schematized area than assumed in the schematic calculations. Subsequently, this will cause a higher water level near the Feni dam than the reduced water level, which was calculated making the schematizations.

The water levels near the Feni dam derived from the monsoon relation with Chittagong can be considered as an upper limit and the reduced water levels derived by means of the mentioned overtopping schematization can be considered as a lower limit. In reality the extreme water level will be somewhere in between the two values.

For further design purposes the extreme water levels during cyclone conditions near the Feni dam were estimated to be the average of the upper and lower limit. For various return periods, the water level values are given in Table D.12.

Return period (years)	10	20	25	40	50	100
<b>A:</b> Water level (m + PWD) cyclone conditions Feni dam derived from monsoon relation.	7.56	8.81	9.20	10.02	10.44	11.65
<b>B:</b> Water level (m + PWD) cyclone conditions Feni dam after overestimated reduction due to inundation.	7.56	8.55	8.71	8.96	9.06	9.33
<b>(A+B)/2:</b> Water level (m + PWD) cyclone conditions Feni dam used for further design.	7.56	8.68	8.96	9.50	9.75	10.49

**Table D.12:** Derivation of the water levels for cyclone conditions, used as a basis for the redesign, for various return periods.

## ANNEX E

### THE SET-UP OF A NUMERICAL WAVE HINDCAST MODEL

#### TABLE OF CONTENTS

E.1	<u>MODEL AREA</u> .....	E - 3
	E.1.1 SOUTHERN BOUNDARY .....	E - 3
	E.1.2 LATERAL AND NORTHERN BOUNDARIES .....	E - 3
E.2	<u>MESH SIZES</u> .....	E - 4
	E.2.1 INPUT GRID MESH SIZES .....	E - 4
	E.2.2 COMPUTATIONAL GRID MESH SIZES .....	E - 6
E.3	<u>MODEL PARAMETERS</u> .....	E - 6
E.4	<u>BATHYMETRY</u> .....	E - 6



## ANNEX E THE SET-UP OF A NUMERICAL HINDCAST MODEL

In this annex the set-up of the numerical model used to estimate the wave climate is described.

### E.1 MODEL AREA

In order to define the model area the southern lateral and northern boundaries are determined in this chapter.

#### E.1.1 SOUTHERN BOUNDARY

First the model boundaries, which determine the model area were chosen. The southern boundary was determined at a location, where short waves have not yet been influenced by the bottom through dissipation, breaking or refraction. This is the case at "deep water". In literature the following condition is valid for deep water:

$$\frac{h}{L_{op}} = \frac{h * 2 * \pi}{g * T_p^2} > 0.25$$

in which:

h	= the water depth	[ m ]
L <sub>op</sub>	= wave length in deep water	[ m ]
g	= gravity acceleration = 9.81	[ m <sup>2</sup> /s ]
T <sub>p</sub>	= wave period for the peak of the wave energy spectrum	[ s ]

For a wave generated at the ocean having a return period of about 50 years, the wave peak period is approximately 14 seconds. The wave length is about 300 meters then. In this case the water can be considered deep where the depth is more than  $0.25 * 300 = 75$  meters. When considering the used bottom charts, it was concluded that the southern boundary should be located at 21° latitude to fulfil the deep water condition.

#### E.1.2 LATERAL AND NORTHERN BOUNDARIES

The lateral boundary at the west side is partly an open boundary, where no waves will be introduced in the model. In this direction the width of the model area should be larger than the area of interest, because along the western lateral boundary a region exist where the wave field is disturbed by the import of zero wave energy. This extension of the model area is determined by the half power width of the directional energy distribution of the waves. This half power width is typically 20° to 40° for waves generated in the model area and 5° to 10° for swell. In this way the western boundary has been determined to be at 90° longitude.

The eastern and northern boundary were imposed by the topography of the coast. The model area is given in Figure E.1.

## **E.2 MESH SIZES**

Three sorts of grids are used in Hiswa; the input, the computational and the output grid. For an explanation of this, reference is made to the Hiswa manual (ref. [9]). The mesh sizes of the input and computational grid are successively determined in Sections E.2.1 and E.2.2.

### **E.2.1 INPUT GRID MESH SIZES**

For running Hiswa, the bottom levels are required for all grid points of the input grid. The mesh size of the input grid should be chosen in such way that relevant details in the bottom are well resolved. At the southern boundary, where depths reach large values, the bottom influence plays a minor role. Because of this and to simplify the introduction of the bathymetry, the mesh size of the input grid near the southern boundary can be rather large and may reach a magnitude of about 3,000 meters.

For the wave climate near the Feni River Closure Dam the detailed description of the bottom directly in front of the dam is rather important. To describe this bottom in a rather accurate way, an input grid mesh size of at least 300 meters is needed here.

It was determined that mesh refinements would be applied in a part of the overall model. This procedure is generally called nesting and is carried out twice. In this way three model areas could be determined.

#### **Overall model**

The input grid for the bathymetry has a mesh size of 3,300 meters and covers the whole model area.

#### **Interior model**

This model has a mesh size of 1,100 meters, which extends to about 80 kilometres south of the dam and covers the Sandwip region. This interior model obtains its boundary conditions from the overall model.

#### **Detailed model**

This model covers the area close to the Feni River Closure Dam up to about 4,500 meters south of the dam, where detailed soundings were carried out. Its mesh size was determined to be 275 meters to describe the bathymetry in this area well. The boundary conditions were provided by the interior model.



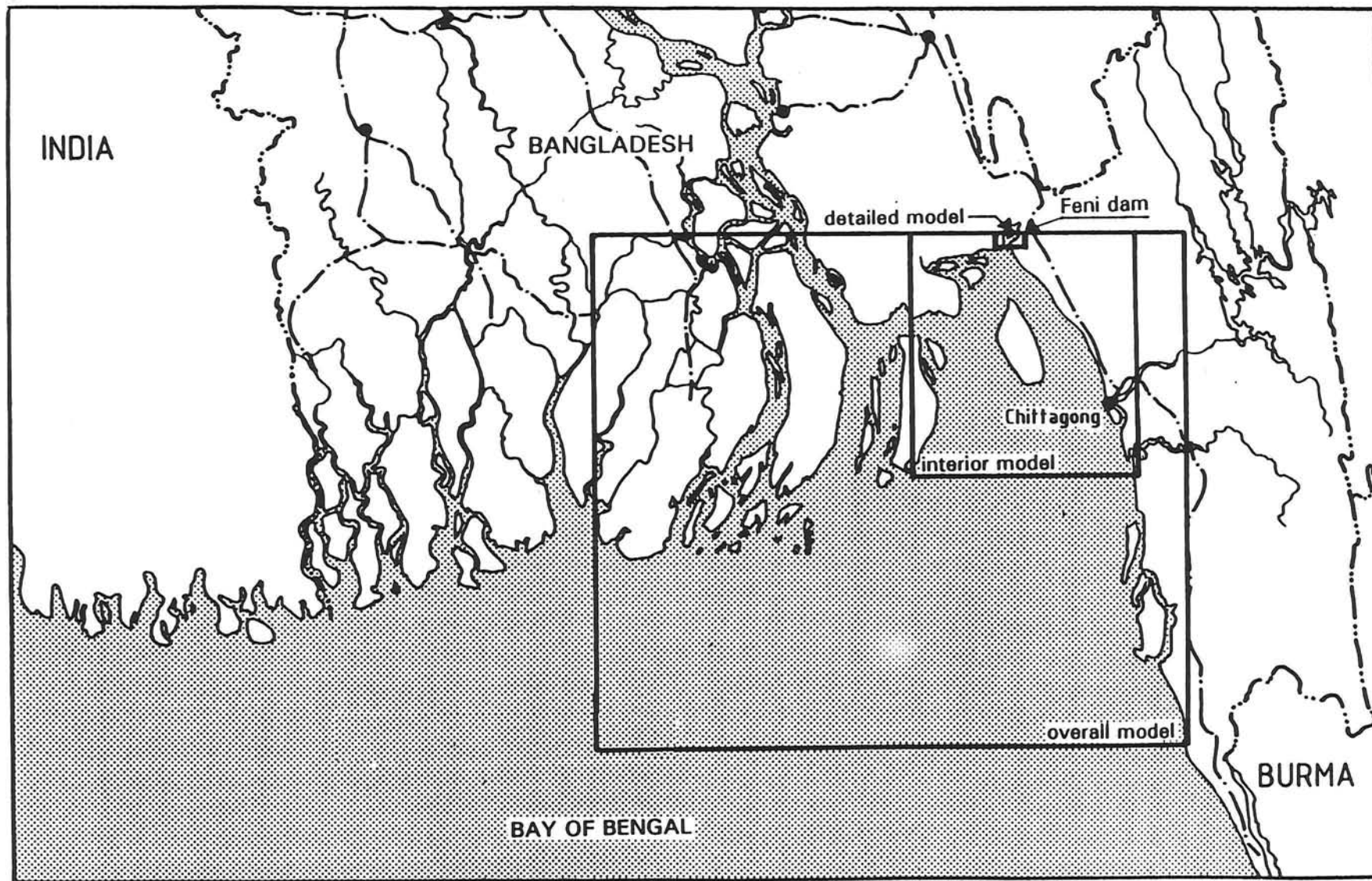


Figure E.1 : Illustration of the used Hiswa model areas.

## **E.2.2 COMPUTATIONAL GRID MESH SIZES**

For the definition of the computational grid, the following aspects had to be chosen:

- The x-axis of the computational grid has to be chosen more or less equal to the mean propagating direction of the waves in the model area.
- The directional sector around the positive x-axis in which Hiswa computes information at spectral directions. In the Hiswa manual (ref. [9]) a sector of 120° is advised.
- The number of subdivisions of the directional sector.
- The mesh sizes in x and y direction for the computational grid. The values should be chosen in such way that the condition for numerical stability and accuracy is answered. The stability criterion yields:

$$Dx/Dy < \cotg ( 0.5 * \text{directional sector} ) \approx 0.58$$

The requirement for considerable accurate results is that the amount of grid points, having a negative action density is minimal. This is also governed by the value of  $Dx / Dy$ .

The latter requirement turned out to be governing. Finally for this factor a value of 0.1 had to be applied, using a mesh size in y-direction which is more or less equal to the mesh size of the bottom input grid.

## **E.3 MODEL PARAMETERS**

The model parameters are not known accurately and as a result of the lack of wave observations near the Feni Dam, the model could not be calibrated. In general the default values of the input parameters can be considered to be a good estimation. For the following parameters these default values are applied:

- Water density
- Coefficients that describe the following processes:
  - wave growth
  - wave breaking
  - bottom friction
  - current blocking

## **E.4 BATHYMETRY**

The bathymetric charts used for the set-up of this model are given below:

- British Admiralty charts were used for the input of the bathymetry for the overall and interior model.
- Bathymetric charts obtained from the Land Reclamation Project.
  - LRP chart 1: A chart comprising the northern Sandwip region,
  - LRP chart 2: Charts made out of soundings, carried out by the Land Reclamation Project in the years 1982, 1986 and 1987 these soundings were carried out in the dam area to an extend of about 2,000 meters perpendicular to the dam.

## **Transition between the LRP chart 1 and the Admiralty chart**

As mentioned in previous chapters there is a transition between bottom charts obtained by the Land Reclamation Project north of Chittagong and the Admiralty charts, which cover the area south of Chittagong. Reference is made to Annex B section 4.2, where the same problem is explained, during the set-up of the Duchess model.

## **Transition between the two LRP charts**

The northern boundary of the LRP chart 1 is located at about 11 kilometres south of the Feni Dam. As the detailed soundings in front of the dam extend only to about 2 kilometres south of the dam, an area with a length of about 9 kilometers appears to be uncovered by soundings! The bottom depth at the northern side of the LRP chart 1, is known to be 5.0 meters below PWD. North of this, no depth values are known, but only the location of the various embankments could be derived from a satellite picture, made in 1992 and obtained from the Muhuri Irrigation Project. In the uncovered area, the bottom depth is assumed to be constantly 5.0 meters below PWD up to 3.5 kilometres south of the Feni Dam. North of this point the bottom depths have been interpolated to the known bathymetry of the detailed bottom chart near the dam. In reality the bottom depth is thought to decrease gradually to the coast, thus in northern direction. Furthermore the bottom generally incorporates many gullies and shoals in this area. These aspects cause a decrease of wave height through a.o. breaking, bottom dissipation and refraction. By assuming a constant bottom level in the area which is uncovered by soundings, the model will probably generate design wave heights near the dam that are a little bit higher than in reality, which yields a safer design.

### **E.4.1 Boundary conditions**

Apart from the bathymetry, the following boundary conditions had to be introduced in the model:

#### **Water level**

Hiswa assumes that the water level, which is introduced, is flat and horizontal. Hiswa will only calculate the wave conditions for this water level and will not generate a water level elevation caused by wind set-up.

#### **Waves entering the southern boundary**

At the southern model boundary waves enter the model area. These waves are generated by ocean depressions and have generally a relatively large period, of about 12 seconds. These waves can be introduced in the numerical model by giving the parameters of the significant wave height and period and mean propagating direction. Furthermore, the width of the directional energy distribution of the incident waves had to be determined. For swell, which enters the model, a relatively small value of  $10^\circ$  is advised and for waves generated in the model area a larger directional spread has to be used.

#### **Local wind fields**

In the numerical model waves are generated by means of wind fields in the model area. In Hiswa the parameters for wave growth can be modified, but as no wave observations are available in the model area, the default values were taken into account.



## ANNEX F

### DESIGN PROCEDURE FOR THE GEOMETRIC DAM PROFILE

#### TABLE OF CONTENTS

F.1	<u>INTRODUCTION</u>	F - 4
F.2	<u>COSTS</u>	F - 4
F.2.1	TOTAL BASE CONSTRUCTION COSTS	F - 4
F.2.1.1	Construction costs independent of the geometric dam profile	F - 4
F.2.1.2	Unit rates	F - 5
F.2.1.3	First estimation of slope protection costs	F - 6
F.2.2	TOTAL CONSTRUCTION COSTS	F - 8
F.2.3	INVESTMENT COSTS	F - 8
F.2.4	OPERATION, MAINTENANCE AND REPLACEMENT COSTS	F - 8
F.3	<u>BENEFITS</u>	F - 8
F.3.1	POTENTIAL AGRICULTURAL YIELD	F - 9
F.3.2	EXPECTED ANNUAL DAMAGE	F - 9
F.3.2.1	Methodology	F - 9
F.3.2.2	Assumptions for the damage-frequency curve	F - 10
F.3.2.3	Derivation of overtopping volumes for the water quality limits	F - 13
F.3.2.4	Derivation of return periods of the overtopping volumes for the water quality limits	F - 14
F.3.3	ANNUAL BENEFITS	F - 15
F.4	<u>OPTIMIZATION OF NET PRESENT VALUE</u>	F - 15
F.4.1	METHODOLOGY	F - 15
F.4.2	RESULTS OF THE OPTIMIZATION	F - 16
F.4.3	EXAMPLE OF DERIVATION OF NPV FOR CHOSEN DAM PROFILE	F - 17
F.5	<u>VERIFICATION OF MONSOON CRITERION</u>	F - 18
F.6	<u>DESIGN OF DAM PROFILE WHEN THE CPP II CRITERIA WOULD BE APPLIED</u>	F - 19
F.6.1	MONSOON DESIGN CONDITION	F - 19
F.6.2	CYCLONE DESIGN CONDITION	F - 19



## **ANNEX F     DESIGN PROCEDURE FOR THE GEOMETRIC DAM PROFILE**

### **F.1     INTRODUCTION**

In this annex the method used to derive the geometric dam profile is described. In accordance with the design criteria (see chapter 7.1 of the main report), the monsoon and cyclone conditions have to be treated separately. For cyclone conditions the dam profile was decided to be derived using an economic optimization procedure. Subsequently this dam profile had to be checked on fulfilment of the monsoon criterion. For the mentioned economic optimization procedure the costs and benefits of the Feni dam had to be estimated for each year of the economic life time of the structure. This is done in Section F.2 and F.3. In Section F.4 the optimization procedure is described and an example of the derivation of the Net Present Value, which is used for this procedure as a main indicator for the economic feasibility, is given. In Section F.5 it is checked, whether the resulting dam profile meets the monsoon criterion. Just for an illustration, the dam profile is determined, when the design criteria used for the coastal embankments which are subject to the Cyclone Protection Project II would be imposed to the Feni dam. This is done in Section F.6.

### **F.2     COSTS**

In this chapter, the costs to be made for the construction and maintenance of the Feni dam are estimated for each year of the economic life time. For the calculations of the costs various definitions are commonly used. In Section F.2.1 the total base construction costs and in Section F.2.2 the total construction costs are derived. From these costs the investment costs, to be made at the start of the structures life time, can be calculated as explained in Section F.2.3. Finally, the operation, maintenance and replacement costs, which are expected to be made each year of the structures life time, can be calculated in Section F.2.4.

#### **F.2.1    TOTAL BASE CONSTRUCTION COSTS**

The total base construction costs can be divided into two parts; dependent and independent of the geometric dam profile. In the Section F.2.1.1 the costs are given, which are independent of the dam profile. In order to estimate the costs which depend on the volumes to be used in the geometric profile, the unit rates have to be determined first. This is done in Section F.2.1.2. The costs of the slope protection depend besides on the length of the slope to be protected on the necessary thickness of the cover layer. This latter aspect is related to the slope angle. In Section F.2.1.3 the method to estimate the cover later thickness is described. Finally the total construction costs could be calculated for each considered dam profile. This calculation was carried out using a spread sheet computer program.

##### **F.2.1.1            Construction costs independent of the geometric dam profile**

The costs of the parts of the structure, which are independent of the crest level and sea side slope angle, were derived from ref. [3] and are given in the Table F.1.

Description of item	Unit	Quantity	Unit rate (Tk)	Amount (10 <sup>6</sup> Tk)
Mobilisation & demobilisation	-	-	-	166.24
Bed protection	m <sup>2</sup>	190,000	600	114.00
Sill	m <sup>3</sup>	93,000	400	37,20
Neap tide dam	m <sup>3</sup>	19,700	800	15.76
Winter spring tide dam	m <sup>3</sup>	114,000	475	54,15
Road (incl. flank embankments)	m <sup>2</sup>	4,500	1000	4,50

**Table F.1:** Costs independent of the final dam profile.

#### F.2.1.2 Unit rates

For the calculation of the construction costs, which depend on the geometric dam profile, the dam profile including the overheight due to geometric settlement had to be taken into account. In order to derive these costs, the unit rates were estimated first. This was done by using the figures of ref. [3]. In this report no detailed information about the unit rates are given. For the slope protection for example, only the total costs per m<sup>2</sup> is given. From these figures, unit rates for each part of the slope protection were estimated using information from ref. [24]. These unit rates are given in Table F.2.

Part of the dam	Materials	Unit	Unit rate (Tk)
Final profile main dam	Earth works	m <sup>3</sup>	100
Final profile flank embankments	Earth works	m <sup>3</sup>	75
Sub layer	Clay	m <sup>3</sup>	300
Filter layers	Geotextile	m <sup>2</sup>	150
	Chipped bricks	m <sup>3</sup>	1200
	Pea gravel	m <sup>3</sup>	750
Cover layer	Concrete blocks, gravel aggreg.	m <sup>3</sup>	2400
	Concrete blocks, brick aggreg.	m <sup>3</sup>	2000
	Brick blocks	m <sup>3</sup>	1300
	Bricks	m <sup>3</sup>	1200

**Table F.2:** Material rates for items of the Feni dam, which are depending on the geometric profile.



### **F.2.1.3 First estimation of slope protection costs**

In order to estimate the costs per surface area for the slope protection, the following assumptions have been made:

**Flank embankments:**

In this stage of the redesign, the slope protection for the right and left flank embankment was chosen to be the same as the original design. The costs per surface area were estimated for the original design and these were subsequently assumed to be equal to the costs per surface area for the redesign.

**Main dam:**

The following items were chosen equal to the original design:

- The sub layer of the slope protection is clay, which is 0.60 meter thick.
- On top of this clay layer a filter fabric was chosen of the same sort as used in the original design.
- On top of this filter fabric a filter layer of chipped bricks with a thickness of 0.10 meter was chosen.
- On top of this filter, placed blocks were used. For each part of the slope, the material of these blocks was initially assumed to be the same as for the original design.

As a first estimation of the cover layer thickness, the global design method is used, which is described below. The thickness of the cover layer is only depending on the slope angle. Subsequently, the costs for the slope protection per surface area could be derived using the mentioned unit rates.

#### **Explanation of the use of the Global method**

In order to estimate the cover layer thickness for the main dam, the global design method for placed revetments was used. For more detailed information reference is made to ref. [12]. The global method is based on the following items:

- Results of extensive research
- Calculations using the analytical method, which is described in Section 7.6.3 (main report)
- Results of numerical calculations

For the global method the breaker index  $\xi$ , has to be derived. The following relation is valid for  $\xi$ :

$$\xi = \frac{\tan \alpha}{\frac{H_{sig}}{L_{op}}} \quad ; \quad L_{op} = \frac{g * T_p^2}{2 * \pi}$$

in which:

$\xi$	= breaker index	[ - ]
$\alpha$	= slope angle	[ ° ]
$H_{sig}$	= significant wave height	[ m ]
$L_{op}$	= wave length at deep water	[ m ]
$g$	= acceleration of gravity	[ m/s <sup>2</sup> ]
$T_p$	= wave period of the peak in the wave energy spectrum	[ s ]

The global method is relating this breaker index to the parameter  $H_{sig}/\Delta * D$ . In this relation  $\Delta$  is the relative density under water and  $D$  is the thickness of the cover layer. The relation between  $\xi$  and  $H_{sig}/\Delta * D$  is depending on the construction type. In this case, the relation can be applied for a "normal construction". For this case design figures were made, see Figure F.1. For a certain breaker index the parameter  $H_{sig}/\Delta D$  and accordingly the necessary thickness  $D$  could be calculated, using this figure.

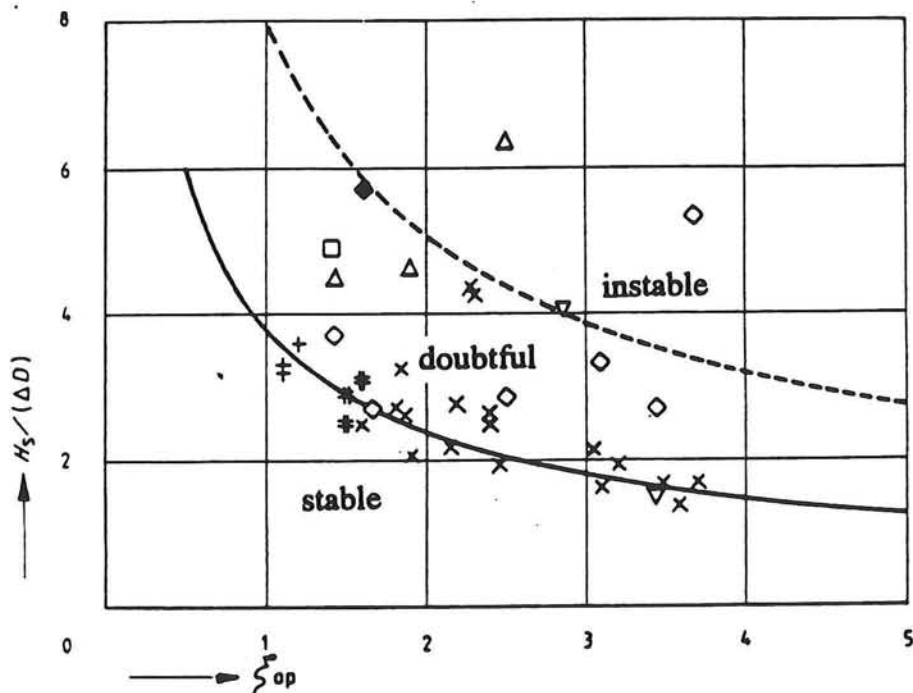


Figure F.1: Design figure of the global method for pitched stones on a geotextile on a granular filter. ("normal construction") see ref. [12].

For more details of this method and for the design figures, reference is made to ref. [12]. For various slope angles, the necessary thicknesses of the cover layer for the main dam were derived using the global method. The used wave conditions for the return period of 50 years were:  $H_{sig} = 1.4$  meter and  $T_p = 4.6$  seconds as determined before in Table 14 of Section 7.4.5.3 of the main report. The results are given in the Table F.3.

Slope angle	1:4	1:4.5	1:5	1:5.5	1:6
Minimum cover layer thickness (m)	0.45	0.40	0.40	0.35	0.30

**Table F.3:** Results of the determination of the cover layer thickness using the global design method.

The costs of the dam parts, which are dependent on the geometric profile, are the costs for the earth work and the slope protection. Using the mentioned unit rates and estimated cover layer thicknesses, the costs could be derived, which are depending on the profile. Subsequently the total base construction costs could be obtained by adding these costs to the costs, which are independent of the geometric profile.

## F.2.2 TOTAL CONSTRUCTION COSTS

In order to derive the total construction costs, physical contingencies have to be taken into account to cover unforeseen works. These contingencies are usually a percentage of the total base construction costs. In the Bangladeshi guidelines (ref. [15]), which have to be applied for projects in the scope of the flood action plan, a percentage of 15 % is advised for feasibility studies. This figure was used here too.

## F.2.3 INVESTMENT COSTS

The total investment costs are defined as the sum of the total construction costs and the engineering costs. These engineering costs comprise costs for survey, investigation, design, preparation of tender documents and supervision of construction. These costs were determined at 15% of the total construction costs. The investment costs have to be made in the year of construction.

## F.2.4 OPERATION, MAINTENANCE AND REPLACEMENT COSTS

These costs include among others costs for technical staff, operation and maintenance of structures and costs for annual repair. These costs were taken into account for every year of the discounting period and are thought to be a certain percentage of the total construction costs. According to the Bangladeshi FAP guidelines (ref. [15]), a percentage of 6% was applied.

## F.3 BENEFITS

In this chapter the annual benefits are derived. As explained in the main report, the annual benefit is defined to be the potential agricultural yield minus the expected annual damage due to overtopping waves at the sea side. In Section F.3.1 it is explained how the potential agricultural was determined. The estimation of the expected annual damage is described in Section F.3.2. Finally the annual benefits could be determined in Section F.3.3.

### F.3.1 POTENTIAL AGRICULTURAL YIELD

The potential agricultural yield is the theoretical maximum possible yield of the crops in one year, when no damage is occurring at all. In order to calculate this value, some data about the area to be cultivated and the cropping pattern have to be known. The gross area comprises about 40,000 ha. of which 27,175 ha. is arable. On this arable land, the objective was to cultivate two crops per year. These crops are HYV (= High Yield Variety) Aus, which is planted in March / April and harvested in June / July and transplanted HYV Aman, which is planted from July till September during the monsoon and harvested from November till January. From comparable irrigation projects (the Baranai Polder Project) in Bangladesh, the estimated yield is 3.3 tons per ha. for both concerned rice varieties. Reference is made to ref. [25]. Also for this comparable project, the market price was estimated to be about 4,000 Taka per ton for both varieties for 1985, which is the year of construction of the Feni River Closure Dam. For the Muhuri Irrigation Project the yield per ha. and the market price is assumed to be equal to the Baranai Polder Project. Using these figures, the potential agricultural yield could be calculated to be:

$$2 \text{ crops per year} * 3.3 \text{ tons per ha.} * 27,175 \text{ ha.} * 4,000 \text{ Taka's per ton} = \\ 720 \text{ million Taka's per year}$$

During the first years after the closure of the Feni river, the irrigation area has to be developed. The area ready for cultivation is not equal to the total possible arable area in this year. Here the Bangladeshi guidelines were followed again. Here it is advised to take a potential agricultural yield of 20 % of the total during the first year, increasing with 20 % each year until the total potential yield is reached 5 years after the closure of the Feni river.

### F.3.2 EXPECTED ANNUAL DAMAGE

#### F.3.2.1 Methodology

The damage to the crop can be caused by several effects. The main cause is the poor water quality in the reservoir, through which no irrigation is possible any more. This poor water quality is mainly caused by sea water overtopping the dam, which makes the reservoir saline. For the optimization procedure, only the damage to the crop due to overtopping waves during cyclonic conditions was considered.

In the following one geometric dam profile is considered, for the annual damage depends on the dam profile. In order to calculate the expected annual damage, a damage-frequency curve had to be derived for each geometric dam profile. For an accurate estimation of this curve, damage cases should be available from history. Unfortunately this is not the case. In spite of this a curve had to be constructed, for which it was necessary to make some assumptions.

The assumptions necessary to construct a schematic damage frequency curve are given in Section F.3.2.2. In this section some distinct points on this curve are defined for which the value of the damage is determined. This is done using the commonly used water quality limits for irrigation purposes. The accompanying probabilities of exceedance of these points are derived in the next sections.

When the return periods of the overtopping volumes necessary to reach the water quality requirements would be derived, the probabilities of exceedance required for the damage-frequency curve are known.

In Section F.3.2.3 the overtopping volumes necessary to reach the water quality requirements are calculated first.

Subsequently, the overtopping volume of sea water was calculated for the concerned dam profile and for various return periods as explained in Section F.3.2.4. Here it is described that the volume of sea water that overtopped the Feni dam can be related to the return period of the cyclonic situation.

From this relation the return period for the overtopping volume of sea water, necessary to reach the water quality requirements can be derived. Accordingly the probabilities of exceedance required for the damage-frequency curve are known.

When the damage-frequency curve of the concerned dam profile is known, the expected annual damage can be derived from this. According to the Bangladeshi guidelines, it is assumed that hydraulic situations exceeding the design situation will cause the same damage as without the dam structure. Accordingly, the surface area had to be determined under the damage-frequency curve below the probability of exceedance for the design situation. The resulting value is equal to the expected annual damage for the considered dam profile.

### F.3.2.2 Assumptions for the damage-frequency curve

As mentioned before, only the damage to the crop due overtopping saline sea water was considered. Accordingly, the water quality requirements for irrigation purposes have to be known. These requirements were obtained from ref. [26]. These requirements are among others:

	Unit	Degree of restriction on use		
		None	Slight to moderate	Severe
The Total Dissolved Solids (TDS)	mg/l	< 450	450 - 2000	> 2000

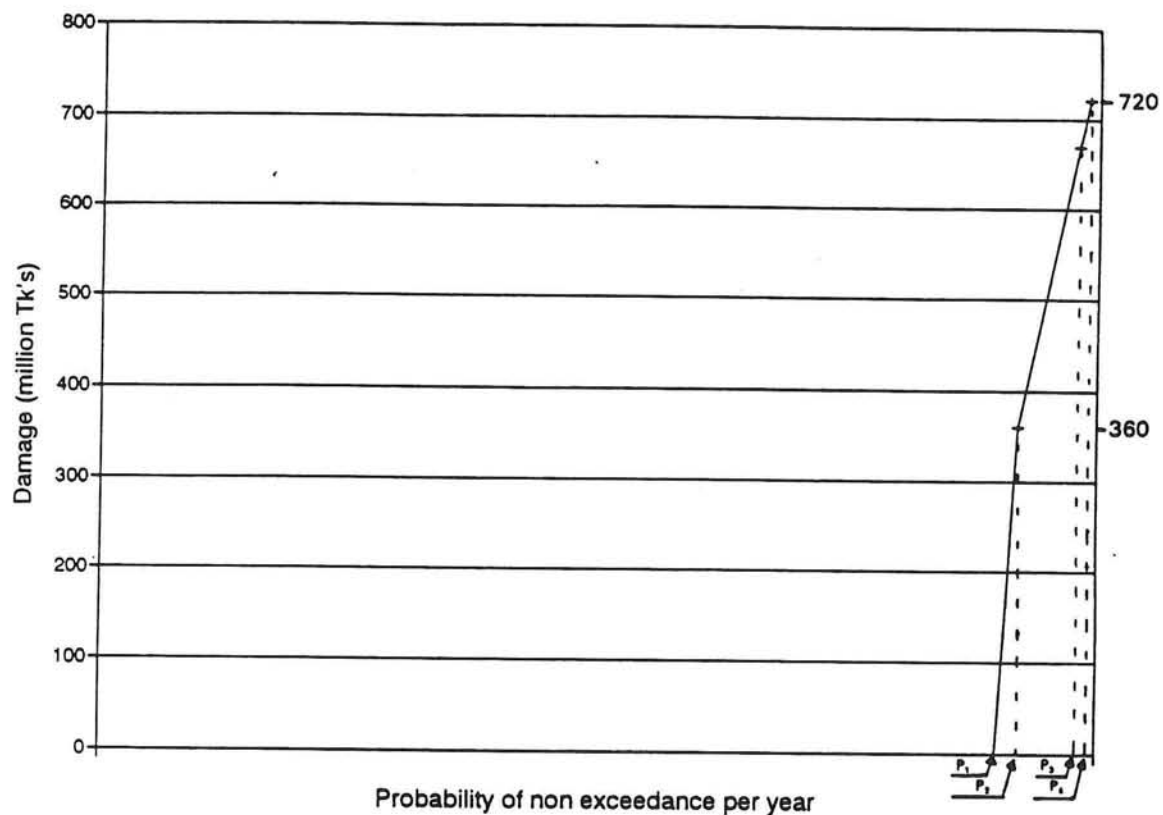
Table F.4: Water quality requirements for irrigation.

For the damage-frequency curve, the following assumptions were made in which the parameter TDS stands for Total Dissolved Solids in kilograms per m<sup>3</sup>:

- 1) TDS ≤ 0.45 kg/m<sup>3</sup>: No damage to the crop is assumed, because there is no restriction on the use for irrigation then. Thus below the probability of exceedance for TDS = 0.45 kg/m<sup>3</sup>, the damage is assumed to be zero.
- 2) TDS = 2.0 kg/m<sup>3</sup>: It is assumed that the reservoir will not be refreshed by the discharge of the Feni river quickly. The high TDS will prevail for a few weeks, which will be illustrated later. During this period, the reservoir water quality is not sufficient for irrigation. When TDS = 2.0 kg/m<sup>3</sup>, the complete crop is assumed to be lost. For the probability of exceedance of this situation, the damage is equal to one crop yield, which is half of the annual potential agricultural yield = 0.5 \* 720 = 360 million Taka's.

- 3) TDS = 2.0 kg/m<sup>3</sup> in both the pre- and post monsoon: This is the case when two cyclones occur in one year, in both periods mentioned. Then two crops are assumed to be completely lost. The probability of exceedance of this situation is assumed to be the square of the probability of exceedance for the situation which yields a TDS of 2.0 kg/m<sup>3</sup>. The accompanying damage is estimated to be the total agricultural yield for one year = 720 million Taka's.
- 4) Between the mentioned three points of the curve, linear interpolation is carried out.
- 5) The probability of exceedance for the design situation above which the dam will breach is assumed to be 1/design return period = 1/50 = 0.02 per year. This is the same value as used in the original design.

In Figure F.2 the schematic damage frequency curve is given.



- $P_1$  = Probability of non exceedance of TDS = 0.45 kg/m<sup>3</sup> per year
- $P_2$  = Probability of non exceedance of TDS = 2.0 kg/m<sup>3</sup> per year
- $P_4$  = Probability of occurrence that two crops are lost in one year
- $P_3$  = Probability of non exceedance of the design conditions = 0.98

Figure F.2: Schematization of the damage-frequency curve.

In order to derive the expected annual damage, the various probabilities of exceedance  $P_1$ ,  $P_2$ ,  $P_3$  and  $P_4$  had to be derived. This is done in the next sections.

### Estimation of the required time necessary to refresh the reservoir

As an illustration of the second assumption, the approximate duration, required to refresh the reservoir is estimated, after a TDS of 2.0 kg/m<sup>3</sup> was reached. The time needed for the TDS in the reservoir to decrease from 2.0 kg/m<sup>3</sup> to the value for which no restrictions on irrigation are valid (0.45 kg/m<sup>3</sup>) was estimated roughly.

For the reservoir the following equation of continuity of dissolved solids could be drawn up:

$$I_{res} * \frac{d TDS_{res}(t)}{d t} = Q_{Feni} * TDS_{Feni}(t) - Q_{out} * TDS_{out}(t)$$

in which:

$I_{res}$	= storage of the reservoir	[ m <sup>3</sup> ]
$t$	= time variable	[ s ]
$TDS_{res}(t)$	= TDS value in the reservoir	[ kg/m <sup>3</sup> ]
$TDS_{Feni}(t)$	= TDS value in the Feni river	[ kg/m <sup>3</sup> ]
$TDS_{out}(t)$	= TDS value of the water that is discharged through the regulator	[ kg/m <sup>3</sup> ]
$Q_{Feni}$	= Feni river discharge into the reservoir	[ m <sup>3</sup> /s ]
$Q_{out}$	= Discharge through regulator	[ m <sup>3</sup> /s ]

The following assumptions were made:  $Q_{out} = Q_{Feni}$  and thus  $I_{res} = \text{constant}$ ,  $TDS_{Feni} = 0$  and  $TDS_{out} = TDS_{res}$ .

Now the equation can be rewritten:

$$\frac{d TDS_{res}(t)}{d t} = -\frac{Q_{Feni}}{I_{res}} * TDS_{res}(t)$$

In general the solution can be written like:

$$TDS_{res}(t) = TDS_{res}(0) * e^{-\frac{Q_{Feni} * t}{I_{res} * TDS_{res}(0)}}$$

For:  $TDS_{res}(0) = 2.0 \text{ kg/m}^3$ ,  
 $TDS_{res}(t_1) = 0.45 \text{ kg/m}^3$ ,  
 $I_{res} = \text{storage for normal operating level} + \text{overtopping amount} = 6.0 * 10^7 \text{ m}^3$  and  
 $Q_{Feni} = 150 \text{ m}^3/\text{s}$  during the post monsoon,

The necessary time  $t_1$  can be calculated to be about  $1.2 * 10^6$  seconds  $\approx 14$  days.

The mentioned method is a very rough schematization, but it gives an estimation of the order of time necessary to refresh the reservoir.

It can be concluded that it takes about 2 weeks to refresh the reservoir and to enable unrestricted irrigation again, when initially the TDS was about 2.0 kg/m<sup>3</sup>. This is a relatively long period, which will cause damage to the standing crop.

### F.3.2.3 Derivation of overtopping volumes for the water quality limits

In order to calculate the expected annual damage for a certain geometric dam profile, the wave overtopping volumes for the three points of the damage-frequency curve have to be estimated first. Subsequently, the probability of exceedance of these overtopping amounts were estimated in the following sections and accordingly the damage frequency curve is known for the concerned dam profile.

For the derivation of the necessary overtopping amounts, to reach the two water quality requirements, the following assumptions were made:

- Only overtopping waves during cyclonic conditions were considered, because these govern the overtopping amounts.
- Prior to the overtopping period, the TDS of the reservoir is assumed to be zero.
- The reservoir level is at normal operating level (= 4.26 + PWD) at the time of overtopping.
- $\rho_{\text{sea water}} = 1025 \text{ kg/m}^3$ . This value was taken into account for the calculation, although this parameter is depending on the fresh water discharge of the lower Meghna river,
- For each part of the Feni dam, thus for the main dam and the both flank embankments, the overtopping amount per linear meter dam axis is equal.
- Saline percentage is constant over the whole reservoir.
- The overtopping amount over the regulator has been assumed to be negligible, because its crest level is relatively high.

For normal operating level of the reservoir, the storage could be derived from the water level - storage relation of ref. [27]. This storage is about  $5.8 * 10^7 \text{ m}^3$ .

Using ref. [28], the salinity percentage could be derived. As the density of sea water is always more than  $1000 \text{ kg/m}^3$ , this value can be subtracted from the density value:

$$\sigma_t = \rho_{\text{sea water}} - 1000 = 25 \text{ kg/m}^3$$

From this value the salinity promilage can be calculated, neglecting pressure and temperature influences:

$$S = 1/0.75 * \sigma_t = 33 \text{ ‰} = \text{salinity promilage}$$

The mass of the amount of fresh water in  $1.0 \text{ m}^3$  sea water is:

$$1.0 \text{ m}^3 * (1-0.033) * \rho_{\text{fresh water}} = 1.0 \text{ m}^3 * 0.967 * 1000 \text{ kg/m}^3 = 967 \text{ kg fresh water.}$$

The mass of dissolved solids in  $1.0 \text{ m}^3$  sea water is:

$$\begin{aligned} \rho_{\text{sea water}} * 1.0 \text{ m}^3 - 967 \text{ kg fresh water} &= 1025 \text{ kg/m}^3 * 1.0 \text{ m}^3 - 967 \text{ kg} = \\ &= 58 \text{ kg dissolved solids.} \end{aligned}$$

When the amount of overtopping sea water is  $x \text{ m}^3$ , the total dissolved solids coefficient (TDS) in the reservoir is:

$$\text{TDS} = \frac{\text{mass overtopping desolved solids}}{\text{reservoir storage} + \text{overtopping amount}} = \frac{58 * x}{5.81 * 10^7 + x} \quad [ \text{kg/m}^3 ]$$

The reservoir storage when the reservoir level is equal to the normal operating level was previously determined to be about  $5.8 * 10^7 \text{ m}^3$ , according to ref. [27].



Since the assumption was made that the overtopping amount per linear meter is equal for the whole dam, the overtopping amounts per linear meter for the two water quality limits can be computed as the total overtopping amount (x) divided by the total dam length. The total dam length measures 3,265 meters. Thus the overtopping amount per m' = x m<sup>3</sup> / 3,265 m.

The resulting overtopping amounts for the two water quality limits are given in Table F.5.

TDS	total overtopping amount	overtopping amount per m'
0.45 kg/m <sup>3</sup>	0.46 * 10 <sup>6</sup> m <sup>3</sup>	140 m <sup>3</sup> /m'
2.0 kg/m <sup>3</sup>	2.08 * 10 <sup>6</sup> m <sup>3</sup>	640 m <sup>3</sup> /m'

**Table F.5:** Overtopping amounts of sea water for the two water quality limits.

When a cyclonic surge causes a TDS of 2.0 kg/m<sup>3</sup> and when the surface area of the reservoir is estimated to be 12 \* 10<sup>6</sup>, m<sup>2</sup> the rise of the reservoir level is about:

$$\text{reservoir rise} = \frac{\text{overtopping amount}}{\text{reservoir surface area}} \approx \frac{2.0 * 10^6}{12 * 10^6} \approx 17 \text{ cm.}$$

This is a rather small rise. There is no inundation to be expected for the irrigation areas, so the damage is assumed to comprise only the damage due to the poor water quality.

Now the annual frequencies for both water quality limits have to be derived.

#### F.3.2.4 Derivation of return periods of the overtopping volumes for the water quality limits

In this section the return periods of the overtopping volumes, that are necessary to reach the water quality limits are derived. For this, the relation between the return periods and the wave overtopping amounts were derived for a certain geometric dam profile. Subsequently, the return period for the two mentioned water quality limits could be determined from this relation. How this was done will be explained in this section.

For various hydraulic situations having return periods of 15, 20, 25, 30, 35, 40, 45, 50 and 100 years, the wave overtopping amounts over the concerned dam profile were estimated. This was done by means of schematization of the high water wave caused by a cyclonic storm as a half sinus curve having a period of 12 hours for each return period. The equation for the water level variation during a high water wave reads:

$$h(t) = h_{\max} * \sin \left( \frac{2 * \pi}{12} * t \right)$$

in which:

$$\begin{aligned} h(t) &= \text{time related water level above PWD} && [ \text{m} ] \\ h_{\max} &= \text{extreme water level (+ PWD) for the concerned return period.} && [ \text{m} ] \end{aligned}$$

The water level variation was divided into several time intervals of 0.5 hour. For each time interval the average overtopping discharge can be estimated, depending on the wave parameters (  $H_{ig}$ ,  $T_z$  and  $\beta$  ), the slope angle and wind velocity, for a certain dam profile. This was done, using the HRS method for the average overtopping discharge caused by waves. Reference is made to ref. [29] for an explanation of this HRS method. The total of the overtopping amounts for all time intervals yielded the total overtopping amount of saline sea water for the concerned return period and dam profile. This procedure was carried out for the various return periods. By means of linear interpolation between these return periods, the return period for the overtopping volumes ( 140 and 640 m<sup>3</sup>/m' which yield the water quality limits could be derived for a specific dam profile. All this was calculated, using a spread sheet computer program.

Subsequently, the probabilities of exceedance for the various points in the damage-frequency curve could be derived and thus the damage-frequency curve is known for each geometric dam profile. Finally, the surface area under the curve below the probability of exceedance of the design situation, which is 0.02 per year, could be calculated. This value is equal to the expected annual damage for the concerned dam profile.

### F.3.3 ANNUAL BENEFITS

The annual benefit is defined to be the annual potential agricultural yield minus the expected annual damage due to overtopping waves. According to the Bangladeshi guidelines (ref. [15]), an economic growth factor had to be taken into account. Due to various agricultural improvements, the potential annual yield will increase in the course of time. The guidelines advise to take an economic growth rate of 3% into account. This means that the annual benefits yearly have to be increased by 3% .

## F.4 OPTIMIZATION OF NET PRESENT VALUE

### F.4.1 METHODOLOGY

For each year after closure of the Feni river, represented by the number n, counting from 0 in 1985, the costs and benefits could be derived now. The difference of the annual benefits and costs of year n had to be discounted to the basic year 1985, in which the closure took place. This was carried out taking a discounting rate of 12 % into account, which is a commonly used rate in Bangladesh and which is also in accordance with ref. [15]. For each year the discounted difference between benefits and costs was calculated. This is also called the Present Value (PV). Thus the PV can be calculated from:

$$PV = ( \text{benefits}_{\text{year } n} - \text{costs}_{\text{year } n} ) * \frac{1}{(1 + \text{discounting rate})^n}$$

The discounting period is assumed to be the economic life time of the structure. According to the Bangladeshi guidelines, 30 years is advised for the discounting period. As there is no reason to deviate from this, a period of 30 years was considered for this study as well.

The sum of the PV's of the discounting period is defined to be the Net Present Value (NPV). For each different dam profile the NPV could be derived.

Then the dam profile which yields the highest NPV was determined. This is thought to be the most economic dam profile, and was therefore chosen for the redesign.

#### F.4.2 RESULTS OF THE OPTIMIZATION

By systematically varying the crest levels and upper sea side slope angles, the relation between the NPV and both the crest levels and sea side slope angles could be derived. This is done in Figure F.3. The resulting optimum crest levels for the different sea side slope angles are given in Table F.6.

Slope angle	1:4	1:4.5	1:5	1:5.5	1:6
Optimum crest level (m. + PWD)	10.4	10.3	10.1	10.1	10.1
NPV (million Taka's)	4985.0	4994.9	4996.3	4990.8	4986.3

Table F.6: Results of the optimization procedure

The optimum crest level appeared to be more or less independent of the slope angle, when the tangent of the slope angle is less than 1:5. The slope angle which yields the highest NPV appeared to have a tangent of 1:5. It was determined, that the optimum dam profile for cyclone conditions has a crest level of 10.1 m. + PWD and a slope angle tangent of 1:5. The return period for the situation that one crop is completely lost appears to be about 25 years.

The mentioned method to calculate the NPV is rather incomplete. The derivation of the benefits is rather inaccurate, as damage figures are not available from practice. The used damage-frequency curve is just a first estimation. Several assumptions and schematizations had to be made in order to estimate the annual benefits. This is why no other conclusions should be drawn from the NPV's. The mentioned method is only a means to derive a geometric dam profile, which is thought to be the most economic for cyclonic conditions.

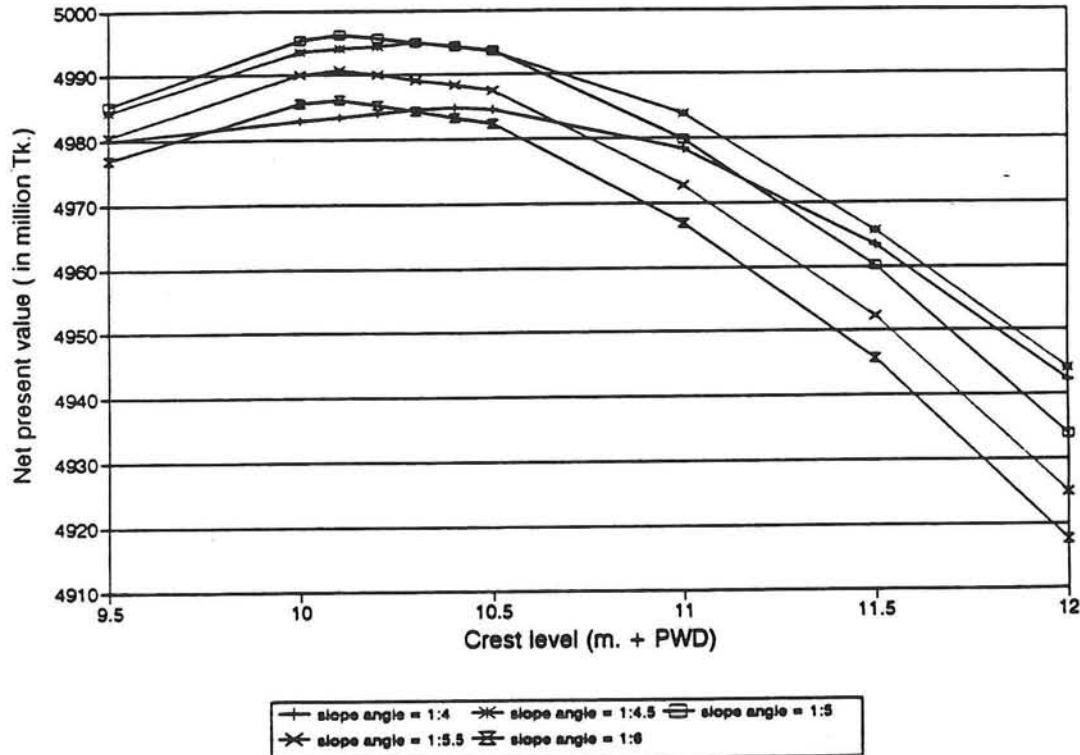


Figure F.3: Optimization of dam profile, using the NPV.

### F.4.3 EXAMPLE OF DERIVATION OF NPV FOR CHOSEN DAM PROFILE

As an example to calculate the NPV, this procedure is given in Table F.7 for the chosen dam profile, which comprises a crest level of 10.6 meter + PWD (including geotechnical settlement) and an upper slope tangent of 1:5.

Year after closure	Values in million Taka's			Annual benefit = 710.98 million Tk
	Investment costs	O&M costs	Benefite	PV
0	768.70	0.00	0.00	-768.70
1	0.00	40.11	142.20	91.15
2	0.00	40.11	292.92	201.54
3	0.00	40.11	452.56	293.58
4	0.00	40.11	621.52	369.50
5	0.00	40.11	800.21	431.30
6	0.00	40.11	824.22	397.25
7	0.00	40.11	848.94	365.88
8	0.00	40.11	874.41	336.96
9	0.00	40.11	900.64	310.32
10	0.00	40.11	927.66	285.77
11	0.00	40.11	955.49	263.15
12	0.00	40.11	984.16	242.31
13	0.00	40.11	1013.68	223.12
14	0.00	40.11	1044.09	205.44
15	0.00	40.11	1075.41	189.15
16	0.00	40.11	1107.68	174.14
17	0.00	40.11	1140.91	160.33
18	0.00	40.11	1175.13	147.60
19	0.00	40.11	1210.39	135.88
20	0.00	40.11	1246.70	125.08
21	0.00	40.11	1284.10	115.14
22	0.00	40.11	1322.62	105.99
23	0.00	40.11	1362.30	97.56
24	0.00	40.11	1403.17	89.80
25	0.00	40.11	1445.27	82.66
26	0.00	40.11	1488.62	76.08
27	0.00	40.11	1533.28	70.02
28	0.00	40.11	1579.28	64.44
29	0.00	40.11	1626.66	59.31
30	0.00	40.11	1675.46	54.58
NPV :				4996.34

Table F.7: Example to calculate the NPV for the chosen dam profile.

## F.5 VERIFICATION OF MONSOON CRITERION

As mentioned in the main report, it had to be checked, whether the crest level fulfils the monsoon criterion. For this the run-up, which will be exceeded by 2% of the waves, had to be added to the still water level for a monsoon return period of 50 years. In general, the wave run-up can be calculated using the formula, which became available recently:

$$z_{2\%} = 1.5 * H_{sig} * \gamma_b * \gamma_r * \gamma_\beta * \xi \quad \text{for } \xi < 2.0$$

$$z_{2\%} = 3.0 * H_{sig} * \gamma_b * \gamma_r * \gamma_\beta * \xi \quad \text{for } \xi \geq 2.0$$

in which:

$z_{2\%}$	= run-up exceeded by 2% of the waves	[ m ]
$H_{sig}$	= significant wave height	[ m ]
$\gamma_b$	= reduction factor with respect to berm influence	[ - ]
$\gamma_r$	= reduction factor with respect to roughness of slope surface	[ - ]
$\gamma_\beta$	= reduction factor with respect to direction of wave front	[ - ]
$\xi$	= breaker index see section 1.1.3 of this annex	[ - ]

In this formula the following values were introduced for a 50 years return period:

$$H_{sig} = 1.4 \text{ m}$$

$$T_z = 4.6 \text{ s}$$

$$T_p = 1.15 * 4.6 = 5.29 \text{ s}$$

$$\tan \alpha = 1/5 = 0.2$$

This yields a  $\xi$  of 1.1. Furthermore:

$$\gamma_b = 1.0 \text{ (no berm)}$$

$$\gamma_r = 1.0 \text{ (smooth placed blocks)}$$

$$\gamma_\beta = 1.0 \text{ for } \beta \leq 30^\circ \text{ and } 1.12 - 0.004 * \beta \text{ for } \beta > 30^\circ$$

$$\beta = \text{angle between the wave fronts and the dam axis} = 30^\circ$$

Thus  $\gamma_\beta = 1.0$

This yields a run-up of 2.31 m.

For a 50 years return period the still water level = 7.69 m for monsoon conditions. The monsoon criterion requires a minimum crest level of the still water level plus the run-up for a 50 years return period, which yields: 7.69 + 2.31 = 10.0 meters + PWD. This value is less than the crest level derived by means of the optimization procedure for cyclonic conditions. When the most economic dam profile during cyclone conditions would be applied, this dam profile would fulfil the monsoon criterion as well.

Accordingly, a slope angle of 1:5 and a crest level of 10.1 m. + PWD, without the influence of the geotechnical settlement, was chosen for the redesign of the main dam.

## F.6 DESIGN OF DAM PROFILE WHEN THE CPP II CRITERIA WOULD BE APPLIED

### F.6.1 MONSOON DESIGN CONDITION

Just as an illustration, the dam profile is determined in this section, when the design criteria, used for the design of the coastal embankments which are subject to the Cyclone Protection Project II, would be imposed to the Feni dam. These criteria were chosen more or less arbitrarily and are not prescribed by the Bangladeshi government.

According to ref. [5], the monsoon criterion used by the Cyclone Protection Project II reads: Less than 13% of the waves should overtop the structure for a situation having a return period of 5 years. For this the following parameters were introduced in the wave run-up formula:

$$\begin{aligned}H_{sig} &= 1.18 \text{ m} \\T_z &= 4.3 \text{ s} \\T_p &= 1.15 * 4.3 = 4.95 \text{ s} \\\tan \alpha &= 1/5 = 0.2 \\\gamma_b &= 1.0 \text{ (no berm)} \\\gamma_r &= 1.0 \text{ (smooth placed blocks)} \\\gamma_\beta &= 1.0 \text{ for } \beta \leq 30^\circ \text{ and } 1.12 - 0.004 * \beta \text{ for } \beta > 30^\circ \\\beta &= \text{angle between the wave fronts and the dam axis} = 30^\circ. \\\text{Thus } \gamma_\beta &= 1.0\end{aligned}$$

This yields a  $\xi$  of 1.14.

According to the most recent wave run-up formula, this yields a wave run-up of 2.01 meter which is exceeded by 2% of the waves. A run-up which is exceeded by 13% of the waves can be calculated using the following formula, according to ref. [29].

$$z_{n\%} = 0.767 * \sqrt{2 - \log n} * z_{2\%}$$

in which:

$$\begin{aligned}z_{n\%} &= \text{run-up exceeded by } n \% \text{ of the waves.} & [ \text{ m } ] \\z_{2\%} &= \text{run-up exceeded by } 2 \% \text{ of the waves.} & [ \text{ m } ]\end{aligned}$$

Thus:  $z_{13\%} \approx 0.72 * z_{2\%} = 0.72 * 2.01 = 1.45$  meter.

The SWL for this monsoon return period is about 6.62 meters. So the required crest level for this criterion is  $6.62 + 1.45 \text{ m} + \text{PWD} = 8.07 \text{ m} + \text{PWD}$ .

### F.6.2 CYCLONE DESIGN CONDITION

The cyclone design criterion reads:

- For a return period of 20 years, the resulting average water depth in the polder (here the reservoir should not attain values higher than 1.0 meter.
- For a return period of 40 years, the water level should be lower than the crest level.

First criterion a) is considered. The volume of sea water, necessary to yield an elevation of the reservoir level by 1.0 meter can be estimated from the water level - storage relation of ref. [27]. Taking the normal operating level as a starting point, an elevation of 1.0 meter requires a total overtopping volume of sea water of 65 million m<sup>3</sup>.

By means of an iteration procedure the necessary crest level, which yields the mentioned overtopping volume, can be derived using the HRS method as described in ref. [29]. The required crest level turns out to be about 8.0 m. + PWD then.

For cyclone criterion b) the dam crest level should be higher than the cyclonic water level corresponding to a return period of 40 years. For the used water level distribution for cyclone conditions this yields a necessary crest level of 9.50 meter + PWD.

Finally it can be concluded that the last mentioned cyclone design criterion governs the geometric design of the dam profile. When the same design criteria as for the CPP II would be applied, the crest level would be about 9.50 meters above PWD (without taking the geotechnical settlement into account). This is only 0.60 meter lower than the crest level chosen in this study.





## ANNEX G

### CALCULATIONS USING THE ANALYTICAL METHOD FOR THE DESIGN OF PLACED BLOCK REVETMENTS

#### TABLE OF CONTENTS

G.1	<u>INTRODUCTION</u> .....	G - 3
G.2	<u>CALCULATIONS FOR THE SLOPE PROTECTION OF THE ULTIMATE REDESIGN</u> .....	G - 4
	G.2.1 STRUCTURAL INPUT PARAMETERS .....	G - 4
	G.2.2 DETERMINATION OF THE LEAKAGE LENGTH .....	G - 4
	G.2.3 REQUIREMENT OF GEOMETRIC STABILITY OF THE GEOTEXTILE .....	G - 6
	G.2.4 STABILITY REQUIREMENT FOR $H = H_{ig}$ .....	G - 6
	G.2.5 STABILITY REQUIREMENT FOR $H = 1.4 * H_{ig}$ .....	G - 8
	G.2.6 REQUIREMENT OF GEOTECHNICAL MICRO STABILITY .....	G - 9
G.3	<u>CALCULATIONS FOR THE SLOPE PROTECTION OF THE ORIGINAL DESIGN</u> .....	G - 10
	G.3.1 STRUCTURAL INPUT PARAMETERS .....	G - 10
	G.3.2 DETERMINATION OF THE LEAKAGE LENGTH .....	G - 10
	G.3.3 REQUIREMENT OF GEOMETRIC STABILITY OF THE GEOTEXTILE .....	G - 10
	G.3.4 STABILITY REQUIREMENT FOR $H = H_{ig}$ .....	G - 10



## ANNEX G      CALCULATIONS USING THE ANALYTICAL METHOD FOR THE DESIGN OF PLACED BLOCK REVETMENTS

### G.1      INTRODUCTION

By means of an example, it is tried to explain the analytical method in this annex. For a more detailed explanation, reference is made to ref. [12].

First hydraulic and structural parameters, which are necessary for this method have to be drawn up. Then, the leakage length should be determined. This is an important parameter, which governs the strength of the slope protection. This parameter represents the relation between the permeabilities of the cover and filter layers. Subsequently, it should be checked, whether the slope protection structure meets all the following requirements:

- Requirement of geometric stability of the geotextile. The mesh sizes of the filter fabric should be sufficiently small to prevent the infiltration of base material through the geotextile into the filter layer.
- Stability requirement for a wave height  $H = H_{sig}$ . When the slope revetment is attacked by these wave heights there should be no block movements.
- Stability requirement for a wave height  $H = 1.4 * H_{sig}$ . For these waves, some block movements are permitted. Here, the block movements should be less than 0.1 times the block thickness. Then the blocks are assumed to fall back on their place after the wave attack.
- Requirement of geotechnical micro stability. When the slope protection is under severe wave attack, no geotechnical failure planes should occur directly underneath the slope protection. The geotechnical macro stability of the total dam body is checked in Section 7.5.2 of the main report.

When all these requirements are fulfilled for a certain slope protection, this slope protection is thought to be stable for the design conditions. Using this method, the stability of a given slope protection can only be checked. By means of an iteration procedure the most economical slope protection, which meets the requirements can be obtained.

In Section G.2 the analytical method is applied to the ultimately chosen main slope protection for the redesign of the main dam. Furthermore, the stability of the slope protection, which was chosen for the original design, is checked in Section G.3.

## G.2 CALCULATIONS FOR THE SLOPE PROTECTION OF THE ULTIMATE REDESIGN WITHOUT ACCRETION INFLUENCE

### G.2.1 STRUCTURAL INPUT PARAMETERS

With regard to the structural properties of the slope protection, the following parameters were determined:

- Slope angle:  $\tan \alpha_{avg} = \text{tangent of the average slope angle between SWL and SWL-2*H}_{sig} = 0.225$
- Cover layer:  $D = \text{cover layer thickness} = 0.20 \text{ m}$   
 $\Delta = (\rho_{block} - \rho_{water})/\rho_{water} \quad [ - ]$   
 $\rho_{block} = \text{density of the blocks} = 2250 \text{ kg/m}^3$   
 $\rho_{water} = \text{density of water} = 1025 \text{ kg/m}^3$   
 Thus,  $\Delta = 1.2,$
- $B = L = \text{width and length of the blocks} = 0.25 \text{ meter}$   
 $s = \text{average joint width between two adjacent blocks} = 2 \text{ mm}$
- Filter layer:  $b_n = \text{filter thickness} = 0.05 \text{ meter}$   
 $n = \text{filter porosity} = 0.4$   
 $D_{n,15} = \text{grain size of the filter material, which is not exceeded by 15 \% of the material based on weight} = 2 \text{ mm for pea gravel.}$   
 $D_{n,90} = \text{grain size of the filter material, which is not exceeded by 90 \% of the material based on weight} \approx 6 \text{ mm for pea gravel.}$
- Filter fabric:  $O_{90} = \text{characteristic mesh size of the filter fabric} = 0.10 \text{ mm.}$
- Sub layer:  $D_{b,50} = \text{grain size of the base material, which is not exceeded by 50 \% of the material based on weight} = 0.01 \text{ mm.}$   
 $D_{b,90} = \text{grain size of the base material, which is not exceeded by 90 \% of the material, based on weight} = 0.03 \text{ mm.}$

### G.2.2 DETERMINATION OF THE LEAKAGE LENGTH

The equation for the leakage length reads:

$$\Lambda = \sqrt{\frac{k * b_{f1} * D}{k'}}$$

in which:

- $\Lambda = \text{leakage length} \quad [ \text{m} ]$   
 $k = \text{permeability of the filter layer} \quad [ \text{mm/s} ]$   
 $k' = \text{average permeability of the cover layer} \quad [ \text{mm/s} ]$

For the calculation of the leakage length the permeability of the filter layer,  $k$ , should be read from the Figure G.1, according to ref. [12]. For the values  $D_{f,15} = 2 \text{ mm}$  and  $n = 0.4$ , the resulting  $k = 30 \text{ mm/s}$ .

For the calculation of the permeability of the cover layer, Figure G.2 should be used. For the values  $s = 2 \text{ mm}$ , no joint fill,  $n = 0.4$ ,  $D_{f,15} = 2 \text{ mm}$  and  $B = L = 0.25$ , the resulting  $k' = 8 \text{ mm/s}$ .

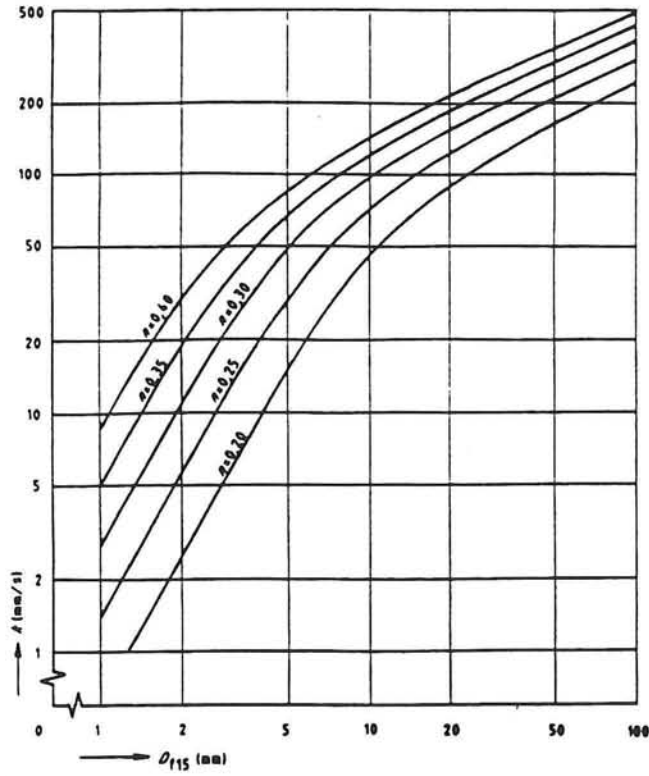


Figure G.1: permeability of the filter layer, according to ref. [12].

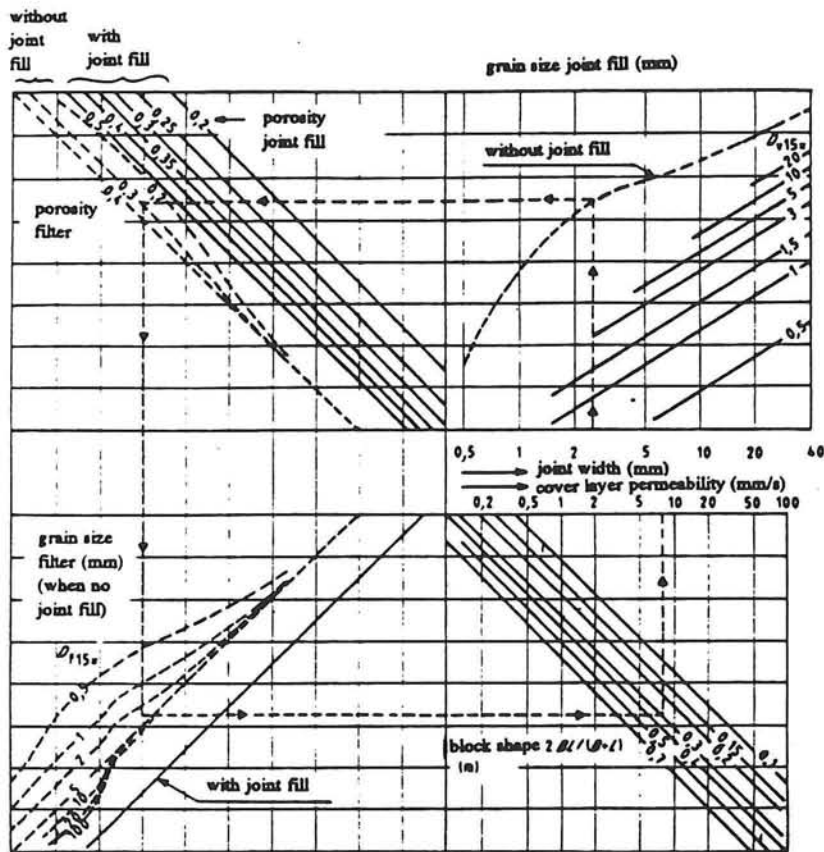


Figure G.2: permeability of the cover layer, according to ref. [12].

When no geotextile is applied directly under the cover layer, it should be checked, whether filter material is likely to wash through the joints. For this the requirement has been set to  $D_{n,90} > s$ . In this case,  $D_{n,90} \approx 6$  mm and  $s = 2$  mm and thus, the requirement is fulfilled.

Finally, the leakage length turns out to be: 
$$\Lambda = \sqrt{\frac{30 * 0.05 * 0.20}{8}} = 0.19 \text{ meter}$$

### G.2.3 REQUIREMENT OF GEOMETRIC STABILITY OF THE GEOTEXTILE

One of the requirements of the analytical method is that no base material should be washed through the filter fabric into the filter layer. The filter fabric should therefore be geometrically stable and it should meet the following requirement:

$$O_{90} < 10 * D_{b,50} \text{ and } O_{90} < D_{b,90} \text{ and } O_{90} \leq 0.10 \text{ mm.}$$

For the clay in the region of the Feni dam, two grain size distributions were used as obtained from ref. [11]. From this,  $D_{b,50} \approx 0.01$  mm and  $D_{b,90} \approx 0.03$  mm. According to the requirement:

$O_{90} < 0.1$  mm. Accordingly, for the chosen filter fabric, having a  $O_{90} = 0.1$  mm, the requirement is more or less fulfilled.

### G.2.4 STABILITY REQUIREMENT FOR $H = H_{sig}$

A wave height, which is equal to  $H_{sig}$ , should not result in any block movements. For the design condition, having a return period of 50 years  $H_{sig} = 1.4$  meter and  $T_z = 4.6$  seconds. For a  $\tan \alpha_{avg} = 0.225$  this yields a breaker index  $\xi = 1.25$ .

First it should be checked, whether the stability of the cover layer is influenced by transitions in the slope protection. As the main slope protection is applied from the crest to  $2 * H_{sig}$  beneath SWL, there are no transitions near the SWL and the influence is thought to be zero.  $\Gamma_0$ , which is the influence factor for transitions is therefore determined to be 1.0.

Subsequently, the influence of friction between the blocks has to be analyzed. For the determination of this influence Figure G.3 has to be used.

For  $\cotan \alpha_{avg,2} \approx 4.5$  and the factor  $B/D = 0.25/0.2 = 1.25$ , the influence factor  $\Gamma_1$  can be read from the figure. This yields:  $\Gamma_1 = 1.11$ .

The total influence factor  $\Gamma$  is defined as:  $\Gamma = \Gamma_1/\Gamma_0 = 1.11 / 1.0 = 1.11$ . Now the critical wave height  $H_{cr}$  can be derived by means of Figure G.4. For this the following strength factor is needed:

$$\Gamma^{1.25} * \sqrt{\frac{\Delta * D}{\Lambda}} = 1.11^{1.25} * \sqrt{\frac{1.2 * 0.20}{0.19}} = 1.28$$

For  $\xi = 1.25$ , the factor  $H_{cr}/\Delta D$  appears to be about 6.0. This yields a  $H_{cr} = 1.44$  meter. As the wave height is 1.4 meter, the slope protection appears to meet the requirement.

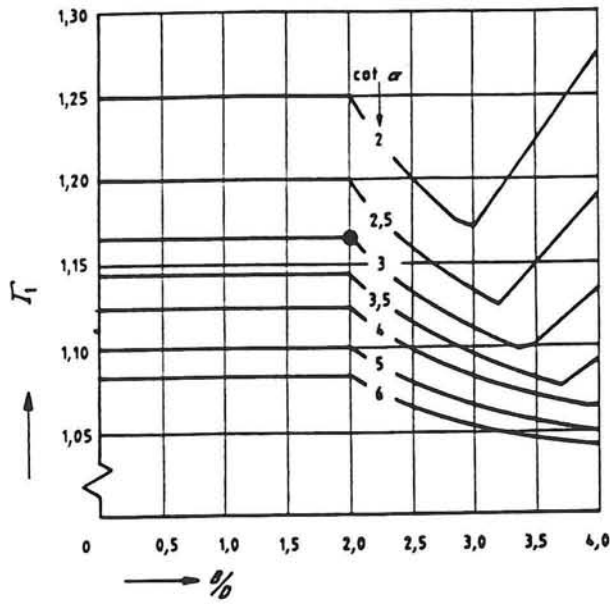


Figure G.3: Influence factor for the friction between the blocks, according to ref. [12].

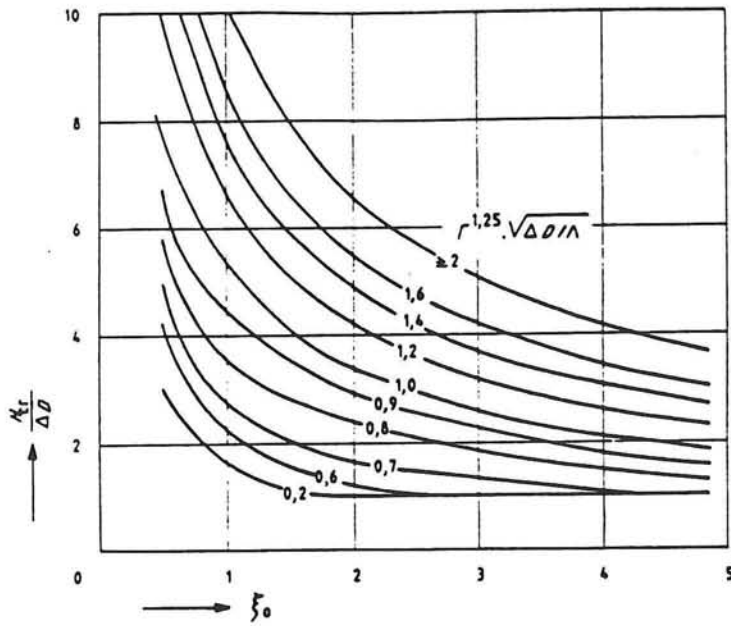


Figure G.4: Critical wave height with respect to the uplifting of the block, according to ref. [12].

## G.2.5 STABILITY REQUIREMENT FOR $H = 1.4 * H_{sig}$

When the slope protection is stable for wave heights,  $H$ , which are equal to  $H_{sig}$ , it should be checked whether the block movements are less than 0.1 times the block thickness for a wave height  $H = 1.4 * H_{sig}$ . For the design wave climate, this wave height is only exceeded by 2% of the waves.  $H = 1.4 * 1.4 \text{ m} = 1.96 \text{ m}$ . The breaker index for this wave height is calculated to be:  $\xi = 1.06$ .

Now several additional influence factors have to be determined. Using Figure G.5, the influence factor for the flow of water beneath the cover layer to the joints can be derived. For this the factor  $(BL/\Lambda)^{0.5} = (0.25 * 0.25/0.19)^{0.5} = 0.57$  and for the factor  $D/(k'\Delta) = 0.20 / (8*1.2) = 21$  are needed. These factors yield an influence factor  $\Gamma_3 \approx 0.3$ .

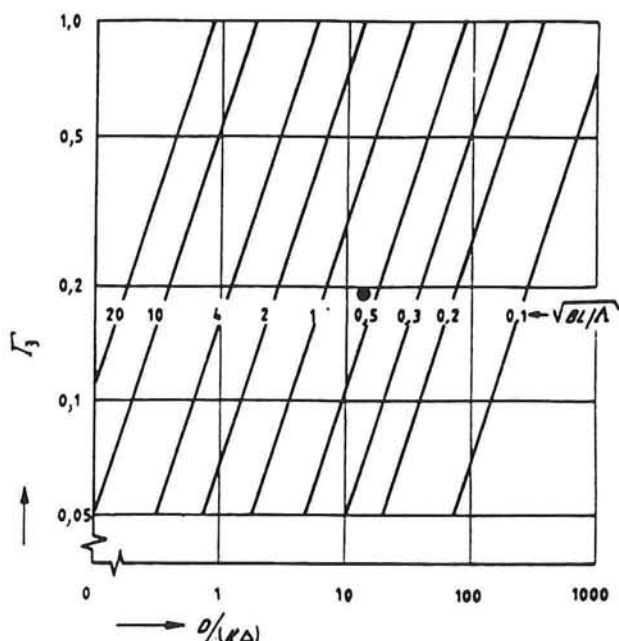


Figure G.5: Influence factor for the flow  $\Gamma_3$ , if the block movement is permissible.

The influence factor for inertia of mass,  $\Gamma_2$ , should be derived from Figure G.6. For  $\Delta = 1.2$  and  $D = 0.2$ ,  $\Gamma_2$  appears to be about 0.06.

Now  $\Gamma$  can be derived as:  $\Gamma = (\Gamma_1 + \Gamma_2 + \Gamma_3) / \Gamma_0 = (1.11 + 0.06 + 0.3) / 1.0 = 1.47$ . For  $\xi = 1.06$  and the strength factor:

$$\Gamma^{1.25} * \sqrt{\frac{\Delta * D}{\Lambda}} = 1.47^{1.25} * \sqrt{\frac{1.2 * 0.20}{0.19}} = 1.82$$

the factor  $H_{cr}/\Delta D$  can be read from Figure G.4.

$H_{cr}/\Delta D$  appears to be about 9.0. This yields  $H_{cr} = 2.16 \text{ m} > 1.96 \text{ m}$ . Therefore, the slope protection meets this requirement as well, when some block movements are permissible. In order to shorten the calculations,  $\Gamma_2$  does not have to be calculated when  $\Gamma_3 > 0.2$ . In this case, the mentioned requirement is thought to be fulfilled.



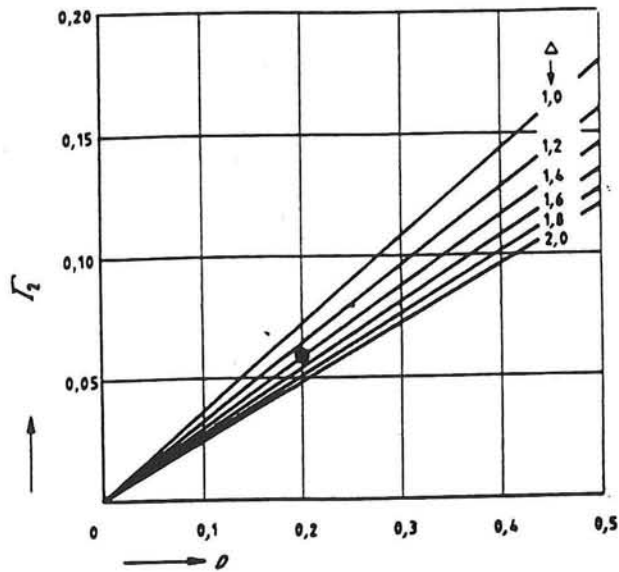


Figure G.6: Influence factor for the inertia of mass, if the stone movement is permissible.

### G.2.6 REQUIREMENT OF GEOTECHNICAL MICRO STABILITY

Subsequently, the geotechnical micro stability was analyzed which concerns the development of geotechnical failure planes directly under the slope protection. The macro stability of the entire dam body is discussed in section 7.5.2 of the main report.

Two loading conditions should be considered:

- 1) Local sliding caused by maximum wave back-rush.
- 2) Local sliding caused by wave slamming.

In contrast to sub layers consisting of sand, the first failure mechanism is not to be expected for a sub layer consisting of clay. As clay is a cohesive material, deeper slide planes are governing. Failure planes, directly underneath the slope protection are not likely to develop.

When the second loading condition is considered, the water cannot be discharged through the clay layer due to the short duration of this loading condition. For clay sub layers there is generally no danger for sliding, caused by this mechanism, according to ref. [12].

It can thus be concluded that this requirement is fulfilled as well.

The concerned slope protection meets all the requirements for a monsoon condition having a return period of 50 years. Accordingly, this structure is thought to be sufficiently stable.

### G.3 CALCULATIONS FOR THE SLOPE PROTECTION OF THE ORIGINAL DESIGN

Using the analytical method, the original slope protection can be checked. As the originally used design wave parameters are not thought to occur in nature (see Section 8.2), the newly derived values for the wave characteristics were used.

#### G.3.1 STRUCTURAL INPUT PARAMETERS

Again the structural parameters have to be drawn up first. This is done below:

Slope angle:  $\tan \alpha_{avg} = 0.194$   
Cover layer:  $D = 0.20 \text{ m}$   
 $\Delta = 1.2$   
 $B = L = \text{width and length of the blocks} = 0.50 \text{ meter}$   
 $s = 2 \text{ mm}$   
Filter layer:  $b_n = 0.10 \text{ meter}$   
 $n = 0.4$   
 $D_{n,15} = 28 \text{ mm}$   
 $D_{n,90} = 45 \text{ mm for chipped bricks.}$   
Filter fabric:  $O_{90} = 0.18 \text{ mm.}$   
Sub layer:  $D_{b,50} = 0.01 \text{ mm.}$   
 $D_{b,90} = 0.03 \text{ mm.}$

#### G.3.2 DETERMINATION OF THE LEAKAGE LENGTH

For  $D_{n,15} = 28$  and  $n = 0.4$ , the permeability of the filter layer,  $k$ , can be obtained from Figure G.1. This parameter appears to be:  $k \approx 25 \text{ mm/s.}$

A joint width of 2 mm, no joint fill,  $n = 0.4$ ,  $D_{n,15} = 28 \text{ mm}$  and  $B = L = 0.50 \text{ meter}$  yields a permeability of the cover layer of about 6 mm/s, according to Figure G.2. Than the leakage length can be determined to be about 1.02 meter.

#### G.3.3 REQUIREMENT OF GEOMETRIC STABILITY OF THE GEOTEXTILE

As mentioned before in section 2.3 of this annex, a filter fabric is required, having a characteristic mesh size  $O_{90}$  bigger than 0.10 mm. The  $O_{90}$  of the filter fabric applied for the original design = 0.18 mm. This filter fabric turns out not to meet the requirement!

#### G.3.4 STABILITY REQUIREMENT FOR $H = H_{sig}$

For  $H_{sig} = 1.4 \text{ meter}$  and  $T_z = 4.6 \text{ seconds}$  and  $\tan \alpha_{avg,2} = 0.194$  the breaker index  $\xi = 1.08$ . Again the influence factor for transitions ( $\Gamma_0$ ) thought to be 1.0. The influence factor for friction between the blocks ( $\Gamma_1$ ) can be read from Figure G.3. For  $B/D = 0.50 / 0.25 = 2.0$  and  $\cotan \alpha_{avg,2} = 1/0.194 \approx 5$ ,  $\Gamma_1 = 1.10$ . Thus the total influence factor  $\Gamma = 1.10/1.0 = 1.10$ .

All this yields a factor for  $H_{cr}/\Delta D = 2.0$ .  $H_{cr}$  appears to be 0.60 meter, which is much smaller than  $H_{sig} = 1.4 \text{ meter}$ . It can be concluded that the original slope protection is far from stable!

**ANNEX H**

**COST CALCULATION OF THE ORIGINAL AND REDESIGN**

**TABLE OF CONTENTS**

H.1	COSTS FOR THE ORIGINAL DESIGN .....	H - 3
H.2	COSTS FOR THE REDESIGN .....	H - 4



## ANNEX H COSTS FOR THE ORIGINAL AND REDESIGN

### H.1 COSTS FOR THE ORIGINAL DESIGN

In the tables H.1 and H.2 the costs for the different items for the original design is given as obtained from ref. [3] and ref. [24].

MAIN DAM				
Item description	Unit	Amount	Unit rate (Tk)	Costs (10 <sup>6</sup> Tk)
(de-) mobilization	-	-	-	166.2
Bed protection	m <sup>2</sup>	190,000	600	114.0
Sill	m <sup>3</sup>	93,000	400	37.2
Neap Tide Dam	m <sup>3</sup>	19,700	800	15.8
Winter Spring Tide Dam	m <sup>3</sup>	114,000	475	54.2
Earth works final profile	m <sup>3</sup>	420,000	100	42.0
Slope protection	m <sup>2</sup>	87,000	800	69.6
Road on main dam	m <sup>2</sup>	4,500	1,000	4.5
Total base construction costs main dam				503.5

Table H.1: Costs of the main dam for the original design.

FLANK EMBANKMENTS				
Item description	Unit	Amount	Unit rate (Tk)	Costs (10 <sup>6</sup> Tk)
Earth works	m <sup>3</sup>	250,000	75	18.8
slope and fore shore protection	m <sup>2</sup>	116,000	570	65.8
road of flank embankments	m <sup>2</sup>	8,000	658	8.0
Total base costs				92.6

Table H.2: Cost of flank embankments for the original design.

## H.2 COSTS FOR THE REDESIGN

After redesigning the Feni River Closure Dam, the total costs can be derived for both cases; with and without accurate anticipation of the accretion process downstream of the dam. This cost calculation is given in the Tables H.3 and H.4, using the unit rates which was estimated in section 1.1 of annex F.

MAIN DAM		unit	unit	without accret.		with accret.	
Item description			rate (Tk)	amount	costs 10 <sup>6</sup> Tk	amount	costs 10 <sup>6</sup> Tk
(de -) mobilization		-	-	-	166.2	-	166.2
Bed protection		m <sup>2</sup>	600	190,000	114.0	190,000	114.0
Sill		m <sup>3</sup>	400	93,000	37.2	190,000	37.2
Neap Tide Dam		m <sup>3</sup>	800	19,700	15.8	19,700	15.8
Winter Spring Tide Dam		m <sup>3</sup>	475	114,000	54.2	114,000	54.2
Road on dam		m <sup>2</sup>	1000	4,500	4.5	4,500	4.5
Earth works final profile		m <sup>3</sup>	100	346,000	34.6	327,000	32.7
Reservoir side slope protection : below 6.46 m. + PWD	0.40 m clay - filter fabric - 0.10 m filter - 0.25 m conc. + brick aggr.	m <sup>2</sup>	890	16,600	15.8	16,600	15.8
above 6.46 m. + PWD	0.40 m clay - 0.10 m bricks	m <sup>2</sup>	240	17,400	4.2	16,500	4.0
Sea side slope protection: crest to 4.9 m. + PWD	0.60 m clay - filter fabric - 0.05 m filter - 0.20 m conc. + gravel aggr.	m <sup>2</sup>	850	29,000	24.7	27,950	23.8
4.9 m to 3.0 m + PWD	0.60 m clay - filter fabric - 0.05 m filter - 0.20 m brick blocks	m <sup>2</sup>	630	9,100	5.7	9,100	5.7
3.0 m + PWD to toe, without siltation influence	idem,	m <sup>2</sup>	630	8,600	5.4	-	-
3.0 m + PWD to toe, with siltation influence	0.60 m clay - filter fabric - 0.05 m filter - 0.10 m bricks	m <sup>2</sup>	490	-	-	8,600	4.2
Total base construction costs for the main dam					482.3		478.1

Table H.3: Cost calculation for the redesign of the main dam with and without accretion influence.

Item description	unit	unitrate Tk	amount	costs 10 <sup>6</sup> Tk.	
<b>LEFT F.E.</b>					
Road on dam	m <sup>2</sup>	1000	1,800	1.8	
Earth works	m <sup>3</sup>	75	44,160	3.3	
Reservoir side slope protection	0.40 m clay - 0.10 m bricks	m <sup>2</sup>	240	7,750	1.9
Sea side slope and fore shore protection	0.60 m clay - filter fabric - 0.05 m filter - 0.20 m conc. + gravel aggr.	m <sup>2</sup>	850	9,580	8.1
<b>RIGHT F.E.</b>					
Road on dam	m <sup>2</sup>	1000	6,200	6.2	
Earth works	m <sup>3</sup>	75	136,000	10.2	
Reservoir side slope protection	0.40 m clay - 0.10 m bricks	m <sup>2</sup>	240	26,000	6.2
Sea side slope protection	0.60 m clay - filter fabric - 0.05 m filter - 0.15 m conc. + gravel aggr.	m <sup>2</sup>	730	26,000	19.0
Total base	construction costs flank emb.			56.7	

**Table H.4:** Cost calculation for the flank embankments of the redesign.

